A Survey on DCSK-based Communication Systems and Their Application to UWB Scenarios

Yi Fang, *Member, IEEE*, Guojun Han, *Senior Member, IEEE*, Pingping Chen, *Member, IEEE*, Francis C. M. Lau, *Senior Member, IEEE*, Guanrong Chen, *Fellow, IEEE*, and Lin Wang, *Senior Member, IEEE*

***Abstract*—In the past two decades, chaotic modulations have drawn a great deal of attention in low-power and low-complexity wireless communication applications due to their excellent anti-fading and anti-intercept capabilities. Of particular interest is the differential chaos shift keying (DCSK), which is considered as a very promising chaotic modulation scheme that achieves not only good error performance, but also low implementation complexity. In this treatise, we provide an insightful survey on the state-of-the-art research in DCSK-based communication systems through an extensive open literature search. In doing so, we firstly review the principles of DCSK modulation and the significant milestones since its inception. Subsequently, we introduce meritorious variants of DCSK, all of which can outperform the original one in certain aspects. We also present the joint design guidelines when combining DCSK with other critical techniques, e.g., error-correction coding and cooperative communication, in wireless communications under both single-user and multi-access scenarios. Besides, we summarize research progress in the application of DCSK-based communication systems to ultra-wideband scenarios and their corresponding advantages. Specifically, we restrict our attention to the relevant modulation and system designs, as well as their performance-analysis methodologies. This survey aims not only to allow researchers understanding the development and current status of DCSK-based communication systems, but also to inspire further research in this area.**

***Index Terms*—Chaotic communication, chaotic modulation, differential chaos shift keying (DCSK), multipath fading channel, ultra-wideband (UWB).**

I. Introduction

As a type of non-periodic and random-like signals, chaotic signals are derived from nonlinear dynamical systems [1]. Due to their inherent wideband characteristic, chaotic signals are naturally suitable for spread-spectrum (SS) modulations/communications [2]. In traditional SS communication systems, binary pseudo-random noise (PN) sequences, such as m-sequences and Gold sequences, are extensively utilized as the spreading sequences and to form the so-called direct-sequence (DS) SS systems [3]–[5]. Such type of spreading sequences possesses very desirable auto-correlation property but poor cross-correlation property because of the large spikes occurring in the cross-correlation functions. To address this weakness, Heidari-Bateni and McGillem [6], [7] have applied chaotic signals to the conventional SS communication systems. The basic principle is to replace the PN sequences by the chaotic sequences which are directly generated by a discrete-time nonlinear map (e.g., logistic map). The use of spreading sequences generated by the chaotic basis functions not only accomplishes all the benefits of conventional DSSS schemes, such as difficulty of uninformed detection, good anti-multipath-fading and anti-jamming abilities, but also results in some extra beneficial properties such as ease of generation and excellent cross-correlation property [6], [7].

In 1992, the (digital) chaotic modulation was first reported by Parlitz *et al*. [8]. Following this work, a great deal of research effort has been devoted to developing new chaotic modulation schemes accomplishing both excellent error-performance and low implementation complexity [9]–[12]. Among all the chaotic modulation schemes, the coherent chaos shift keying (CSK) [9] and non-coherent differential CSK (DCSK) [12] can achieve very desirable performance and therefore have been considered as two most outstanding alternatives for SS communications. Nevertheless, similar to the DSSS, the CSK belongs to coherent SS techniques and thus the locally-generated carriers have to be synchronized at the receiver terminal[1]. Aiming at improving the performance of CSK systems, many researchers have tried to explore the effective chaos-synchronization algorithms but merely attained very slow progress [13]–[16]. Perfect chaos synchronization remains as a challenging problem and is considered as one practical drawback of the CSK systems. In contrast, a DCSK receiver requires only an auto-coherent demodulator (i.e., differentially coherent (DC) demodulator) and does not need to reproduce the chaotic carrier. Moreover, DCSK systems exhibit lower implementation complexity and more powerful near-far resilience as compared to CSK and DSSS systems [12], [17]–[20].

Motivated by the aforementioned DCSK superiorities, a significant amount of work has been done with an aim to investigating the fundamental limits and theoretical performance of the DCSK systems under different channel environments, such as additive white Gaussian noise channels [21]–[26] and fading channels [19], [27], [28]. Furthermore, an improved demodulator for DCSK, namely the generalized-maximum-likelihood (GML) detector, has been proposed by Kolumban *et*

Y. Fang and G. Han are with the School of Information Engineering, Guangdong University of Technology, China (email: {fangyi, gjhan}@gdut.edu.cn).

P. Chen is with the Department of Electronic Information, Fuzhou University, China (email: ppchen.xm@gmail.com).

F. C. M. Lau is with the Department of Electronic and Information Engineering, Hong Kong Polytechnic University, Hong Kong (email: encm-lau@polyu.edu.hk).

G. Chen is with the Department of Electronic Engineering, City University of Hong Kong, Hong Kong (e-mail: eegchen@cityu.edu.hk).

L. Wang is with the Department of Communication Engineering, Xiamen University, China (email: wanglin@xmu.edu.cn).

[1]The procedure of reproducing the locally-generated chaotic carrier is defined as chaos synchronization.

al. [29]. Compared with the conventional DC demodulator, the GML demodulator possesses a distinguished advantage, i.e., it can be operated without a correlator. Currently, DCSK systems have been considered as very good candidates for low-power and low-complexity wireless communication applications, e.g., wireless personal area networks (WPANs) and wireless sensor networks (WSNs). Tutorial-like coverages of DCSK systems can be found in [20], [23], [30].

Because of its attractive advantages, DCSK has been extended to the non-binary domain, forming M-ary DCSK [30]. Moreover, as the conventional DCSK is not energy-stable, frequency modulation has been incorporated into DCSK such that the energy per bit can be kept constant [31]. Nevertheless, due to the differential property, the aforementioned DCSK systems suffer from two major drawbacks — relatively low data-rate and requirement of a radio-frequency (RF) delay line. To overcome such limitations, several meritorious variants of DCSK, e.g., enhanced DCSKs [32], [33], quadrature CSK (QCSK) [34], coded-shifted (CS) DCSK [35], high-efficiency DCSK [36], multi-carrier (MC) DCSK [37], have been further developed. To be specific, the enhanced DCSKs, QCSK and MC-DCSK can increase the data rate, while the CS-DCSK and high-efficiency DCSK can avoid using delay lines at the receiver terminal. In the CS-DCSK system, a high-date-rate (HDR) scheme has been proposed to further boost the bandwidth efficiency [38]. As DCSK spreads the spectrum of the original signal over a large bandwidth, it offers a relatively low spectral efficiency. For this reason, some multiple-access (MA) schemes[2], including the Walsh-coded (WC) DCSK scheme, have been conceived so as to increase the user capacity [23], [39]–[42]. Xu *et al*. [35] and Kaddoum *et al*. [43] have respectively extended the CS-DCSK and MC-DCSK to multi-user scenario. In addition to the above-mentioned aspects, Chen *et al*. [44], [45] have proposed an improved version of DCSK, namely the differentially DCSK (DDCSK) WC, and a novel detector to enhance the error performance of the conventional MA-DCSK systems. As a further advance, the coexistence of the DCSK-based systems and conventional digital communication systems, e.g., binary-phase-shift-keying (BPSK) and DSSS systems, has been intensely discussed [46]–[48].

Along with the development of DCSK-based systems, a lot of attention has been turned to investigating the concatenation of the modulation scheme with other crucial techniques as well as their corresponding designs. In 2010, Wang *et al*. [49] have firstly investigated the performance of M-ary DCSK in multiple-input-multiple-output (MIMO) multipath fading channels, and have proposed two transceiver schemes for such a system to achieve spatial diversity effectively. Aiming at validating the feasibility of the usage of chaotic communications in MIMO multipath fading scenarios, two different types of space-time block code (STBC)-based DCSK systems have been designed and analyzed [50]–[52]. In particular, the channel state information (CSI) is required in one STBC-DCSK system [50], [51] but not in the other [52]. In some practical scenarios, the transmitters may not be able to support multiple antennas owing to the constraints of size, complexity, power, cost, etc. To tackle this problem, a novel MIMO relay DCSK cooperative-diversity (DCSK-CD) system, which consists of a single-antenna transmitter, a multi-antenna relay and a multi-antenna receiver, has been formulated [53]. Alternatively, cooperation between two single-antenna users can also yield spatial diversity with relatively lower implementation complexity [54], [55]. Inspired by such an idea, some DCSK-CC systems have been constructed in [17], [56]–[58]. Besides spatial-diversity techniques, error-control techniques [59]–[62] can be exploited to dramatically boost the error performance and throughput of wireless communication systems. For example, error-correction codes (ECCs) [63]–[69] and automatic repeat request/cooperative automatic repeat request (ARQ/CARQ) [18] have been taken into account in designing DCSK-based systems. Additionally, bandwidth-efficient network coding (NC)-DCSK systems [70], [71] and multiresolution (MR)-based M-ary DCSK system [72] have been proposed over multipath fading channels with the use of the network coding techniques [73]–[75] and MR modulation [76], [77].

Although chaos-based communication systems have received a significant amount of attention in the past two decades, they are mostly restricted to academic research. To speed up the real-life deployment of such technologies, greater effort has been dedicated to expanding their application scenarios. Recently, it has been proved that DCSK-based modulations are particularly suitable for short-range ultra-wideband (UWB) wireless communications [78]–[82]. As a non-coherent transmitted-reference (TR) system, the frequency-modulated (FM)-DCSK not only inherits the advantages of conventional DCSK but also possesses the benefits of TR systems [83]–[85]. In consequence, FM-DCSK stands out as a very desirable scheme for UWB transmission, especially for low-cost, low-power and low-complexity WPAN/WSN applications [56], [86], [87]. Inspired by the aforementioned superiorities, a variety of DCSK-based systems have been extended to UWB transmission environments, forming various FM-DCSK-based UWB systems such as cooperative FM-DCSK UWB system [88], single-input multiple-output (SIMO) FM-DCSK UWB system [89], MIMO-relay FM-DCSK UWB system [90], STBC-FM-DCSK UWB system [52] as well as ARQ-based FM-DCSK UWB system [91]. Huang *et al*. [92] have also investigated the performance of FM-DCSK UWB for wireless medical applications. At the same time, several chaotic modulation schemes have been proposed as possible solutions for the UWB radio standards in WPANs by the IEEE 802.15.4a Task Group [93]–[95]. In addition, the chaos-based UWB pulse has already been involved in the latest international standard for wireless body area networks (WBANs), i.e., IEEE 802.15.6 [96]. All the above-mentioned applications and standards have indicated that DCSK possesses a great potential to becoming an excellent alternative for low-power short-range wireless communications.

This paper provides a comprehensive survey of the state-of-the-art DCSK-based communication system design and analysis over AWGN and multipath fading channels, as well

[2]"Multiple-access" and "multi-user" may be used interchangeably in this paper.

as their applications to UWB transmission scenarios. To begin with, the basic principles of chaotic modulations including CSK and DCSK are reviewed. Afterwards, some classical variants of DCSK as well as their corresponding advantages are elaborated. Following these foundations, a compact overview of the design of DCSK in conjunction with various critical techniques in wireless communications is presented. Furthermore, the research endeavors in the application of DCSK-based systems to UWB scenarios and the optimization techniques are described.

Although the list of the references may not be exhaustive, the articles cited as well as the references therein can be served as a good starting point for further reading by the interested readers. In particular, tutorial-style articles, such as [20], [23], [30], have reviewed the fundamental principles of CSK, DCSK, FM-DCSK, M-ary DCSK, and their performance over AWGN channels. In fact, the aforementioned articles have limited their attention to the available advancements till 2004. Against this background, this survey focuses on the latest development and important milestones of DCSK-based communication systems in the recent decade. To the best of our knowledge, this is the first general survey on DCSK-based communication systems over multipath fading channels, and hence can be considered as a useful reading for the interested researchers.

The remainder of this paper is organized as follows. In Section II, the basic principles and a historical overview of DCSK-based communication system are provided. In Section III, the research achievement in the structure improvement of DCSK (i.e., variants of DCSK) is summarized. The development of DCSK-based modulations in wireless communication systems, i.e., the joint design of DCSK and other crucial techniques in wireless communications, is described in Section IV. In Section V, we survey a promising application of DCSK, i.e., FM-DCSK-based UWB systems, and the corresponding optimization methodologies. Finally, the concluding remarks and future research directions are outlined in Section VI. To facilitate the reading of this treatise, the list of abbreviations used in this survey is shown in Table I.

TABLE I
LIST OF ABBREVIATIONS USED IN THIS SURVEY

ACK/NACK	acknowledgement/negative ACK
AF	amplify-and-forward
ANC	analog network coding
AR4JA	accumulate-repeat-by-4-jagged-accumulate
ARQ/CARQ	automatic repeat request/cooperative ARQ
AWGN	additive white Gaussian noise
BCJR	Bahl-Cocke-Jelinek-Raviv
BER	bit-error-rate
BP	belief propagation
BSC/SBC	bit-to-symbol/symbol-to-bit conversion
CC/CD	cooperative communication/cooperative diversity
CM	channel model
CMOS	complementary metal oxide semiconductor
COOK	chaotic on-off keying
CPC	chaotic-pulse-cluster
CS/GCS	coded-shifted/generalized CS
CSI	channel state information
CSK/DCSK	chaos shift keying/differential CSK
DC	differentially coherent
DDCSK	differentially DCSK
DF/EF	decode-and-forward/error-free
DPSK	differential phase shift keying
DS/DSSS	direct-sequence/DS spread-spectrum
ECC	error-correction code
EGC	equal-gain combiner
FER	frame-error-rate
FM	frequency-modulated
FSK	frequency-shift-keying
GA	Gaussian approximation
GML	generalized-maximum-likelihood
HDR	high-data-rate
IUI/IPI	inter-user/pulse interference
ITI/ISI	inter-transmit-antenna/symbol interference
IR/NIR	iterative receiver/non-IR
LDPC	low-density parity-check
LLR	log-likelihood-ratio
LOS/NLOS	line-of-sight/non-LOS
LTE	Long Term Evolution
MA/CDMA	multi-access/code-division MA
MC/MR	multi-carrier/multiresolution
MGF	moment generating function
MIMO	multiple-input-multiple-output
MRC	maximum-ratio combiner
MT-EGC	multicode transmission with EGC
NC	non-cooperative
PA	product-accumulate
PDF	probability density function
PN	pseudo-random noise
PNC/IPNC	physical-layer network coding/improved PNC
PSC/SPC	parallel-to-serial/serial-to-parallel converter
PSK/BPSK	phase-shift-keying/binary-PSK
QAM	quadrature amplitude modulation
QoS	quality of service
RF	radio-frequency
SG-BF	stochastic-gradient method for beamformer update
SIMO	single-input multiple-output
SISO	single-input-single-output
SNC	straightforward network coding
SNR	signal-to-noise-ratio
STBC	space-time block code
SU	single-user
TR	transmitted-reference
USRP	universal software radio peripheral
UWB	ultra-wideband
VBLAST	vertical-Bell-Labs-layered-space-time
VDMA	variant-delay MA
WBAN/WPAN	wireless body/personal area network
WC	Walsh code
WSN	wireless sensor network

II. PRINCIPLES OF DCSK COMMUNICATION SYSTEMS

As a typical chaotic modulation scheme, the CSK, which was first proposed by Dedieu *et al*. [9], is considered as the fundamental basis of DCSK. More importantly, it can provide a benchmark for the performance evaluation of other chaotic modulations, e.g., DCSK and its variants. For this reason, the working principles of CSK are first introduced in this section. Then the basic knowledge of DCSK together with the channel models (CMs) under which DCSK systems will be considered are presented. Afterwards, the major contributions made in the field of DCSK-based communication systems are summarized.

A. CSK System

The block diagram of a (binary) CSK communication system is depicted in Fig. 1 [23], [97]. As can be observed, only one chaos generator is used at the transmitter terminal. In such a system, the i-th bit $b_i \in \{+1, -1\}$ is

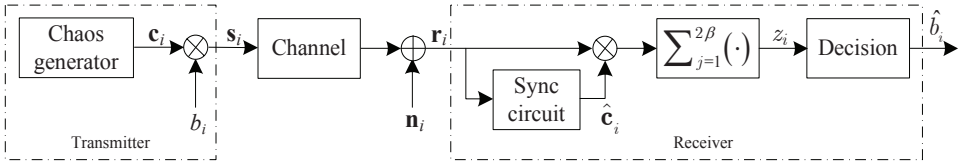

Fig. 1. Block diagram of a typical CSK communication system.

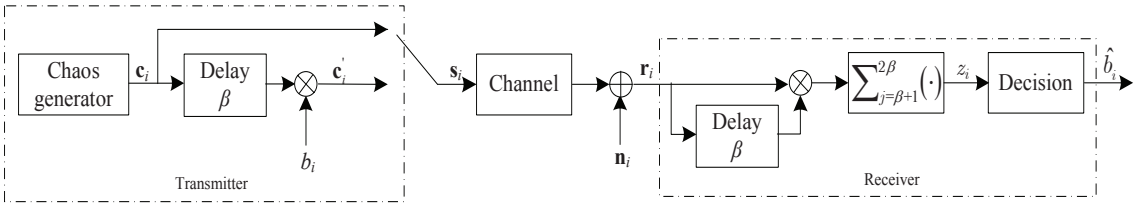

Fig. 2. Block diagram of a typical SU-DCSK communication system.

represented by one chaotic sequence $\mathbf{c}_i = \{c_{i,j}\}$, where $i = 1, 2, \ldots$; $j = 1, 2, \ldots$; $c_{i,j}$ is the i-th component chaotic sample; and $\mathbb{E}(c_{i,j}) = 0$. Assume that the durations of a chaotic sample and a bit are denoted by T_s and T, respectively, and the global spreading factor is denoted by $2\beta = T/T_s$. As a result, the j-th modulated sample output from a CSK modulator corresponding to b_i is expressed as $s_{i,j} = b_i c_{i,j}$, where $j = 1, 2, \ldots, 2\beta$; $c_{i,j}$ serves as the carrier; and $\mathbf{s}_i = [s_{i,1}, s_{i,2}, \ldots, s_{i,2\beta}]$ denotes the overall baseband transmitted signal during the i-th bit duration. Especially, both $s_{i,j}$ and $c_{i,j}$ are real numbers. As a result, the transmit energy per bit is $E_b = \sum_{j=1}^{2\beta} s_{i,j}^2 = \sum_{j=1}^{2\beta} c_{i,j}^2 = 2\beta\mathbb{E}(c_{i,j}^2)$, where $\mathbb{E}(\cdot)$ denotes the expectation operator. This signal is then passed through a given channel[3] and detected by a coherent demodulator. Based on the signal vector $\mathbf{r}_i = [r_{i,1}, r_{i,2}, \ldots, r_{i,2\beta}]$ received in the i-th transmission period (i.e., bit duration), a decision metric (demodulator output) z_i is computed using $z_i = \sum_{j=1}^{2\beta} r_{i,j} c_{i,j}$. Then the decoded bit is determined based on a hard-decision rule: $\hat{b}_i = +1$ if $z_i \geq 0$ and $\hat{b}_i = -1$ otherwise [97].

As can be seen from Fig. 1, the *synchronization circuit* plays a crucial role in the detection process because it is required to recover the "noise-like" chaotic carrier $\hat{\mathbf{c}}_i$ based on the noisy received signal $\mathbf{r}_i$. When the noise is extremely small and the channel varies slowly, synchronization of chaotic circuits and chaotic maps can be achieved using adaptive controllers [174] or neural networks [175]. Unfortunately, the existing chaos-synchronization algorithms are not able to provide satisfactory performance in noisy environments, and thus the realization of synchronization circuit is still an intractable problem at present [19], [81], [109]. Precisely speaking, the realization of chaos-synchronization circuit should be a profound technical subject, which is outside the scope of this treatise. We therefore refer the interested readers to the aforementioned publications for more details.

Note also that

- In this paper, $\mathbf{n}_i = [n_{i,1}, n_{i,2}, \ldots, n_{i,2\beta}]$ represents an additive-white-Gaussian-noise (AWGN) sequence of length 2β, unless otherwise specified. Moreover, $n_{i,j}$ has a zero mean and variance σ_n^2, i.e., $n_{i,j} \sim \mathcal{N}(0, \sigma_n^2)$; and $N_0 = 2\sigma_n^2$ denotes the noise power-spectral density.
- Many maps, e.g., logistic map, cubic map, and Bernoulli-shift map, can be employed to generate different chaotic sequences [23]. In this paper, the logistic map (i.e., $c_{i,j+1} = 1 - 2c_{i,j}^2$) is used because of its simplicity.

B. DCSK System

1) Single-user DCSK system: For the sake of tackling the practical weakness of CSK system, a more robust chaos-based system equipped with a DC demodulator — *DCSK system* — has been proposed by Kolumban *et al*. [12]. Fig. 2 shows the block diagram of a single-user (SU) DCSK communication system, in which the synchronization circuit is not required. Distinguished from the CSK system, the DCSK system represents each information bit by two chaotic sequences (i.e., fragments) of length β, i.e., the chaotic-reference sequence and the information-bearing sequence. To be specific, the information-bearing sequence equals the reference sequence if $b_i = 1$; otherwise (i.e., $b_i = -1$), it equals the negative of the reference sequence. Mathematically, the j-th output sample of the DCSK transmitter can be written as

$$s_{i,j} = \begin{cases} c_{i,j} & \text{if } 1 \leq j \leq \beta, \\ b_i c_{i,j-\beta} & \text{if } \beta + 1 \leq j \leq 2\beta, \end{cases} \tag{1}$$

As indicated by (1), the transmitted signal can be further expressed as $\mathbf{s}_i = [\mathbf{c}_i \ \mathbf{c}_i']$, where $\mathbf{c}_i = [c_{i,1}, c_{i,2}, \ldots, c_{i,\beta}]$ denotes the reference sequence and $\mathbf{c}_i' = b_i \mathbf{c}_i$ denotes the information-bearing sequence.

At the receiver, a DC demodulator (instead of a coherent demodulator in CSK) is utilized to demodulate the received signal $\mathbf{r}_i$ [12], while the decision rule is the same as that in the CSK system. In particular, there is no need to capture the CSI (or the chaotic carrier) when performing the detection in DCSK-based communication systems [23], [28]. Consequently, such a demodulator does belong to the noncoherent-demodulator category[4]. In comparison with the CSK system,

[3]The description of the CMs for chaotic modulations is ignored here but will be thoroughly discussed in Sect. II-B3.

[4]In this paper, we distinguish the coherent demodulator and noncoherent demodulator by the requirement of the *chaos synchronization* (i.e., the regeneration of the chaotic carrier), as in most other related publications [18]–[20], [23], [28].

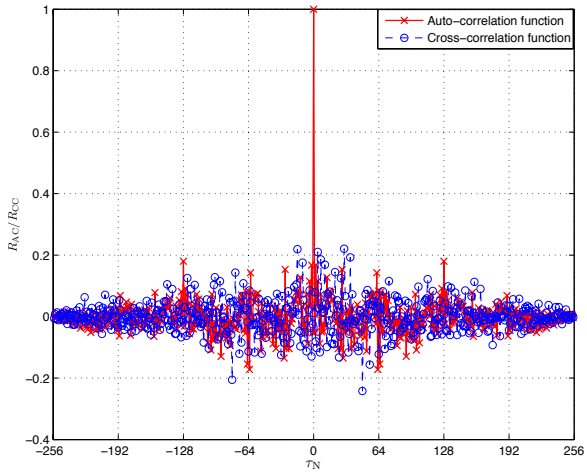

Fig. 3. Normalized auto-correlation and cross-correlation functions of DCSK sequences. The parameter used is $\beta = 128$.

the DCSK system possesses an easier implementation architecture at the expense of about 6 dB performance degradation over AWGN channels [20], [23], [28]. Yet, the performance degradation will be reduced under multipath fading scenarios because DCSK can significantly mitigate the effect of such channel imperfections.

To elaborate a little further, we discuss the cross-correlation property of DCSK signals, which is of great importance when attempting to generalize an SU case to an MA scenario. Fig. 3 illustrates the normalized auto-correlation function (i.e., $R_{\rm AC}$) and cross-correlation function (i.e., $R_{\rm CC}$) of DCSK sequences of length $2\beta = 256$, where $\tau_{\rm N}$ denotes the normalized time delay. It can be observed that due to the finite-length property, two different DCSK sequences have low cross-correlations rather than are perfectly orthogonal ($R_{\rm CC} \to 0$). To deal with this issue, a chaotic sequence can be multiplied with a 2^n-order WC [98] to produce n different DCSK sequences that strictly satisfy the orthogonality property [20].

In 2004, Kolumban *et al*. [29] have further proposed a new energy-based detector configuration (referred to as GML detector), for the DCSK/FM-DCSK system. Moreover, it is applicable to most variants of the DCSK/FM-DCSK system. The GML detector exploits the available *a-priori* information of the DCSK signal and thus achieves better error performance than the conventional DC detector.

2) MA-DCSK system: Similar to the existing DSSS systems [99], [100], MA is also considered as an essential feature in the application of DCSK-based systems. In fact, there exist several different MA-DCSK systems such as variable-delay-MA (VDMA) DCSK system [40], [101], code-division-MA (CDMA) DCSK system [102] and WC-DCSK system [20]. Among these systems, the WC-DCSK system has the best error performance and hence has been intensely investigated over the past ten years[5].

In an N-user MA-DCSK system where $N = 2^n/2$, a $2N$-order orthogonal WC sequence, defined as [20]

$$\mathbf{W}_{2^n} = \begin{bmatrix} \mathbf{W}_{2^{n-1}} & \mathbf{W}_{2^{n-1}} \\ \mathbf{W}_{2^{n-1}} & -\mathbf{W}_{2^{n-1}} \end{bmatrix} \quad n = 1, 2, \ldots \tag{2}$$

where $\mathbf{W}_{2^0} = \mathbf{W}_1 = 1$, is exploited to avoid the inter-user interference (IUI). In this case, each DCSK-modulated signal consists of $2^n = 2N$ fragments and each fragment length equals $f = 2\beta/(2N)$. Here, we consider the i-th bit period of the k-th user U_k. Denote $\mathbf{c}_{k,i}$ as the reference-chaotic sequence of length f used for the i-th bit. Furthermore, the k-th user is assigned with the $(2k-1)$-th and $2k$-th row vectors in $\mathbf{W}_{2^n}$. If the i-th bit b_i equals 1, the $(2k-1)$-th row vector is used for the transmission; and if the i-th bit b_i equals -1, the $2k$-th row vector is used. Denoting $w_{l,m}$ as the (l,m)-th element of the $2N$-order WC, the transmitted DCSK signal of the k-th user during the i-th bit period can be written as $\mathbf{s}_{k,i} = [w_{2k-b'_i,1}\mathbf{c}_{k,i}, w_{2k-b'_i,2}\mathbf{c}_{k,i}, \ldots, w_{2k-b'_i,2N}\mathbf{c}_{k,i}]$ where $b'_i = (b_i+1)/2$.

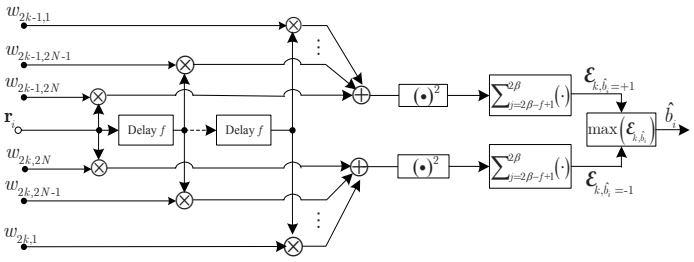

Fig. 4. Block diagram of the GML detector for U_k in an MA-DCSK system.

At the receiving end, a GML detector, whose structure is shown in Fig. 4, is employed to estimate the source information. Referring to Fig. 4, $\mathbf{r}_i$ denotes the received signal from the channel while $\mathcal{E}_{k,\hat{b}_i=\pm1}$ denotes the weighted energy corresponding to $\hat{b}_i = \pm 1$. *Note that* we omit here the expressions for $\mathbf{r}_i$ and $\mathcal{E}_{k,\hat{b}_i=\pm1}$, the details of which can be found in [17], [20], [44]. One can also refer to these references for more comprehensive knowledge of the MA-DCSK framework.

Remark: In this paper, we assume that the WCs (i.e., the system) are synchronized perfectly as in [17], [18], [40], [48], [54], [55], [71], [103] and therefore the IUI can be substantially eliminated. In a practical wireless environment, the WCs used in the downlink channels can be considered as synchronous while those in the uplink channels are always asynchronous. Yet, due to the good cross-correlation properties of chaotic sequences and WCs [17], [18], [40], it has been pointed out that the performance of DCSK-based systems does not vary much even if the channels corresponding to different users are not synchronized perfectly.

3) Channel Models: Broadly speaking, DCSK-based systems have been studied under two different channel models (CMs) in the literature. Initially, most contributions related to DCSK-based systems were investigated over AWGN channels with or without delay spread [20], [23], [30], [40], [41], [83]. In fact, the AWGN channel represents a type of simplest noisy CM and therefore the corresponding theoretical analysis and design can be easily carried out. Since 2003, more and

[5]For this reason, we will focus our attention on the "WC-based MA-DCSK systems" in this paper. Also for simplicity, "MA-DCSK system" will be used instead of "WC-based MA-DCSK system" in the remaining parts of this paper.

more research effort [19], [27], [28], [49]–[53], [56]–[58] has been spent on investigating DCSK-based systems over multipath fading channels — a type of wireless channel that can substantially degrade the quality of the received signals.

Mathematically, the input and output relationship of a multipath fading channel in an SU-DCSK system is given by

$$r_{i,j} = \sum_{l=1}^{L} \alpha_l s_{i,j-\tau_l/T_s} + n_{i,j}, \quad 1 \le j \le 2\beta, \qquad (3)$$

where $\mathbf{r}_i = \{r_{i,j}\}$ is the received signal; L denotes the total number of paths; α_l and $\tau_l = \kappa T_s$ are, respectively, the channel gain and the time delay of the l-th path; κ (i.e., normalized time delay) is a non-negative integer that satisfies $\kappa \ll 2\beta$; and $n_{i,j} \sim \mathcal{N}(0, N_0/2)$ is the Gaussian noise. In particular, α_l is a random variable subject to a certain distribution, e.g., Rayleigh fading [17], [28], Ricean fading [19], [27], and Nakagami-m fading [104], [105].

In the last ten years or so, research on DCSK-based systems are usually focused on Rayleigh fading channels [17], [28], [35], [36], [42]–[44], [49]–[52]. However, Rayleigh-fading does not satisfy the statistical characteristics of land-mobile systems, complex indoor environments, as well as ionospheric radio links. Fortunately, Nakagami-m fading can provide the best fit for the characteristics of such wireless channels [106]. As a result, Nakagami-m fading appears to be a more generalized distribution by which a myriad of fading environments (e.g., severe, light, or non-fading) can be accurately characterized. For these reasons, a great deal of research work has been dedicated to designing and analyzing DCSK-based systems in Nakagami fading channels [18], [48], [53], [57], [101].

Based on the above discussions, we will summarize the research achievements of DCSK-based systems over both AWGN channels and fading channels in the next subsection. Without loss of generality, however, for all the simulations carried out in this paper, we assume that the fading gains in the multipath fading channels follow a Nakagami-m distribution.

Example 1: We simulate the bit-error-rate (BER) performance of a two-user (i) MA-DCSK system, (ii) MA-CSK system, and (ii) CDMA system over a multipath Nakagami fading channel with a fading depth of $m = 2$, and show the results in Fig. 5. For the CDMA system, maximal sequences are used for spreading[6]. It can be observed that the MA-CSK and CDMA systems outperform the DCSK system in the low signal-to-noise-ratio (SNR) region because coherent detectors have been adopted in these systems. Yet, they become inferior to the MA-DCSK system in the high-SNR region. It is because the BER is dominated by noise in the low-SNR region but becomes more affected by the multipath fading in the high-SNR region. *It is worth noting that* owing to its stronger robustness against channel imperfection (i.e., multipath fading and time delay) [18], [19], [28], [97], the performance advantage of DCSK will become more obvious as the total number of paths (i.e., L) increases. In accordance

[6]For the sake of a fair comparison, an extra "0" is added at the end of the maximal sequences to produce an even sequence length [107], [108].

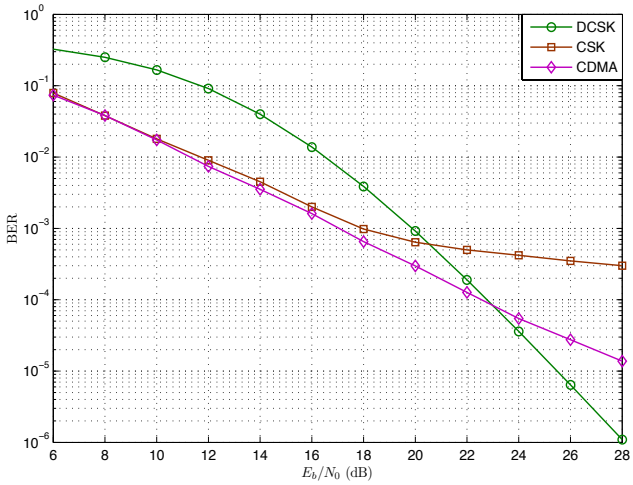

Fig. 5. BER curves of the MA-DCSK system, MA-CSK system, and CDMA system over a multipath Nakagami fading channel. The parameters used are $N = 2, m = 2, L = 2, (\tau_1, \tau_2) = (0, T_s)$, and $f = 64$.

to such advantages, the DCSK stands out as a better alternative for SS systems with respect to the other two schemes.

Note that DCSK applies a noncoherent receiver while both CSK and CDMA use a coherent receiver. For multipath fading channels, the BER performance is limited by noise in the low SNR region and hence the coherent receivers perform better than the noncoherent one. In the high SNR region, however, noise is negligible and the performance becomes limited by the "interference" caused by the late-arriving signals. Suppose there are only two arriving signals, the first-arriving signal and the second-arriving one. In the case of the coherent receivers, the second-arriving signal has two effects on the system performance. Firstly, it reduces the useful received signal strength (i.e., the first-arriving signal). Secondly, the second-arriving signal contributes to extra "interference" at the demodulator output when it correlates with the output from the synchronization circuit. Due to these two effects, the BER of both CSK and CDMA improves very slowly in the high SNR region. For the noncoherent receiver, the second-arriving signal (i) reduces the useful received signal strength, (ii) causes some interference to the first-arriving signal, (iii) but at the same time contributes positively to the decision metric z_i when it correlates with its own β-delayed signal (see Fig. 2). Due to the last attribute, DCSK continues to improve its BER in the high SNR region. The relative performance among the DCSK system, CSK system, CDMA system over multipath fading channel has also been illustrated by [28], [97]. The same arguments can be applied to explain why the MA-DCSK system is more appropriate for multipath fading channels.

C. Historical Development of DCSK-based Systems

In the past twenty years, DCSK-based modulations have received significant attention from the wireless-communication community and hence they represent another major direction for SS communication systems. As a consequence, taking into consideration the features of chaotic sequences, researchers have endeavored to design a large set of DCSK-based communication systems [17], [18], [20], [23], [50], [52], [53], [109],

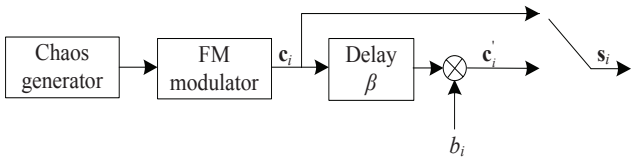

Fig. 6. Block diagram of the transmitter in an FM-DCSK system.

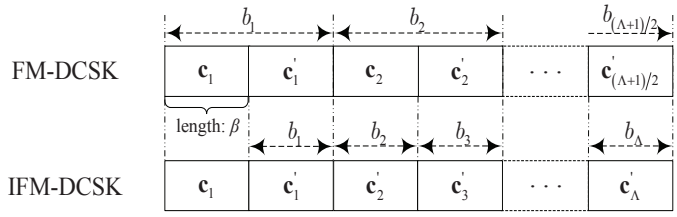

Fig. 7. Signal formats of the FM-DCSK and IFM-DCSK, where the number of chaotic fragments in each transmission period is assumed as $\Lambda + 1$.

[110] as well as their promising variants [30]–[37], [39], [44], [49], [111], [112]. Meanwhile, all the aforementioned systems have been carefully analyzed via Gaussian approximation (GA) [19], [27], [28], [113], moment generating function (MGF) [53], [88], as well as some other approaches [19], [26], [51]. Additionally, the application of DCSK-based systems to short-distance UWB transmissions has been extensively studied [79]–[92]. In Table II, we summarize the major contributions in the field of DCSK-based systems.

III. Variants of DCSK

Motivated by its desirable properties, DCSK has been thoroughly studied in terms of error performance, energy efficiency, data rate, etc. For the sake of further improving such a technique, a variety of variants have been developed and each of them can outperform the conventional DCSK in certain aspects. In this section, we cover the development in the design and analysis of some meritorious variants of DCSK.

A. FM-DCSK

1) Principles of FM-DCSK: Due to the inherent non-periodic property of chaotic signals, the bit energy of a DCSK modulation system cannot be kept constant but varies from bit to bit. To avoid this problem, FM-DCSK has been proposed by Kolumban *et al*. [31]. It seamlessly combines DCSK with FM so as to produce a constant-bit-energy wideband chaotic signal with no compromise in the attainable error performance. Fig. 6 presents the transmitter configuration of an FM-DCSK system, whereas the receiver is the same as that in the conventional DCSK system.

Inspired by this work, a great deal of attention has been paid to this research area and a significant amount of research achievements have been attained [29], [32], [56], [63], [64], [78], [83], [84], [84]–[92], [111], [114]–[116], [120]. Aiming to illustrate a little further, we also introduce some important milestones in the development of FM-DCSK.

2) Performance improvement: As a further advance, the structure of FM-DCSK has been modified by Kolumban *et al*. [32] so as to form an improved version of FM-DCSK (referred to as IFM-DCSK). In the IFM-DCSK system, suppose that there are totally Λ bits to be transmitted in each transmission period[7]. The information-bearing sequences that correspond to Λ source bits employ the same chaotic sequence as the reference sequence. The signal formats of the conventional FM-DCSK and IFM-DCSK are depicted in Fig. 7. Referring to this figure, we have $\mathbf{c}_i' = b_i\mathbf{c}_i$ for the FM-DCSK scheme, where $1 \leq i \leq (\Lambda+1)/2$, b_i, $\mathbf{c}_i$, and $\mathbf{c}_i'$ denote the i-th bit, i-th reference-chaotic sequence, and i-th information-bearing sequence, respectively. On the other hand, we have $\mathbf{c}_1' = b_1\mathbf{c}_1$ and $\mathbf{c}_i' = b_i\mathbf{c}_{i-1}'$ for the IFM-DCSK scheme, where $2 \leq i \leq \Lambda$. In general, $\mathbf{c}_i' \in \{+\mathbf{c}_1, -\mathbf{c}_1\}$ $(1 \leq i \leq (\Lambda+1)/2)$ for the IFM-DCSK scheme. In accordance to the above description, the information-bearing sequence $\mathbf{c}_i'$ $(2 \leq i \leq (\Lambda+1)/2)$ in the FM-DCSK scheme should be different from that in the IFM-DCSK scheme since the reference-chaotic sequence $\mathbf{c}_i$ in the former scheme varies from bit to bit.

Based on the structure of IFM-DCSK, a noise-mitigation methodology has also been proposed in the same paper to further enhance the error performance. Interested readers can refer to [32] for more details.

As compared with FM-DCSK, IFM-DCSK possesses some outstanding advantages.

- The data rate is increased from $1/2$ to $\Lambda/(\Lambda+1)$.
- The transmitted energy per bit is reduced from E_b to $(\Lambda+1)E_b/(2\Lambda)$, provided that the transmitted energy per fragment keeps as $E_b/2$.
- The error performance is improved with the same demodulator.

Nevertheless, the IFM-DCSK suffers from a more complicated transmitter.

In addition to the improvement of the transmitted signal (i.e., transmitter), some research effort has been made to enhance the performance of FM-DCSK system from other perspectives. For instance, Kolumban *et al*. [29] have conceived an optimum non-coherent detector, i.e., GML detector, for FM-DCSK systems. The superiority of GML detector, whose structure has been depicted in Fig. 4, will be more obvious for MA scenarios.

3) Implementation: Along with the information-theoretical development of FM-DCSK systems, some researchers have devoted efforts to the hardware realization of such systems. In 2012, Krebesz *et al*. [120] have successfully implemented the FM-DCSK system on the universal-software-radio-peripheral (USRP) platform based on a complex-envelope approach. Moreover, the theoretical error performance of FM-DCSK system has been validated by real measurements on the aforementioned platform. Strictly speaking, such a platform does belong to the soft-radio-based platforms but not hardware platforms. Thus, more endeavors in the field of hardware realization is expected.

In summary, FM-DCSK has already exhibited very promising characteristics (e.g., stable bit energy, excellent perfor-

[7]It has been shown in [32] that the number of information-bearing sequences should be between 2 and 4. Otherwise high spikes may appear in the spectrum of the overall transmitted signal.

TABLE II
MAJOR CONTRIBUTIONS IN THE STUDY OF DCSK-BASED COMMUNICATION SYSTEMS.

Year	Author(s)	Contribution
1996	Kolumban *et al*. [12]	Proposed the DCSK modulation.
1997	Kolumban *et al*. [39]	Developed an MA technique for the DCSK system, forming the first MA-DCSK system.
1998	Kolumban *et al*. [31]	Proposed the FM-DCSK, which possesses both excellent error performance and constant bit-energy.
1998	Kolumban *et al*. [15]	Reviewed the existing chaos-synchronization algorithms for chaos-based communication systems.
1999	Kolumban *et al*. [32]	Proposed two enhanced versions of DCSK/FM-DCSK in order to improve the energy efficiency and performance.
1999	Kennedy *et al*. [78]	First investigation on the simulated error performance of FM-DCSK systems over multipath fading channels.
2000	Abel *et al*. [21]	Presented the cumulant analysis tools, which are particularly suitable for DCSK systems, for chaos-based communication systems in AWGN channels.
2001	Galias *et al*. [34]	Introduced a multilevel version of DCSK modulation, i.e., QCSK, which exhibits similar error performance but has higher a data rate as compared to DCSK.
2001	Krol *et al*. [114]	Built the first experimental FM-DCSK chaos radio system to predict the error performance in a realistic radio communication environment.
2002	Lau *et al*. [40]	Proposed a novel MA-DCSK system, namely the VDMA-DCSK system, and derived the numerical BER formula of the corresponding system.
2002	Kolumban *et al*. [20]	Characterized the performance of the DCSK system in multipath channels, and introduced the WC sequence into the DCSK system so as to realize MA capability.
2003	Lau *et al*. [23]	Provided a fundamental tutorial for CSK/DCSK systems and addressed their design and analysis principles over AWGN channels.
2003	Kolumban *et al*. [115]	Extended the DCSK/FM-DCSK to non-binary domain, forming the M-ary DCSK/FM-DCSK, which accomplishes better performance at the expense of degrading the spectral efficiency.
2003	Lau *et al*. [47]	Analyzed the performance of DCSK system under the influence of a coexisting DSSS system in AWGN channels.
2003	Mandal *et al*. [27]	Attempted to evaluate the error performance of DCSK system in multipath Rayleigh fading channels.
2004	Kolumban *et al*. [29]	Designed a novel energy detector, i.e., GML detector, for DCSK system, which can achieve a better performance in AWGN channels.
2004	Wang *et al*. [63]	Introduced and studied low-density parity-check (LDPC)-coded FM-DCSK system.
2004	Xia *et al*. [28]	Analyzed the BER performance of DCSK system in multipath Rayleigh fading channels with delay spread.
2005	Erkucuk *et al*. [80]	Proposed a new hybrid modulation scheme, i.e., the M-ary code shift/DCSK for low-rate UWB applications.
2005	Ye *et al*. [116]	Illustrated new characteristics and performance advantages of FM-DCSK system in comparison with the conventional DSSS system in multipath fading channels.
2006	Salberg *et al*. [117]	Developed a subspace detector for DCSK system and conducted a performance analysis of the M-ary FM-DCSK system exploiting orthogonal subspace-generating vectors.
2007	Mazzini *et al*. [118]	Proposed a chaos-based DS-UWB system for wireless-sensor-network applications.
2008	Chong *et al*. [81]	Designed an UWB direct chaotic communication system based on the chaotic on-off keying (COOK) and DCSK for the low-cost, low-power, and low-rate WPAN applications.
2008	Wang *et al*. [85]	Conceived a novel SIMO architecture for FM-DCSK system for improving the data rate and BER performance.
2008	Zhou *et al*. [42]	Studied the BER performance of an MA-DCSK system in multipath Rayleigh fading channels.
2009	Ma *et al*. [50]	Discussed the implementation of Alamouti STBC with DCSK in MIMO channels and demonstrated its performance enhancement with respect to the single-input-single-output (SISO) DCSK scheme.
2010	Min *et al*. [86]	Investigated and optimized the critical parameters, e.g., guard interval and integration interval, of the FM-DCSK UWB system over IEEE 802.15.4a indoor channels.
2010	Chen *et al*. [87]	Conceived a low-complexity data-aided timing-synchronization algorithm for FM-DCSK UWB systems.
2011	Xu *et al*. [35]	Proposed CS-DCSK scheme, which does not require any RF delay line at the receiver but achieves comparable performance as the conventional DCSK scheme.
2011	Wang *et al*. [89]	Introduced a novel SIMO FM-DCSK UWB system based on chaotic-pulse-cluster (CPC) signals, which not only reduces the length of time-delay unit but also obtains a significant performance gain over the existing counterparts.
2011	Xu *et al*. [17]	Developed and analyzed a two-user DCSK-CC system over multipath Rayleigh fading channels.
2012	Kaddoum *et al*. [19]	Proposed a generalized BER analytical methodology for DCSK system in both AWGN and fading channels, which can provide an accurate BER prediction for small spreading factors.
2012	Chen *et al*. [44]	Developed WC-DDCSK modulation scheme, which leads to a more satisfactory performance as well as lower sensitivity to ISI in MA transmission environments.
2012	Kaddoum *et al*. [38]	Conceived two HDR CS-DCSK schemes, both of which can outperform the CS-DCSK scheme in AWGN channels in terms of data rate and error performance.
2013	Fang *et al*. [53]	Designed and analyzed a MIMO relay DCSK-CD system over multipath Nakagami fading channels.
2013	Chen *et al*. [52]	Proposed an analog STBC-DCSK system without channel estimation, which can effectively suppress ITI.
2013	Kaddoum *et al*. [37]	Presented an MC-DCSK system, which possesses the benefits of energy efficiency, HDR, as well as excellent performance over AWGN and multipath Rayleigh fading channels.
2014	Kaddoum *et al*. [71]	Developed and analyzed a new bandwidth-efficient ANC-based MC-DCSK system in AWGN and multipath Rayleigh/Rician fading channels.
2014	Xu *et al*. [48]	Investigated the error performance of the combined CS-DCSK-BPSK system over both AWGN and multipath Nakagami fading channels.
2015	Fang *et al*. [18]	Designed a DCSK-ARQ/CARQ system to achieve the goal of boosting the error performance and throughput of DCSK non-cooperative (NC)/CC system.
2015	Lyu *et al*. [69]	Introduced and evaluated performance of LDPC-coded M-ary DCSK system with an iterative receiver (IR).
2015	Wang *et al*. [72]	Applied MR modulation to DCSK system, forming an MR M-ary DCSK system, to satisfy different quality-of-service (QoS) requirements for different transmitted bits within a symbol.
2015	Kaddoum *et al*. [119]	Proposed an MA orthogonal-frequency-division-multiplexing (OFDM)-based DCSK system.

mance and easy implementation) and has become a good candidate for short-range wireless communication applications, such as WPANs/WSNs and UWB communications.

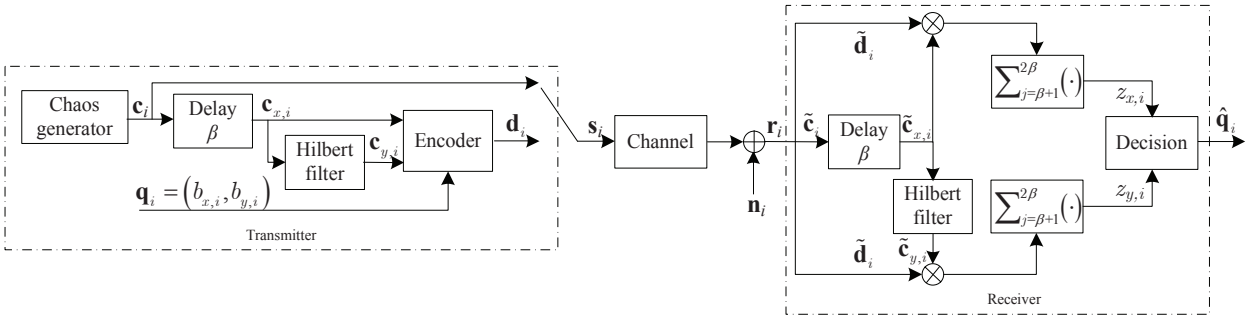

Fig. 8. Block diagram of a typical QCSK communication system.

B. QCSK

Quadrature CSK (QCSK), which is considered as a high-spectral-efficiency multilevel DCSK, was first proposed by Galias *et al*. in 2001 [34]. The block diagram of a QCSK system is shown in Fig. 8. In the sequel, we will describe the transceiver design of such a system as well as its advantage and disadvantage.

1) Transceiver structure: In contrast to DCSK, QCSK transmits a two-bit symbol rather than one bit in each transmission period (i.e., symbol period). We denote the i-th symbol by $\mathbf{q}_i = (b_{x,i}, b_{y,i})$ where $b_{x,i}, b_{y,i} \in \{+1, -1\}$. In fact, each symbol is represented by two chaotic fragments, each of length β — the reference-chaotic fragment $\mathbf{c}_i$ and the information-bearing fragment $\mathbf{d}_i$. The output of the QCSK transmitter during the i-th symbol period can be expressed as $\mathbf{s}_i = [\mathbf{c}_i \ \mathbf{d}_i]$ where $\mathbf{d}_i = b_{x,i}\mathbf{c}_{x,i} + b_{y,i}\mathbf{c}_{y,i}$, $\mathbf{c}_{x,i} = \mathbf{c}_i$, and $\mathbf{c}_{y,i}$ denotes an orthogonal sequence of $\mathbf{c}_{x,i}$[8]. In reality, $\mathbf{c}_{y,i}$ can be generated with by using a Hilbert filter [34].

At the receiver terminal, based on the received signal $\mathbf{r}_i = \mathbf{s}_i + \mathbf{n}_i = [\mathbf{c}_i \ \mathbf{d}_i] + \mathbf{n}_i = [\widetilde{\mathbf{c}}_i \ \widetilde{\mathbf{d}}_i]$, a modified DC detector can be utilized to decode the transmitted symbol $\mathbf{q}_i$, as shown in Fig. 8. Initially, the two "corrupted" orthogonal signals, i.e., $\widetilde{\mathbf{c}}_{x,i}$ and $\widetilde{\mathbf{c}}_{y,i}$, are directly obtained from the noisy reference fragment $\widetilde{\mathbf{c}}_i$. Afterwards, one can perform the detection by correlating $\widetilde{\mathbf{d}}_i$ with $\widetilde{\mathbf{c}}_{x,i}$ and $\widetilde{\mathbf{c}}_{y,i}$, respectively, and calculate the two metric values $z_{x,i}$ and $z_{y,i}$. At the end, the detected signal $\hat{\mathbf{q}}_i$ is yielded utilizing an appropriate decision-making rule.

2) Advantage and disadvantage: As can be seen from Fig. 8, the QCSK system is equivalent to two DCSK systems, with the difference that each information-bearing fragment in the QCSK system contains two bits of information. Benefiting from such an efficient transmission scheme, QCSK system doubles the data rate while keeping the error performance unchanged as compared with the DCSK system. Yet, the above advantage is accomplished at the expense of a relatively higher implementation complexity in both the transmitter and receiver.

Recently, another improved DCSK scheme has been proposed in [33]. It also aims at doubling the data rate of the conventional DCSK system by means of a time-reversal operation. The improved DCSK scheme enables a slight performance gain over the QCSK scheme in multipath fading channels.

C. M-ary DCSK

1) WC-based M-ary DCSK: In some practical applications, non-binary symbols rather than binary bits are to be transmitted in order to achieve a higher throughput. To achieve this aim, WC-based M-ary DCSK was introduced by Kolumban *et al*. in 2003 [115] and further elaborated by Kis in 2005 [30][9]. To ensure the orthogonality of M different transmitted DCSK signals, each DCSK sequence is first split into M chaotic fragments, each of length f. These fragments, denoted by $\mathbf{c}_{i,m}$ ($m = 1, 2, \ldots, M$) for the i-th symbol duration, are further multiplied with a row vector of an M-order WC, which can be generated using (2). Consequently, the transmitted signal corresponding to the i-th symbol $b_i \in \{0, 1, \ldots, M-1\}$ is given as $\mathbf{s}_{b_i} = [w_{b_i+1,1}\mathbf{c}_{i,1}, w_{b_i+1,2}\mathbf{c}_{i,2}, \ldots, w_{b_i+1,M}\mathbf{c}_{i,M}]$.

As in Sect. II-B2, a GML detector can be exploited to retrieve the source information at the receiver. The main difference between the GML detector used here and the one in Fig. 4 is that all the M different metrics, i.e., $\mathcal{E}_{\hat{b}_i=0}, \mathcal{E}_{\hat{b}_i=1}, \ldots, \mathcal{E}_{\hat{b}_i=M-1}$, should be calculated so as to identify the estimated symbol $\hat{b}_i$ in the M-ary scenario. As observed from the above description, the WC-based M-ary DCSK system is reduced to a conventional (binary) DCSK system if $M = 2$. Therefore, the M-ary DCSK is considered as a generalization of the conventional DCSK. More importantly, the error performance of the former scheme is superior to the latter scheme, and the performance gain will become larger as M increases [30].

Motivated by these advantages, more research on M-ary DCSK has been conducted in recent years [25], [68], [69]. For instance, the authors in [25] have delved into the channel capacity of M-ary DCSK in the context of an AWGN channel.

Example 2: Fig. 9 shows the BER results of M-ary DCSK systems over a multipath Nakagami fading channel with fading depth $m = 2$. Referring to this figure, the 4-ary DCSK system achieves a gain of 2.0 dB over the conventional DCSK system (i.e., $M = 2$) at a BER of 6×10^{-5}. However, the 4-ary DCSK system suffers from a lower spectral efficiency and a

[8]Precisely, the orthogonal sequence (i.e., quadrature sequence) $\mathbf{c}_{y,i}$ of $\mathbf{c}_{x,i}$ is defined as the sequence that is obtained via shifting the phase of each frequency component in $\mathbf{c}_{x,i}$ by $\pi/2$. Accordingly, we have $\mathbf{c}_{y,i}(\mathbf{c}_{x,i})^{\mathrm{T}} = 0$, where the superscript "T" denotes the transpose operator.

[9]In the WC-based M-ary DCSK systems, M represents the cardinality of a signal set that are to be transmitted. It is also known as the number of possible symbols in a transmitted signal set. For example, one can assume that a signal set $\mathcal{B} = \{0, 1, \ldots, M-1\}$ rather than {0,1} is to be transmitted.

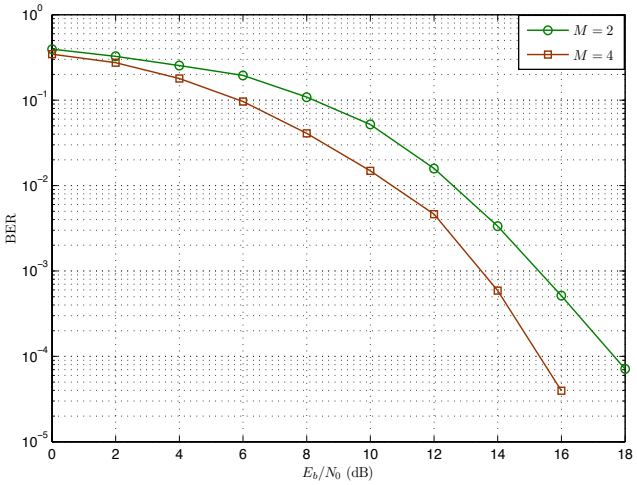

Fig. 9. BER curves of the WC-based M-ary DCSK systems over a multipath Nakagami fading channel. The parameters used are $m = 2, L = 2, (\tau_1, \tau_2) = (0, T_s), M = 2, 4,$ and $f = 40$.

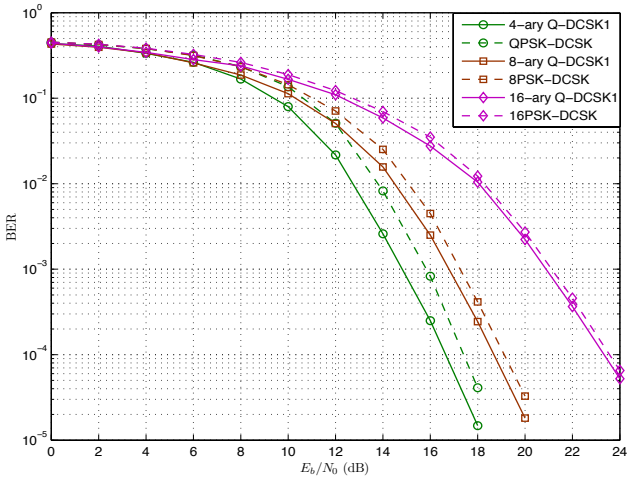

Fig. 10. BER curves of the M-ary Q-DCSK1 system and MPSK-DCSK system over a multipath Nakagami fading channel. The parameters used are $m = 2, L = 2, (\tau_1, \tau_2) = (0, T_s), M = 4, 8, 16,$ and $f = 64$.

higher system complexity. In particular, the most challenging problem for implementing such a system is that all the M chaotic fragments should be perfectly synchronized at symbol level.

2) PSK/QAM-based M-ary DCSK: In 2010, Wang *et al*. [49] have proposed another M-ary DCSK scheme based on phase-shift-keying (PSK)/quadrature amplitude modulation (QAM) and have called it MPSK/MQAM-DCSK. In such a system, each symbol $b_i \in \{0, 1, \ldots, M-1\}$ is spread to a DCSK signal which includes one reference-chaotic fragment and one information-bearing fragment. Particularly, the information-bearing fragment is sent by modulating the reference-chaotic fragment with an M-ary symbol, and the modulation is realized by either MPSK or MQAM. *Note that* as in the conventional DCSK system, the reference-chaotic fragment sent in the PSK/QAM-based M-ary DCSK system is the chaotic sequence produced directly by a chaos generator.

According to the MPSK/MQAM-DCSK signal, two novel transceiver structures, i.e., the multicode transmission with equal-gain combiner (MT-EGC) and stochastic-gradient method for beamformer update (SG-BF), have also been conceived in [49]. Both transceiver schemes can effectively accomplish spatial diversity in MIMO multipath Rayleigh fading channels without the need of having CSI at either transmitter or receiver.

More specifically, the MT-EGC scheme employs a distinct chaotic sequence at each transmit antenna to spread the same symbol prior to transmission, and then uses EGC to process all the weighted signals output from the DC detectors corresponding to the receive antennas. On the other hand, the SG-BF scheme employs a single chaotic sequence and makes use of the adaptive transmit and receive beamforming at the transmitter and receiver, respectively. Here, the beamformers are updated via an SG algorithm, which is detailed in Sect. III-B of [49]. Between the two proposed strategies, the SG-BF scheme significantly outperforms the MT-EGC scheme and obtains a remarkable performance gain in MIMO multipath Rayleigh fading environments.

Remarks:

- The major difference between the PSK/QAM-based M-ary DCSK system and the conventional (binary) DCSK system lies in the structure of the information-bearing fragment.
- Given a fixed modulation order $M \geq 4$ (i.e., a fixed data rate R_{T}), the PSK/QAM-based M-ary DCSK scheme benefits from higher spectral efficiency but suffers from weaker error performance as compared to the WC-based M-ary DCSK scheme.

3) QCSK-based M-ary DCSK: The QCSK (i.e., 4-ary DCSK) can also be generalized to form a QCSK-based M-ary DCSK [34], [72]. Exploiting the idea of MPSK, a constellation of chaotic signals can be generated and hence the information-bearing sequence can be expressed as $\mathbf{d}_i = e^{\sqrt{-1}(2b_i\pi/M)} = \cos(2b_i\pi/M) + \sqrt{-1}\sin(2b_i\pi/M)$, where $\sqrt{-1}$ denotes the *imaginary* unit of a complex number and $b_i \in \{0, 1, \ldots, M-1\}$. This type of DCSK is termed as M-ary Q-DCSK1. Similarly, another type of QCSK-based M-ary DCSK, i.e., M-ary Q-DCSK2, can be formulated by designing a chaotic version of QAM if the constellation signals are not restricted to lie on the unit circle.

Example 3: We now compare the error performance of the M-ary Q-DCSK1 system and MPSK-DCSK system over a multipath Nakagami fading channel. Fig. 10 reveals that the M-ary Q-DCSK1 system outperforms the MPSK-DCSK system for a given value of M. They agree well with the results in an AWGN channel [72]. For example, the former one has a gain of about 1 dB with respect to the latter one in the high SNR region when $M = 4$. However, the performance gap between the two systems is reduced as M increases. *It should be noted that* the performance gain of M-ary Q-DCSK1 system is obtained at a price of a slightly higher complexity.

D. CS-DCSK

1) Principles of CS-DCSK: In most conventional DCSK-based systems, there exist RF delay lines at the receiver terminal. These RF delay lines are extremely difficult to be realized using complementary metal oxide semiconductor

(CMOS) technology. To avoid the use of RF delay lines and to facilitate more practical applications, CS-DCSK system has been proposed by Xu *et al*. [35].

In the conventional DCSK systems, the reference-chaotic sequence and information-bearing sequence are transmitted in two different time slots of one bit duration. In CS-DCSK, the aforementioned two sequences are transmitted in the same time slot and are distinguished by using two different row vectors of a WC. Generally speaking, the transmitted signal corresponding to the i-th bit duration is formulated as $\mathbf{s}_{b_i} = [(w_{\mathrm{R},1} + b_i w_{\mathrm{I},1})\mathbf{c}_i, (w_{\mathrm{R},2} + b_i w_{\mathrm{I},2})\mathbf{c}_i, \ldots, (w_{\mathrm{R},M} + b_i w_{\mathrm{I},M})\mathbf{c}_i]$, where $\mathbf{w}_{\mathrm{R}} = [w_{\mathrm{R},1}, w_{\mathrm{R},2}, \ldots, w_{\mathrm{R},M}]$ and $\mathbf{w}_{\mathrm{I}} = [w_{\mathrm{I},1}, w_{\mathrm{I},2}, \ldots, w_{\mathrm{I},M}]$ denote two different row vectors in the M-order WC. Thus, we have $\mathbf{w}_{\mathrm{I}}(\mathbf{w}_{\mathrm{R}})^{\mathrm{T}} = 0$.

In accordance to the feature of CS-DCSK, a flexible demodulator that does not require any RF delay line has been developed in [35]. Referring to the paper, the demodulator consisting of a rectangular function, a WC generator and an integral operator computes a decision metric $\mathcal{E}$ based on the received signal. Finally, the source information is determined based on the value of $\mathcal{E}$. Here, the detailed description of the demodulator in CS-DCSK system is omitted but can be readily found in [35]. Besides the above-mentioned results, the theoretical error performance of CS-DCSK systems over AWGN and multipath Rayleigh fading channels has been analyzed in [35], where such a system to MA scenarios has also been extended. *Note that* the order of the WC exploited to implement a CS-DCSK modulation scheme should be at least equal to 2 (i.e., $M \geq 2$).

For a given value of M, the CS-DCSK system is similar to the WC-based M-ary DCSK system. Nonetheless, several differences exist between these two systems and are listed below.

(1) Both the reference-chaotic sequence and information-bearing sequence are transmitted in the same time slot for CS-DCSK but they are transmitted in M separate time slots for M-ary DCSK. Therefore, CS-DCSK indeed belongs to binary-DCSK-modulation category while M-ary DCSK belongs to multilevel-DCSK-modulation category.
(2) Although both systems possess RF delay lines at the transmitter, there is no RF delay line at the receiver of CS-DCSK system, which is its most distinguished advantage.
(3) The CS-DCSK system can be reduced to a variant of the conventional DCSK system (i.e., 2-ary DCSK system) if $M = 2$.

Example 4: The BER results of the CS-DCSK system and conventional DCSK system over a multipath Nakagami fading channel with fading depth $m = 2$ are plotted in Fig. 11. For the sake of fair comparison, we adopt a 2-order WC to construct the CS-DCSK signal. It can be seen that the CS-DCSK system and conventional DCSK system produce identical error performance. Nevertheless, the former system benefits from the easier receiver implementation because delay lines are not required. These observations validate the advantage of the CS-DCSK system.

As a further discussion, we show the BER results of the CS-DCSK systems over a multipath Nakagami fading channel with different WC orders in Fig. 12, where the global

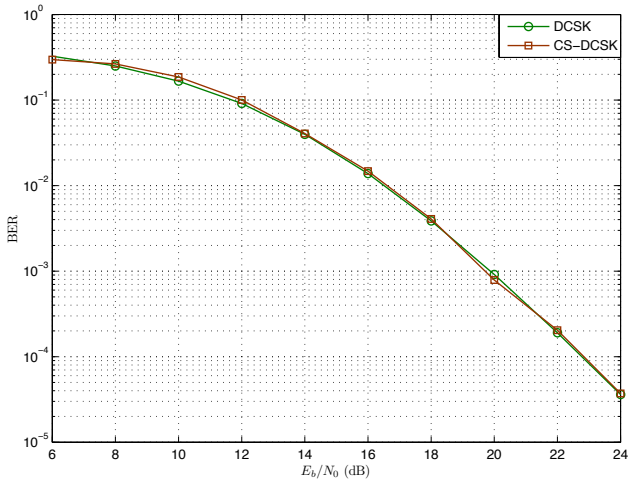

Fig. 11. BER curves of CS-DCSK system and conventional DCSK system over a multipath Nakagami fading channel. The parameters used are $m = 2, L = 2, (\tau_1, \tau_2) = (0, T_s), M = 2,$ and $f = 64$.

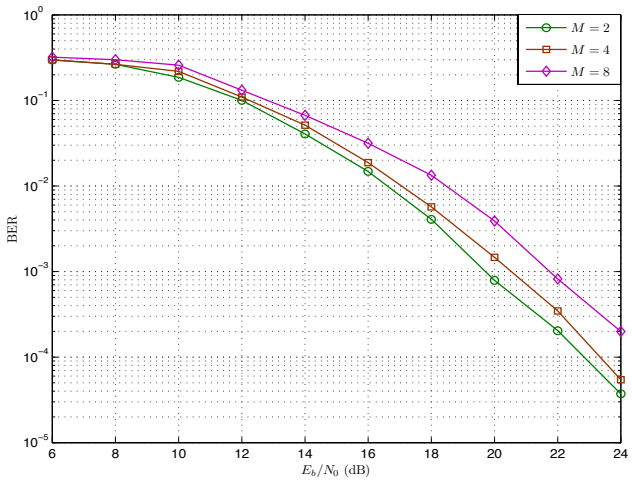

Fig. 12. BER curves of CS-DCSK systems with different WC orders over a Nakagami fading channel. The parameters used are $m = 2, L = 2, (\tau_1, \tau_2) = (0, T_s), M = 2, 4, 8,$ and $2\beta = 128$.

spreading factor 2β is kept constant (i.e., $2\beta = 128$). As can be observed, the system performance is strongly dependent on the order of WC. For a fixed global spreading factor, the system performance deteriorates as M increases. It is because a larger M implies a smaller fragment length ($f = 2\beta/M$), which in turn produces a more severe inter-symbol interference (ISI) [10].

2) HDR-CS-DCSK: As is well known, the orthogonal property of WCs that are used in CS-DCSK systems may be dramatically deteriorated in asynchronous MA situations. Aiming at overcoming this drawback, the authors in [38] have proposed an improved version of CS-DCSK, namely *HDR-CS-DCSK*, which not only can be easily extended to MA scenarios but also can achieve HDR. In HDR-CS-DCSK, chaotic codes (instead of WCs) that possess extremely low auto/cross-correlation are exploited to distinguish the reference sequence from the information-bearing sequence. For every bit in each symbol, the corresponding component information-

[10] It is obvious that a more severe ISI results in worse error performance.

bearing sequence is formed by the multiplication of the reference sequence, a chaotic code, and the bit information. Then the overall information-bearing sequence is computed by summing all component information-bearing sequences.

Inspired by the idea in [35], the authors in [38] have conceived a hardware-friendly detector that does not require any delay lines. They have also proposed an improved framework of HDR-CS-DCSK that can reduce the ISI. The main idea is to form a transmit signal by modulating the information-bearing sequence and reference-chaotic sequence into an *in-phase* signal and *quadrature* signal, respectively. *Note also that* the receiver should be modified accordingly based on the improved modulation scheme.

In addition to the design aspect, the theoretical analyses and simulations have been carried out. The results have demonstrated that HDR-CS-DCSK has more outstanding error performance than CS-DCSK, especially in the low-SNR region.

3) GCS-DCSK: Parallel with the HDR-CS-DCSK, a WC-based generalized CS-DCSK (GCS-DCSK) has been developed to achieve HDR in [112]. The major difference between GCS-DCSK and HDR-CS-DCSK is that the former one uses WCs rather than chaotic codes to isolate the reference-chaotic sequence and information-bearing sequences. Besides, the data rate of GCS-DCSK scheme can be varied in an adaptive manner by adding new or removing some component information-bearing sequences. Yet, as compared to the HDR-CS-DCSK system, the GCS-DCSK system suffers from the drawback of relatively worse auto-/cross-correlation in MA scenarios. *Note that* the authors in [112] have only considered the GCS-DCSK system in an SU scenario but not MA scenario. Thus the application of GCS-DCSK to practical wireless communications is still somewhat limited.

E. DDCSK

1) Principles of DDCSK: The design objective of all the DCSK variants reported previously is to boost the performance of SU-DCSK systems, but little is mentioned about the performance enhancement of MA-DCSK system [109]. In [44], a DDCSK modulation scheme was proposed for MA scenarios.

As in the DCSK system, there is a "reference" sequence and an information-bearing sequence for each information bit in the DDCSK system. DDCSK, however, uses the information-bearing sequence of the previous bit as the "reference" sequence of the current bit. In other words, only the information-bearing sequence is sent for each bit (except the first bit) because the "reference" sequence is already sent in the previous bit duration.

Suppose each frame consists of $N_{\mathrm{F}}+1$ time slots. We let $\mathbf{c}_0$ be an initial reference-chaotic sequence of length f, which is sent in time slot 0. $\mathbf{c}_0$ serves as the reference sequence of the first bit. Then, the information-bearing sequence of the first information bit b_1 is given by $b_1\mathbf{c}_0$ and is sent in time slot 1. Moreover, the information-bearing sequence $\mathbf{c}_1 \triangleq b_1\mathbf{c}_0$ for the first information bit b_1 will serve as the reference sequence for the second information bit b_2. The information-bearing sequence for b_2, which is then given by $\mathbf{c}_2 \triangleq b_2\mathbf{c}_1$, will be sent in time slot 2. In general, $\mathbf{c}_i \triangleq b_i\mathbf{c}_{i-1}$ $(i = 1, 2, \ldots, N_{\mathrm{F}})$ is defined as the information-bearing sequence for the i-th information bit b_i. The sequences sent in one whole frame, which contains $N_{\mathrm{F}}+1$ time slots, are represented by $[\mathbf{c}_0,\ \mathbf{c}_1,\ \mathbf{c}_2, \ldots,\ \mathbf{c}_{N_{\mathrm{F}}}]$. Therefore, $\mathbf{c}_i$ $(i = 1, 2, \ldots, N_{\mathrm{F}}-1)$ transmitted in time slot i is considered as both the information-bearing sequence for b_i and the reference sequence for b_{i+1}. In fact, there are totally N_{F} bits transmitted in each frame and hence we term N_{F} as the frame length.

Based on such a modulation scheme, a new WC-DDCSK system has been further developed for realizing the MA capability and eliminating the IUI. To accommodate $N = 2^n$ users in such a system, an N-order WC (see (2)) has to be constructed and each row vector in the WC is assigned to a user. We denote the k-th row in the WC by $\mathbf{w}_k = [w_{k,1}, w_{k,2}, \ldots, w_{k,N}]$. Furthermore, the k-th user generates an initial chaotic sequence denoted by $\mathbf{c}^k$. Then the reference-chaotic sequence of the k-th user, denoted by $\mathbf{c}_{k,0}$, is written as

$$\mathbf{c}_{k,0} = [w_{k,1}\mathbf{c}^k, w_{k,2}\mathbf{c}^k, \ldots, w_{k,N}\mathbf{c}^k]. \tag{4}$$

Same as the SU system, these reference-chaotic sequences are sent in time slot 0.

The information-bearing sequence $\mathbf{c}_{k,i}$ sent by the k-th user for its i-th bit $b_{k,i}$ is therefore equal to $b_{k,i}\mathbf{c}_{k,i-1}$, i.e., $\mathbf{c}_{k,i} \triangleq b_{k,i}\mathbf{c}_{k,i-1}$ $(i = 1, 2, \ldots, N_{\mathrm{F}})$. As a result, the overall sequence sent by the k-th user can be written as

$$[\mathbf{c}_{k,0}, \mathbf{c}_{k,1}, \mathbf{c}_{k,2}, \ldots, \mathbf{c}_{k,N_{\mathrm{F}}}]. \tag{5}$$

At the receiver terminal, the GML detector can also be used to estimate the source information with minor modification [44].

Remarks:

- Based on the aforementioned way of constructing the reference-chaotic sequences, sequences sent by different users are orthogonal to one another.
- As compared with the conventional MA-DCSK system, the DDCSK system provides better anti-ISI capability over multipath fading channels because of its enhanced auto/cross-correlation property.
- Another advantage of the new DDCSK system is an improvement in the data-rate and energy efficiency. In particular, the improvement will be more remarkable as the number of users (i.e., N) increases.
- Nonetheless, the DDCSK system costs some additional complexity in hardware implementation. Also, the anti-intercept capability of the DDCSK system becomes weaker since all the N_{F} information-bearing sequences in a data frame share the same initial reference-chaotic sequence (i.e., all the N_{F} information-bearing sequences are related to the initial reference-chaotic sequence).
- The DDCSK can also be treated as a variant of differential phase shift keying (DPSK) [121] in the SS domain. Thereby, it is applicable for the SU scenario to achieve a desirable performance gain [32], [44][11].

Example 5: We consider a two-user MA-DDCSK system over a multipath Nakagami fading channel. Then the

[11]Precisely speaking, the IFM-DCSK [32] in Sect. III-A2 is the simplified version of DDCSK in the SU scenario.

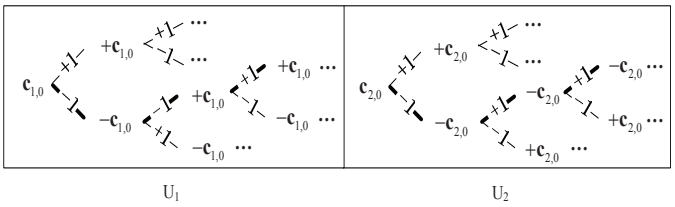

Fig. 13. An example of the transmission strategy in a two-user MA-DDCSK system.

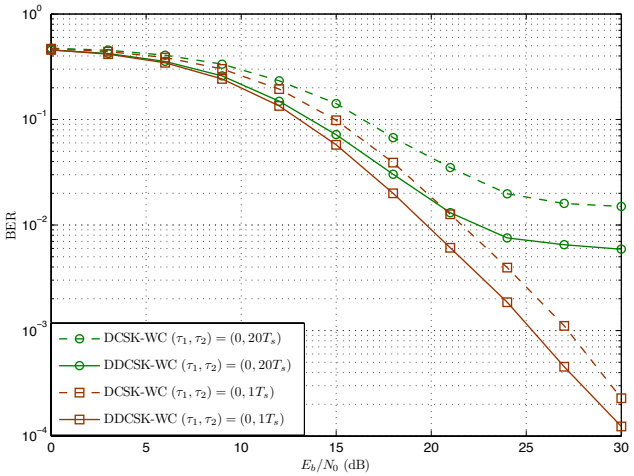

Fig. 14. BER curves of the MA-DDCSK system and MA-DCSK system over a multipath Nakagami fading channel. The parameters used are $N = 2, m = 1, L = 2, (\tau_1, \tau_2) = (0, T_s)$ and $(0, 20T_s), f = 40,$ and $N_{\mathrm{F}} = 1000$.

reference-chaotic sequences of the two users are given by $\mathbf{c}_{1,0} = [w_{1,1}\mathbf{c}^1, w_{1,2}\mathbf{c}^1]$ and $\mathbf{c}_{2,0} = [w_{2,1}\mathbf{c}^2, w_{2,2}\mathbf{c}^2]$, respectively. Fig. 13 shows an example of the transmission strategy of such a system with $N_{\mathrm{F}} = 3$. Assuming that the data sent by U_1 and U_2 are $\{-1 \ -1 \ +1\}$ and $\{-1 \ +1 \ +1\}$, respectively, the overall DDCSK sequence of U_1 is yielded as $[\mathbf{c}_{1,0} \ -\mathbf{c}_{1,0} \ +\mathbf{c}_{1,0} \ +\mathbf{c}_{1,0}]$, while that of U_2 is yielded as $[\mathbf{c}_{2,0} \ -\mathbf{c}_{2,0} \ -\mathbf{c}_{2,0} \ -\mathbf{c}_{2,0}]$. Consequently, these two DDCSK sequences can be produced via the *bold* paths in Fig. 13.

It is insightful to compare the error performance of the MA-DDCSK system and MA-DCSK system over a Nakagami fading channel with different time delays in Fig. 14. Referring to this figure, the MA-DDCSK system performs better than the MA-DCSK system. Moreover, the performance gain is higher in the case of a larger delay spread. For example, at a BER of 10^{-2}, MA-DDCSK accomplishes a gain of about 2 dB with respect to MA-DCSK for the case of $(\tau_1, \tau_2) = (0, T_s)$, while the gain is increased to 7.5 dB for the case of $(\tau_1, \tau_2) = (0, 20T_s)$. The results indicate that the MA-DDCSK system possesses a stronger robustness against ISI compared with MA-DCSK.

2) Improved Detector: Recently, Chen *et al*. [45] have further proposed a novel detector at the receiver of the MA-DDCSK system. The detector adopts the Bahl-Cocke-Jelinek-Raviv (BCJR) decoding algorithm [122], in which soft information rather than hard information is measured. The newly proposed detector exploits the characteristics of chaotic modulation and WC-DDCSK transmission strategy more effectively, and gives rise to a remarkable performance improvement. As shown by the analytical and simulated results in [45], the BCJR-based detector achieves a gain of about 2 dB over the conventional GML detector used in [44] over a multipath Nakagami fading channel with parameters $N = 2, m = 1, (\tau_1, \tau_2) = (0, T_s), f = 64,$ and $N_{\mathrm{F}} = 1000$. Since neither complicated channel estimation nor rake reception is required in the improved WC-DDCSK system, the receiver should be more suitable for energy-constrained wireless networks such as low-power and low-complexity WPANs and WSNs.

F. MC-DCSK

As a critical technique in wireless communication systems, multi-carrier transmission has several attractive advantages as compared with the single-carrier one. For example, the multi-carrier systems, such as OFDM, not only achieve higher spectral efficiency but also possess stronger resistance to frequency-selective fading [123]. Although there exist a significant amount of research achievements on MC-SS systems, e.g., MC-CDMA system [124], [125], the design and analysis of MC-DCSK systems are relatively unexplored. For this reason, an MC-DCSK system have been introduced in [37] to strike a balance among error performance, energy efficiency and data rate. We now elaborate a little further on the architecture of the MC-DCSK system.

1) Transmitter: Assume that a data frame of length N_{F} is to be transmitted in the MC-DCSK system. The data frame is first divided into Q parallel bitstreams $\{\mathbf{b}_q\}$ via a serial-to-parallel converter (SPC), where $\mathbf{b}_q = (b_{q,1}, b_{q,2}, \ldots, b_{q,\Lambda-1})$, $q = 1, 2, \ldots, Q$, and $b_{q,i}$ denotes the i-th bit of the q-th bitstream. We then have $N_{\mathrm{F}} = Q(\Lambda - 1)$. In the MC-DCSK system, a chaotic signal $c_q(t)$ is produced to modulate the first subcarrier in order to form the reference-chaotic signal. Moreover, the product of $c_q(t)$ and $b_{q,i}$ modulates the remaining $\Lambda - 1$ subcarriers, forming the information-bearing signal. Then, the transmitted signal corresponding to the q-th bitstream can be written as

$$s_q(t) = c_q(t)\cos(2\pi f_0 t + \varphi_0) + \sum_{i=1}^{\Lambda-1} b_{q,i} c_q(t)\cos(2\pi f_i t + \varphi_i), \tag{6}$$

where φ_i $(i = 0, 1, \ldots, \Lambda - 1)$ represents the phase angle defined in the i-th carrier modulation process.

For MC-DCSK, all the modulated subcarriers should be mutually orthogonal during one transmission period. To accomplish this goal, one can set the baseband frequency as $f_i = f_{\mathrm{p}} + (i + 1)/T_s$, where f_{p} is defined as the fundamental subcarrier frequency. *Note also that* the minimum guard interval between the neighbouring subcarriers is equal to $T_{\Delta,s} = (1 + \zeta)T_s$, where $0 < \zeta \leq 1$ [125].

2) Receiver: Through a multipath fading channel, the received signals can be detected by means of a robust receiver without using any delay line. The structure and detecting principle of the receiver in MC-DCSK system are detailed in [37]. As observed, the receiver includes Λ multiplication operators, Λ matched filters, two matrix memories, a sign function, and a parallel-to-serial converter (PSC). In the following, we will examine the error performance of such a novel system to validate its superiority.

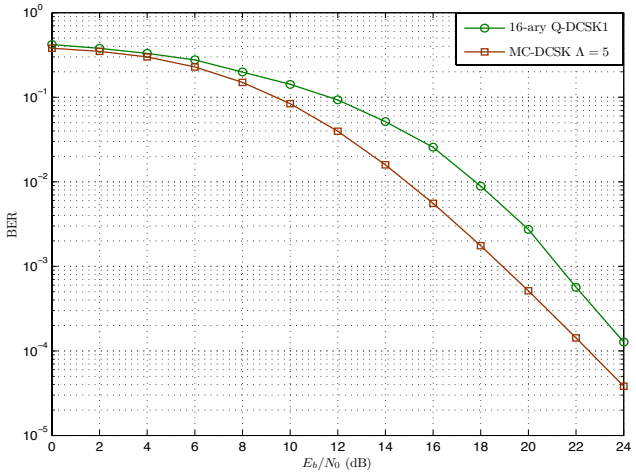

Fig. 15. BER curves of the MC-DCSK system and M-ary Q-DCSK1 system over a multipath Nakagami fading channel. The parameters used are $m = 2, L = 2, (\tau_1, \tau_2) = (0, T_s), f = 40, R_{\rm T} = 4,$ and $N_{\rm F} = 1000$.

Example 6: We consider the MC-DCSK and M-ary Q-DCSK1 systems and assume that the data rate is kept as $R_{\rm T} = 4$ bits/transmission. In other words, $\Lambda = 5$ for the case of MC-DCSK while $M = 16$ for the case of M-ary Q-DCSK1. Fig. 15 presents the BER results of these two multilevel DCSK systems over a Nakagami fading channel. One can observe that the MC-DCSK system is superior to the M-ary DCSK1 system. For example, at a BER of 10^{-3}, the MC-DCSK accomplishes a gain of about 2 dB over the M-ary DCSK1 system. Furthermore, we have performed simulations for other data rates and have found that a larger gain can be obtained if $R_{\rm T}$ increases.

Based on the work of [37], MC-DCSK system has been extended to cover MA scenarios [43]. It has been shown that the transmission scheme exhibits excellent error performance as well as desirable energy efficiency.

IV. Design of DCSK-Related Systems

In the past two decades, a variety of techniques, e.g., multi-antenna techniques, CC, ECC, ARQ, network coding, OFDM, etc., have been proposed to improve the performance of wireless communication systems. In this section, we elaborate the joint design of DCSK and such popular techniques in the current literature. To simplify the descriptions, we refer to all the above-mentioned systems as DCSK-related systems[12].

A. SIMO FM-DCSK System

In wireless communications, fading is a major factor that deteriorates the quality of signal reception. Among all the methodologies proposed to mitigate the effect of fading, the multi-antenna technologies are of particular interest because they can provide significant spatial-diversity/multiplexing improvement [126], [127].

To the best of our knowledge, [85] is the first related work that considers DCSK systems in the context of spatial diversity. In that paper, the authors have proposed a novel SIMO architecture with one transmit antenna and $N_{\rm R}$ receive antennas for FM-DCSK, namely an SIMO FM-DCSK system, to achieve both high data rate and good error performance.

In such a system, Λ information bits are firstly converted from serial to parallel, constructing a bitstream (i.e., $\mathbf{b} = \{b_1, b_2, \ldots, b_\Lambda\}$), where $b_i \in \{+1, -1\}$ is the i-th bit in $\mathbf{b}$. Subsequently, the component bits are modulated by FM-DCSK and distinguished by an M-order WC, where $M = 2\Lambda$. These Λ DCSK signals are then transmitted through the same antenna simultaneously in one transmission period. With this method, the system can accomplish a data rate of $R_{\rm T} = \Lambda$ bits/transmission without increasing the bandwidth. The *multibit* transmission mechanisms used here and in MC-DCSK system (see Sect. III-F) differ in the sense that the former one exploits a code-division multiplexing but the latter one exploits the frequency-division multiplexing. For example, in an SIMO FM-DCSK system with $\Lambda = 2$, a 4-order WC $\mathbf{W}_4$ is utilized by the transmitter, where

$$\mathbf{W}_4 = \begin{bmatrix} +1 & +1 & +1 & +1 \\ +1 & -1 & +1 & -1 \\ +1 & +1 & -1 & -1 \\ +1 & -1 & -1 & +1 \end{bmatrix} \begin{matrix} \} b_1 \\ \\ \} b_2 \end{matrix}. \tag{7}$$

As can be seen, the first two row vectors in $\mathbf{W}_4$ are allocated to b_1 while the remaining two row vectors are allocated to b_2. Likewise, a GML detector can be exploited to demodulate the corresponding signal after passing through the multipath fading channels [85].

As pointed out in [85], the SIMO FM-DCSK scheme outperforms the DS vertical-Bell-Labs-layered-space-time (VBLAST) scheme [128] in the high-SNR region over a multipath Nakagami-fading channel with fading depth $m = 1$. More importantly, in contrast to the DS-VBLAST system which is equipped with a complicated Rake receiver, the SIMO FM-DCSK system allows a much lower receiver implementation complexity. As a result, the *multibit-based* SIMO FM-DCSK system has potential to become a competitive solution for low-complexity and low-cost wireless links.

B. STBC-DCSK Systems

It has been shown theoretically [129], [130] that MIMO technology can dramatically improve the error performance of wireless communication systems. As one of the simplest realizations of an MIMO configuration, STBC was proposed in 1998 [131]. Among all the STBCs [131], [132], Alamouti STBC stands out as one of the most classical schemes as well as a milestone in the development of STBC research. It is because such a transmit approach can achieve remarkable spatial-diversity gain with extremely easy implementation. In 2009, an Alamouti STBC-DCSK system has been designed and analyzed so as to explore the feasibility of employing chaotic communications in MIMO fading channels [50], [51]. Apart from the Alamouti-based architecture, Chen *et al.* [52] have developed a novel analog STBC scheme for the DCSK system to achieve spatial diversity without requiring the knowledge of CSI.

[12]Precisely, a DCSK-related system is defined as a communication system that combines the DCSK-based modulation with other critical wireless-communication techniques.

TABLE III
THE COMPONENT DCSK SEQUENCES IN THE STBC-DCSK TRANSMIT MATRIX $\mathbf{S}$ IN EACH TRANSMISSION PERIOD.

i	1	2
$\mathbf{s}_{1,i}$	$[\mathbf{c}_0\ b_1\mathbf{c}_0]$	$[\mathbf{c}_0\ -b_2\mathbf{c}_0]$
$\mathbf{s}_{2,i}$	$[\mathbf{c}_0\ b_2\mathbf{c}_0]$	$[\mathbf{c}_0\ b_1\mathbf{c}_0]$

TABLE IV
THE RECEIVER SIGNALS AT TWO RECEIVE ANTENNAS IN EACH TRANSMISSION PERIOD.

i	1	2
$\mathbf{r}_{1,i}$	$\alpha_{1,1}\mathbf{s}_{1,1}+\alpha_{2,1}\mathbf{s}_{2,1}+\mathbf{n}_{1,1}$	$\alpha_{1,1}\mathbf{s}_{1,2}+\alpha_{2,1}\mathbf{s}_{2,2}+\mathbf{n}_{1,2}$
$\mathbf{r}_{2,i}$	$\alpha_{1,2}\mathbf{s}_{1,1}+\alpha_{2,2}\mathbf{s}_{2,1}+\mathbf{n}_{2,1}$	$\alpha_{1,2}\mathbf{s}_{1,2}+\alpha_{2,2}\mathbf{s}_{2,2}+\mathbf{n}_{2,2}$

1) Alamouti STBC-DCSK System: As in [50], [51], we consider an *Alamouti* STBC-DCSK system with two transmit antennas and two receive antennas (i.e., $N_{\mathrm{T}}=N_{\mathrm{R}}=2$). The information bits $\{b_i\}$ are firstly mapped onto an $N_{\mathrm{T}}\times T_{\mathrm{b}}$ Alamouti STBC transmit matrix $\mathbf{B}$, where N_{T} and T_{b} denote the numbers of transmit antennas and time slots in a block code, respectively [131][13].

Assuming that $N_{\mathrm{T}}=2$ and $T_{\mathrm{b}}=2$, $\mathbf{B}$ can be written as

$$\mathbf{B}=[\mathbf{b}_1\ \mathbf{b}_2]=\begin{bmatrix} b_1 & -b_2 \\ b_2 & b_1 \end{bmatrix}. \tag{8}$$

Then, in the i-th time slot ($i=1,2$), the two bits in each column vector, i.e., $\mathbf{b}_i$, are respectively exploited by two parallel DCSK modulators to construct two DCSK sequences (i.e., $\mathbf{s}_{1,i}$ and $\mathbf{s}_{2,i}$). The constructed sequences $\mathbf{s}_{1,i}$ and $\mathbf{s}_{2,i}$ are further passed to two different transmit antennas. Consequently, the corresponding STBC-DCSK transmit matrix of $\mathbf{B}$ is resulted as

$$\mathbf{S}=\begin{bmatrix} \mathbf{s}_{\mathrm{T_{x1}}} \\ \mathbf{s}_{\mathrm{T_{x2}}} \end{bmatrix}=\begin{bmatrix} \mathbf{s}_{1,1} & \mathbf{s}_{1,2} \\ \mathbf{s}_{2,1} & \mathbf{s}_{2,2} \end{bmatrix}, \tag{9}$$

where the row vector $\mathbf{s}_{\mathrm{T_{x}}k}$ denotes the transmitted signal from the k-th transmit antenna (i.e., $\mathrm{T_{x}}k$) in one transmission period. According to such a generating rule, the component DCSK sequences in the STBC-DCSK transmit matrix $\mathbf{S}$ are illustrated in Table III, where $\mathbf{c}_0$ denotes the reference-chaotic sequence in the overall transmission period.

The STBC-DCSK signal is then passed through four independent fading channels constructed by four different transmit-receive antenna pairs based on the transmission strategy of Alamouti STBC system [50]. Let $\alpha_{k,\omega}$ be the channel fading gain of the $\mathrm{T_{x}}k\rightarrow\mathrm{R_{x}}\omega$ link; and $\mathbf{n}_{\omega,i}$ be the Gaussian noise vector at the ω-th receiver in the i-th time slot. The signals at the two receive antennas, i.e., $\mathbf{R}_{\mathrm{R_{x1}}}=[\mathbf{r}_{1,1}\ \mathbf{r}_{1,2}]$ and $\mathbf{R}_{\mathrm{R_{x2}}}=[\mathbf{r}_{2,1}\ \mathbf{r}_{2,2}]$, are given in Table IV. The two received signals will be processed by two parallel correlators (i.e, the configuration of a correlator can be referred to Fig. 2) and subsequently be decoded by an STBC decoder. *It is worth noting that* the principle of the well-known Alamouti STBC decoder has been described in [50], [131].

Based on the framework in [50], Kaddoum *et al*. [51] have further carried out theoretical analyses of such an STBC system over an AWGN channel. The analytical method used in [51] is quite different from the conventional GA-based method [28], and it can provide an exact estimation on the error performance even for a very small fragment length. Noticeably, the Alamouti STBC-DCSK system accomplishes a desirable performance gain over the SISO-DCSK one in both AWGN and fading channels [50], [51].

2) Analog STBC-DCSK System: In 2013, Chen *et al*. [52] have proposed another type of STBC-DCSK system. Distinguished from the Alamouti STBC-DCSK system, the new framework combines DCSK with STBC and utilizes the good cross-correlation property of chaotic sequences. This type of STBC-DCSK system is referred to as *analog* STBC-DCSK system because chaotic signals having good analog feature are directly passed into an STBC encoder for further processing [52]. We now provide more details on the design principles of the analog STBC-DCSK system with N_{T} transmit antenna and one receive antenna.

(1) Transmitter: In the analog STBC-DCSK scheme, there are totally $2N_{\mathrm{T}}$ time slots in each transmission period. At the beginning, a date frame $\{b_i\}$ is pre-processed by an SPC to obtain several bitstreams, each of length $2N_{\mathrm{T}}$. In each transmission period, the bits involved in one bitstream are firstly passed into $2N_{\mathrm{T}}$ parallel DCSK modulators in order to generate $2N_{\mathrm{T}}$ different DCSK signals simultaneously. The i-th DCSK signal $\mathbf{s}_i$ comprises a reference-chaotic sequence $\mathbf{c}_i$ and an information-bearing sequence $\mathbf{c}'_i=b_i\mathbf{c}_i$, and is denoted by $\mathbf{s}_i=[\mathbf{c}_i,\ \mathbf{c}'_i]$. In the sequel, the generated $2N_{\mathrm{T}}$ DCSK signals are fed into an STBC encoder.

As seen from Fig. 3, two chaotic sequences representing different bits possess low cross-correlation. They become near-orthogonal if the fragment length is long enough. In consequence, in order to alleviate the ITI at the receiver terminal, chaotic fragments generated by the same DCSK modulator cannot be sent by different transmit antennas in the same time slot. For instance, if $\mathbf{c}_i$ is being transmitted by the first transmit antenna, other transmit antennas must not send $\mathbf{c}_i$ or $\mathbf{c}'_i$ in the same time slot. Based on such a transmission strategy, all the reference-chaotic sequences and information-bearing sequences are re-ordered and then assigned to the transmit antennas in each time slot by the STBC encoder. In general, the major goal of such a transmission strategy is to effectively suppress the ITI by employing the inherently good cross-correlation property of chaotic signals.

For a given transmission period, we define $\mathbf{x}_{k,i}$ as the (re-ordered) signal sent by the k-th transmitted antenna in the i-th ($i=1,2,\ldots,2N_T$) time slot. Assuming a multipath fading channel, the received signal in the i-th time slot can be described as

$$\mathbf{r}_i=\sum_{k=1}^{N_{\mathrm{T}}}\sum_{l=1}^{L}\left[\alpha_{k,l}\mathbf{x}_{k,i,\langle\tau_{k,l}\rangle}\right]+\mathbf{n}_i, \tag{10}$$

where $\alpha_{k,l}$ is the fading gain of the l-th path in a multipath Nakagami fading channel formed by the k-th transmit-receive antenna pair (recall that there are N_T transmit antennas and one receive antenna); $\tau_{k,l}$ is the corresponding time delay; $\mathbf{x}_{k,i,\langle\tau_{k,l}\rangle}$ denotes the signal $\mathbf{x}_{k,i}$ delayed by $\tau_{k,l}$; L is the total number of paths; and $\mathbf{n}_i$ is the overall Gaussian noise vector

[13]Here, T_{b} is also defined as the number of time slots in each transmission period.

TABLE V
THE RE-ORDERED CHAOTIC SIGNALS SENT BY THE k-TH ($k = 1, 2$) TRANSMIT ANTENNA IN EACH TRANSMISSION PERIOD IN THE ANALOG STBC-DCSK SYSTEM WHERE $N_{\mathrm{T}} = 2$.

Transmission period i	1	2	3	4
$\mathbf{x}_{1,i}$	$[\mathbf{c}_1\ \mathbf{c}'_1]$	$[\mathbf{c}_2\ \mathbf{c}_4]$	$[\mathbf{c}'_2\ \mathbf{c}'_4]$	$[\mathbf{c}_3\ \mathbf{c}'_3]$
$\mathbf{x}_{2,i}$	$[\mathbf{c}_2\ \mathbf{c}_4]$	$[\mathbf{c}_1\ \mathbf{c}'_1]$	$[\mathbf{c}_3\ \mathbf{c}'_3]$	$[\mathbf{c}'_2\ \mathbf{c}'_4]$

TABLE VI
THE OUTPUT SIGNAL z_i OF THE i-TH DEMODULATOR IN THE ANALOG STBC-DCSK SYSTEM WHERE $N_{\mathrm{T}} = 2$.

i	Output signal z_i
1	$\mathbf{r}_{1,1} \cdot (\mathbf{r}_{1,2})^{\mathrm{T}} + \mathbf{r}_{2,1} \cdot (\mathbf{r}_{2,2})^{\mathrm{T}}$
2	$\mathbf{r}_{1,1} \cdot (\mathbf{r}_{4,1})^{\mathrm{T}} + \mathbf{r}_{2,1} \cdot (\mathbf{r}_{3,1})^{\mathrm{T}}$
3	$\mathbf{r}_{3,1} \cdot (\mathbf{r}_{3,2})^{\mathrm{T}} + \mathbf{r}_{4,1} \cdot (\mathbf{r}_{4,2})^{\mathrm{T}}$
4	$\mathbf{r}_{1,2} \cdot (\mathbf{r}_{4,2})^{\mathrm{T}} + \mathbf{r}_{2,2} \cdot (\mathbf{r}_{3,2})^{\mathrm{T}}$

at the received antenna. By letting $\mathbf{r}_{i,1}$ and $\mathbf{r}_{i,2}$ represent the first and second fragments of $\mathbf{r}_i$ respectively, we readily have $\mathbf{r}_i = [\mathbf{r}_{i,1}\ \mathbf{r}_{i,2}]$.

(2) Receiver: With an aim to successfully retrieving the original information, a modified DC demodulator has been designed to deal with the received signals in a linear manner, as detailed in [52]. It is obvious that the modified DC demodulator does not require the CSI knowledge and thus leads to an easy implementation. To have more insight, an example of the transceiver design of the analog STBC system with two transmit antennas is given as follows.

Example 7: According to the design principle reported above, there exist several different realizations of the transmitted signals that can achieve the objective of avoiding ITI. We consider an analog STBC system with $N_{\mathrm{T}} = 2$. One realization for the re-ordered chaotic signals sent by the k-th ($k = 1, 2$) transmit antenna in each transmission period is shown in Table V. Referring to this table, in the first time slot, $\mathbf{x}_{1,1} = [\mathbf{c}_1\ \mathbf{c}'_1]$ is sent by the first transmit antenna while $\mathbf{x}_{2,1} = [\mathbf{c}_2\ \mathbf{c}_4]$ is sent by the second antenna.

Based on the transmitted signals in Table V, four DC demodulators are designed respectively for the sake of estimating the four source information bits in each bitstream. The output signal of i-th ($i = 1, 2, 3, 4$) demodulator, i.e, z_i, can be characterized by Table VI. It can be seen that each demodulator involves two correlators and one summation operator. Finally, the information bit b_i is decided as $+1$ if $z_i \geq 0$, and -1 otherwise.

Remarks:

- In the two STBC-DCSK systems, a normalized factor $1/\sqrt{N_{\mathrm{T}}}$ should be used to scale each transmitted DCSK sequence $\mathbf{s}_{k,i}$ in order to keep the transmit energy per bit E_b constant.
- The channel between each transmit-receive antenna pair is assumed to be block-faded, i.e., the fading gain is invariant over at least one transmission period.
- The CSI is required in the demodulating process of the Alamouti STBC-DCSK system, while it is unnecessary for the analog STBC-DCSK system.
- The two STBC-DCSK systems outperform the conventional SISO-DCSK system because of the spatial-diversity gain [50], [52]. According to the results shown in a forthcoming figure (i.e., Fig. 17), the Alamouti STBC-DCSK system possesses better error performance than the analog STBC-DCSK system at the expense of a relatively higher implementation complexity.

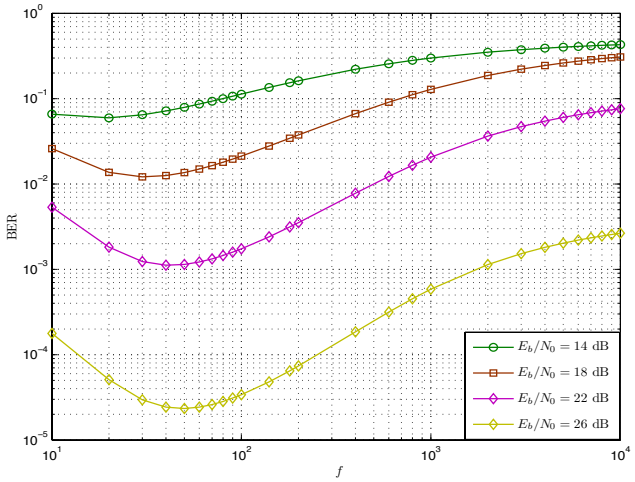

Fig. 16. Theoretical BER curves versus the fragment length f in an analog STBC-DCSK system over a one-ray Nakagami fading channel. The parameters used are $N_{\mathrm{T}} = 2, N_{\mathrm{R}} = 1, m = 2,$ and $L = 1$.

Example 8: Fig. 16 plots the theoretical BER performance[14] versus the chaotic fragment length f in an analog STBC-DCSK system over a one-ray Nakagami fading channel with fading depth $m = 2$. For a fixed value of E_b/N_0, the results reveal that the error performance is firstly improved and then deteriorated as f increases. Accordingly, there exists an optimal fragment length (i.e., f_{th}) which results in the lowest BER value.

In addition, we compare the error performance of the two different STBC-DCSK systems over a one-ray Nakagami fading channel (as in [50]) and present the results in Fig. 17. The parameters used here are the same as those listed in Fig. 16, except that $f = 128$. Results suggest that the Alamouti STBC-DCSK scheme outperforms the analog STBC-DCSK scheme for the range of E_b/N_0 under study and achieves a gain of about 4 dB in the high-SNR region. Nevertheless, the analog STBC-DCSK scheme does not need to estimate the CSI at the receiver and strikes a good tradeoff between error performance and system complexity. Owing to such an advantage, the analog STBC-DCSK system is more suitable for low-cost and low-complexity wireless applications such as UWB communications.

C. MIMO Relay DCSK-CD System

The works in [50]–[52] suggest that MIMO and STBC can offer nice ways to achieve both transmit and receive diversities for DCSK. However, the transmitters may not be able to support multiple antennas in reality due to the constraints of size, complexity, power, cost, etc. Alternatively, a relay channel, which is composed of a source (i.e., a user U), a

[14]The theoretical BER expression of the analog STBC-DCSK system over a multipath Nakagami fading channel can be easily derived in a similar way as in [52].

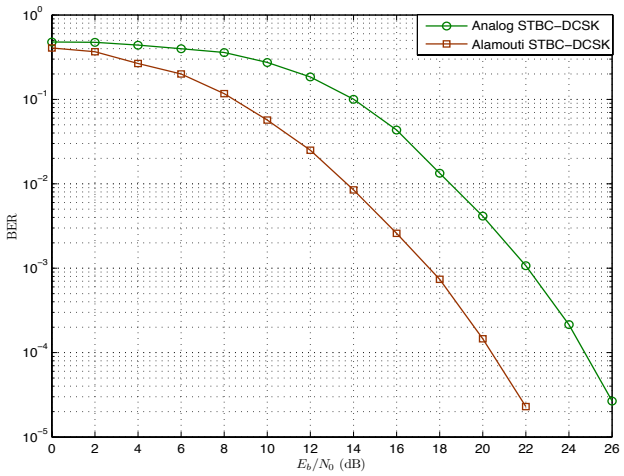

Fig. 17. Simulated BER curves of the analog STBC-DCSK system and Alamouti STBC-DCSK system over a one-ray Nakagami fading channel. The parameters used are $N_{\mathrm{T}} = 2, N_{\mathrm{R}} = 1, m = 2, L = 1,$ and $f = 128$.

relay (R) and a destination (D), can attain spatial diversity with a relatively lower complexity [133]. A relay channel is also considered as the most elementary configuration of CC systems. Actually, a base station equipped with multiple antennas can serve as either a relay or a destination in practical wireless communication systems. Motivated by this idea, some researchers have applied the MIMO technique to relay networks to realize diversity gain, which is termed as cooperative diversity (CD) [134]. Moreover, the information-theoretical advancement of MIMO relay systems, e.g., capacity analysis, has been carried out in [135], [136].

In 2013, the first MIMO relay DCSK-CD system has been developed by Fang *et. al.* [53]. Unlike the conventional MIMO-DCSK and STBC-DCSK systems, the MIMO relay DCSK-CD system installs multi-antenna at the relay and destination instead of the transmitter. In that piece of work, the authors not only have conceived the corresponding transmission mechanism for a two-user scenario, but also have conducted a theoretical analysis of its system performance. Especially, both the exact BER in integral expression and the approximate BER in closed-form expression have been derived and verified. Here, we concisely portray the transmission mechanism of the system.

Consider an MA-MIMO-DCSK relay system that consists of two users ($\{\mathsf{U}_1, \mathsf{U}_2\}$), one relay (R) and one destination (D), where both R and D possess multiple antennas but U_k $(k = 1, 2)$ possesses only one antenna. In such a system, each transmission period is divided to two phases, i.e., broadcast phase and cooperative phase. Each user can send its DCSK signal to D with the help of the multi-antenna R.

In the first phase, both U_1 and U_2 broadcast their corresponding WC-based DCSK signals to R and D. In the second phase, R cooperates with U_1 and U_2 to forward their signals to D. In particular, D will store all the received signals and decode them only at the end of each transmission period. In consequence, for a given user U_k $(k = 1, 2)$, each antenna of D receives "corrupted" DCSK signals from both links $\mathsf{U}_k \rightarrow \mathsf{D}$ and $\mathsf{R} \rightarrow \mathsf{D}$, and hence may obtain a spatial-diversity gain.

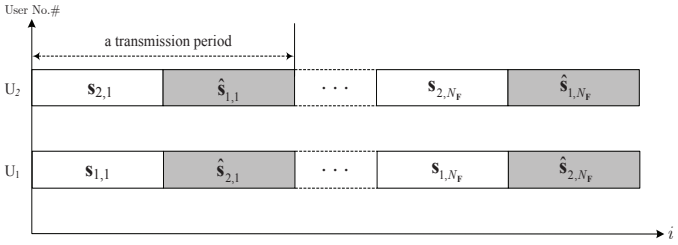

Fig. 18. Cooperative mechanism of the two-user DCSK-CC system.

In practical applications, the error performance of the MIMO relay is determined by the detailed relaying strategy or protocol. In [53], both the error-free (EF) protocol and decode-and-forward (DF) protocol are thoroughly investigated over a multipath Nakagami fading channel. The results have indicated that the EF protocol only achieves a gain of 0.5 dB over the DF protocol when $m = 1$, and the gain will be reduced as the fading depth m increases. In this paper, we assume that the DF protocol is adopted by all the relay-based systems as it not only exhibits good performance close to EF protocol, but also can be easily implemented [136]. *It is worth noting that* the MIMO relay DCSK-CD system can be promptly extended to the scenarios of more users (i.e., $N > 2$).

D. DCSK-CC System

CC between two single-antenna users can also yield spatial diversity and increase the system reliability dramatically [54], [55]. Recently, Xu *et. al.* [17], [56] have incorporated the CC technique into a two-user MA-DCSK system and form a two-user DCSK-CC system.

In the two-user DCSK-CC system, each transmission period is split into two phases, i.e., broadcasting phase and cooperative phase. In the first phase, the user U_k $(k = 1, 2)$ broadcasts its own DCSK signal to the other terminal, i.e., U'_k $(k' \neq k)$, and destination D. In the second phase, U'_k $(k' \neq k)$ may help U_k to forward its message to D, depending on whether U'_k can successfully decode the message from U_k or not.

Specifically, U'_k decodes the received signal from the other user at the end of the first phase. If the signal can be decoded successfully, the retrieved information will be re-modulated using DCSK and forwarded to D in the second phase[15]; otherwise, U'_k remains idling in the second phase. Benefiting from the cooperative diversity, the DCSK-CC system can get remarkable performance improvement with respect to the DCSK-NC system at the price of sacrificing some throughput. Based on the above-mentioned principle, the cooperative mechanism of the two-user DCSK-CC system can be readily described in Fig. 18, where N_{F} denotes the frame length.

Furthermore, DCSK-CC system has been generalized to the scenario of $N > 2$ users by Fang *et. al.* [57], in which a primary user transmits its signal to D with the assistance from the other users (i.e., relays). In that work, the theoretical BER and throughput of the MA-DCSK-CC system have also been

[15]In the i-th transmission period, we define $\mathbf{s}_{k,i}$ as the transmitted signal of U_k and $\hat{\mathbf{s}}_{k,i}$ as its corresponding reconstructed signal at the cooperator U'_k by using DF protocol.

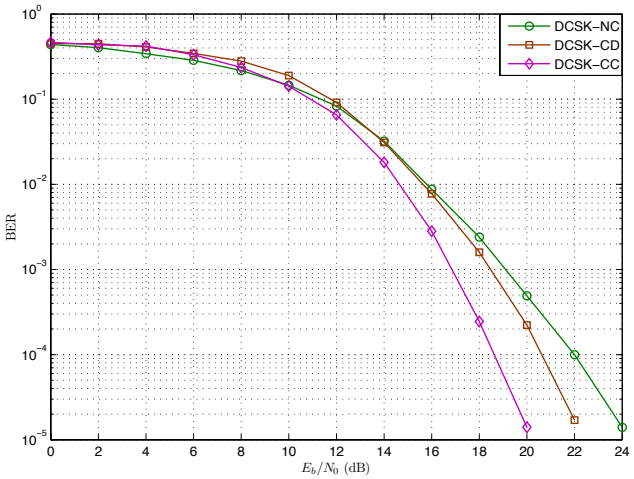

Fig. 19. BER curves of the MA-DCSK-NC system, MIMO relay DCSK-CD system, and DCSK-CC system. The parameters used are $N = 4, m = 2, L = 2, (\tau_1, \tau_2) = (0, T_s), d_{\rm SD} : d_{SR} : d_{RD} = 1 : 1 : 1, f = 32,$ and $N_{\rm F} = 1$.

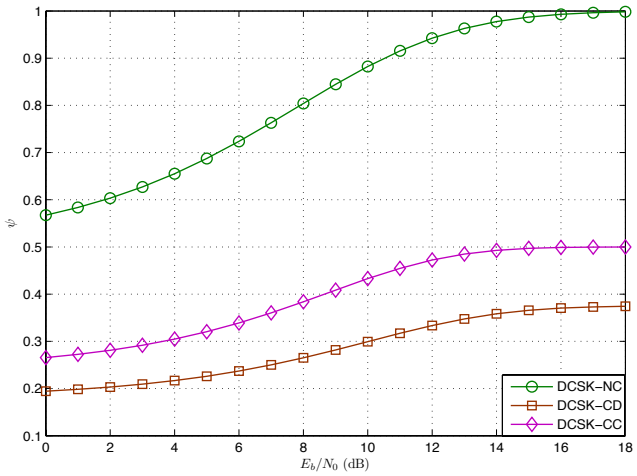

Fig. 20. Normalized throughput of the MA-DCSK-NC system, MIMO relay DCSK-CD system, and DCSK-CC system. The parameters used are $N = 4, m = 2, L = 2, (\tau_1, \tau_2) = (0, T_s), d_{\rm SD} : d_{SR} : d_{RD} = 1 : 1 : 1, f = 32,$ and $N_{\rm F} = 1$.

thoroughly analyzed. For more comprehensive knowledge of the DCSK-CC system, readers can refer to the related literature [17], [56], [57].

Remark: As indicated in [53], [57], the MIMO relay DCSK-CD system is superior to the DCSK-CC system in terms of BER performance in a two-user scenario. However, the former one becomes inferior to the latter one when the number of users $N > 2$.

Example 9: Fig. 19 presents the BER curves of a four-user DCSK-CC system over a multipath Nakagami fading channel[16]. Meanwhile, the results for MA-DCSK-NC system and MIMO relay DCSK-CD system are plotted in the same figure to provide benchmarks for performance evaluation. One can easily observe that DCSK-CC system and DCSK-CD system possess the best and moderate error performance, respectively, while DCSK-NC system has the worst error performance, especially in the high-SNR region.

As a further study, we plot the normalized throughput[17] of the above three DCSK-related systems in Fig. 20. It can be seen that the throughput of the DCSK-NC system is about two times that of DCSK-CC system. It is because the transmission periods of the DCSK-NC and DCSK-CC systems contain one and two time slots, respectively. In general, the DCSK-related systems, from the highest to the lowest throughput, are ranked in the following order: i) DCSK-NC system, ii) DCSK-CC system, and iii) MIMO relay DCSK-CD system.

E. LDPC-Coded DCSK System

In addition to utilizing spatial-diversity strategies, DCSK can be beneficially combined with error-control mechanisms, such as ECCs [59], [60] and ARQ/CARQ [61], [62], to enhance the performance. As an excellent type of ECC, LDPC codes have been investigated over the past twenty years. It has been shown that LDPC codes can achieve near-capacity error performance under different channel conditions and can hence remarkably improve the quality of wireless transmissions [59]. Inspired by this superiority, Wang *et al*. [63] have firstly examined the interplay between LDPC codes and FM-DCSK modulation over an AWGN channel, and have found that an LDPC-coded FM-DCSK system can accomplish a gain of more than 8 dB over the counterpart without ECC at a given BER.

Deferring from conventional (FM) DCSK systems, LDPC-coded DCSK system encodes the source information initially using an LDPC code prior to being modulated by a DCSK modulator. After passing through a wireless channel, the received signal is detected by a concatenated decoder that consists of a DC demodulator and an LDPC decoder [63]. In particular, effective iterative decoding algorithms, e.g., belief-propagation (BP) decoding algorithm, can be employed to implement the LDPC decoder according to the sparse property of LDPC codes [137].

Apart from the works of [63], [85], a simpler coded SIMO FM-DCSK system, namely *product-accumulate (PA)-coded SIMO FM-DCSK system*, was proposed by Zhang *et al*. [64] in 2008. PA codes not only enable good error performance close to channel capacity but also possess regular structures leading to low encoding and decoding complexities [138]. The results in [64] have suggested that the PA-coded SIMO FM-DCSK framework outperforms the LDPC-coded one over an AWGN channel for moderate/large frame length with a relatively lower implementation complexity.

Besides the transmitter design, the receiver design is another challenge for LDPC-coded DCSK systems. As is well known, turbo equalization (i.e., turbo decoder) is particularly suitable for improving the performance of serial concatenated systems, in which an inner detector (or demapper) and an

[16]For the sake of fair comparison, we assume that i) the number of terminals in all three DCSK-related systems are kept constant; ii) all terminals are equipped with only one antenna; and iii) the distance of the link $\mathsf{A} \to \mathsf{B}$ is set to $d_{\rm AB} = 1$, where $\mathsf{A} \in \{\mathsf{U}_k\ (k = 1, 2, \ldots), \mathsf{R}\}$ and $\mathsf{B} \in \{\mathsf{R}, \mathsf{D}\}$. To satisfy condition i), in the MA-MIMO relay DCSK system, one user should serve as the relay and the remaining three users are to transmit messages to the destination.

[17]In this paper, the normalized throughput is defined as the ratio between successfully received frames/transmission period and transmitted frames/transmission period, as in [54], [55].

outer decoder[18] are involved [139]. The main idea of turbo equalization is to exchange the soft *extrinsic* information iteratively between detector and decoder so as to enhance the reliability of the output signal of the receiver [140]. Inspired by this idea, Lyu *et al*. [68], [69] have developed a turbo-like IR for WC-based M-ary DCSK systems. In this M-ary DCSK system [69], the source information is encoded, mapped, and modulated before being transmitted to the destination D. More specifically, the encoder, mapper, and modulator are respectively implemented by a binary protograph code [60], natural mapping [141], and M-ary DCSK.

In fact, natural mapping is one popular technique used for bit-to-symbol conversion (BSC) because it can be easily realized. For instance, given a fixed protograph codeword $\mathcal{V} = (v_1, v_2, \ldots, v_{N_\mathrm{F}})$ with $v_j \in \{0, 1\}$ and $j = 1, 2, \ldots, N_\mathrm{F}$, the N_F bits are split into Q serial bitstreams of length Λ where $\Lambda = \log_2 M$, and $Q = \lceil N_\mathrm{F}/\Lambda \rceil$ with $\lceil x \rceil$ denoting the ceiling of x. Based on the natural-mapping rule, the q-th $(q = 1, 2, \ldots, Q)$ bitstream $(v_{\Lambda(q-1)+1}, v_{\Lambda(q-1)+2}, \ldots, v_{\Lambda q})$ is converted to a symbol $b_q \in \{0, 1, \ldots, M-1\}$, expressed as $b_q = \sum_{i=0}^{\Lambda-1} v_{\Lambda(q-1)+i+1} \cdot 2^i$. For simplicity of exposition, we further define $\vartheta_{q,i} = v_{\Lambda(q-1)+i}$ such that $(\vartheta_{q,1}, \vartheta_{q,2}, \ldots, \vartheta_{q,\Lambda}) \triangleq (v_{\Lambda(q-1)+1}, v_{\Lambda(q-1)+2}, \ldots, v_{\Lambda q})$.

At the receiver terminal, the concatenation of the natural demapper and BP decoder forms a turbo-like decoder, in which the natural demapper and BP decoder are treated as the inner demapper component and outer decoder component, respectively. Firstly, the received signal is demodulated by a GML detector in order to get the weighted-energy vector $\mathbf{\Xi}_q = (\mathcal{E}_{\hat{b}_q=0}, \mathcal{E}_{\hat{b}_q=1}, \ldots, \mathcal{E}_{\hat{b}_q=M-1})$. In particular, $\mathbf{\Xi}_q$ is predefined as the initial information of the turbo-like decoder and will be sufficiently utilized in the overall decoding procedure.

To elaborate a little further on the turbo-like decoder, we firstly introduce the following definition.

Definition 1. The *a-posteriori* log-likelihood-ratio (LLR) of a coded bit $\vartheta_{q,i}$ output from the inner demapper is defined as $L_{\mathrm{app,I}}(\vartheta_{q,i}) = \ln[\Pr(\vartheta_{q,i} = 1|\mathbf{\Xi}_q)/\Pr(\vartheta_{q,i} = 0|\mathbf{\Xi}_q)]$, where $\Pr(\cdot)$ denotes the probability function.

It should be noted that the definition of LLR utilized here is similar to that in [142]. Based on such a definition, one can immediately obtain six other types of LLRs.

- $L_{\mathrm{A,IO}}(\vartheta_{q,j})$ denotes the input *a-priori* LLR of the coded bit $\vartheta_{q,j}$ at the inner demapper.
- $L_{\mathrm{A,OI}}(v_j)$ denotes the input *a-priori* LLR of the coded bit v_j at the outer decoder.
- $L_{\mathrm{E,IO}}(\vartheta_{q,j})$ denotes the output *extrinsic* LLR of the coded bit $\vartheta_{q,j}$ of the inner demapper;
- $L_{\mathrm{E,OI}}(v_j)$ denotes the output *extrinsic* LLR of the coded bit v_j of the outer decoder.
- $L_{\mathrm{app,I}}(\vartheta_{q,j})$ denotes the *a-posteriori* of $\vartheta_{q,j}$ output from the inner demapper.
- $L_{\mathrm{app,O}}(v_j)$ denotes the *a-posteriori* of v_j output from the outer decoder.

The block diagram of the turbo-like decoder in the M-ary DCSK system is depicted in Fig. 21. As seen from this figure, the extrinsic LLR of the demapper is served as the a-priori LLR of the decoder in each iteration, and vice versa, i.e., $L_{\mathrm{A,OI}}(v_j) = L_{\mathrm{E,IO}}(v_j)$ and $L_{\mathrm{A,IO}}(v_j) = L_{\mathrm{E,OI}}(v_j)$.

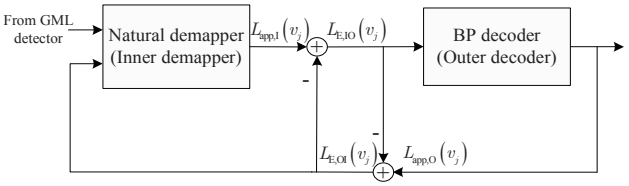

Fig. 21. Block diagram of the turbo-like decoder in the LDPC-coded M-ary DCSK system.

At the beginning, We initialize all the LLRs to zero and the probabilities $\Pr(b_q = \mu)$ to $1/M$ for all $q = 1, 2, \ldots, Q$ and $\mu = 0, 1, 2, \ldots, M-1$. Then, the turbo-like decoding algorithm can be summarized as follows.

Calculating the extrinsic LLR output from the inner demapper

1) For $q = 1, 2, \ldots, Q$, if the knowledge of the CSI is available at the receiver, the conditional probability density function (PDF) $f(\mathbf{\Xi}_q|b_q = \mu)$ can be evaluated based on the initial information $\mathbf{\Xi}_q$ and Bessel function, as shown in [69, eq.(19)][19].
2) For $q = 1, 2, \ldots, Q$, if $\exists v_j \in \mathcal{V}$ and $L_{\mathrm{A,IO}}(v_j) \neq 0$, update the probability $\Pr(b_q = \mu)$ exploiting the sequence $\{L_{\mathrm{A,IO}}(v_j)\}$ and the natural-mapping rule; otherwise, $\Pr(b_q = \mu) = 1/M$.
3) For $q = 1, 2, \ldots, Q$ and $i = 1, 2, \ldots, \Lambda$, calculate the a-posteriori LLR $L_{\mathrm{app,I}}(\vartheta_{q,i})$ by substituting $f(\mathbf{\Xi}_q|b_q = \mu)$ and $\Pr(b_q = \mu)$ into [69, eq.(20)], which is derived with the help of the natural-demapping rule.
4) The Q resultant LLR sequences $\{L_{\mathrm{app,I}}(\vartheta_{1,i})\}$, $\{L_{\mathrm{app,I}}(\vartheta_{2,i})\}, \ldots, \{L_{\mathrm{app,I}}(\vartheta_{Q,i})\}$ are then processed via a symbol-to-bit converter (SBC) in order to construct a serial sequence $\{L_{\mathrm{app,I}}(v_j)\}$ of length N_F, which corresponds to the protograph codeword $\mathcal{V}$.
5) For $j = 1, 2, \ldots, N_\mathrm{F}$, compute the output extrinsic LLR as $L_{\mathrm{E,IO}}(v_j) = L_{\mathrm{app,I}}(v_j) - L_{\mathrm{A,IO}}(v_j) = L_{\mathrm{app,I}}(v_j) - L_{\mathrm{E,OI}}(v_j)$. *Note also that* $\{L_{\mathrm{E,IO}}(v_j)\}$ will be considered as the input a-priori LLR $\{L_{\mathrm{A,OI}}(v_j)\}$ for the outer decoder.

Calculating the extrinsic LLR output from the outer decoder

Based on the sequence $\{L_{\mathrm{A,OI}}(v_j)\}$, one can perform the well-known BP decoder on the Tanner graph of the protograph code $\mathcal{V}$ [60], [137] and hence calculate the corresponding a-posteriori LLR sequence $L_{\mathrm{app,O}}(v_j)$. Also, the output extrinsic LLR sequence $\{L_{\mathrm{E,OI}}(v_j)\}$ can be easily measured through a similar way as the aforementioned Step 5). Finally, the sequence $\{L_{\mathrm{A,IO}}(v_j)\}$ (i.e., where $L_{\mathrm{A,IO}}(v_j) = L_{\mathrm{E,OI}}(v_j)$) is fed back to the inner demapper for the next turbo iteration. *Note also the followings*.

- Although the locally generated M-ary DCSK signal is very difficult to be recovered at the receiver terminal in practice,

[18]*Note that* the detector/decoder in the turbo equalization should be soft-input soft-output.

[19]In the case of no CSI being available, the conditional PDF $f(\mathbf{\Xi}_q|b_q = \mu)$ can be estimated via a GA-based method, as detailed in Sect. III-B of [69].

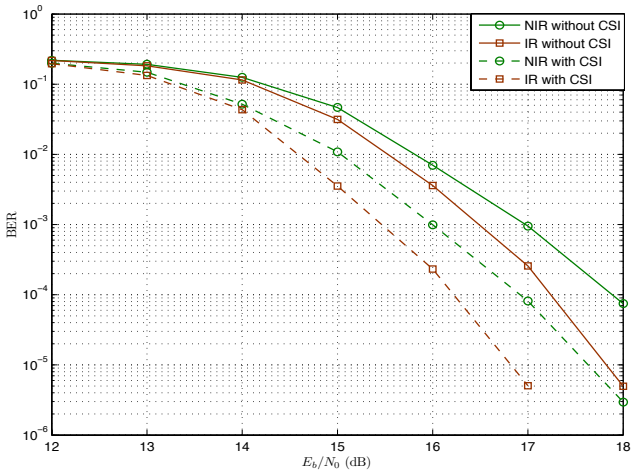

Fig. 22. BER curves of the LDPC-coded M-ary DCSK systems with and without a turbo-like IR over a one-ray Nakagami fading channel. The parameters used are $m = 1$, $f = 20$, and $M = 4$. The rate-$1/2$ accumulate-repeat-by-4-jagged-accumulate (AR4JA) code of length $N_{\rm F} = 500$ is assumed as the channel code.

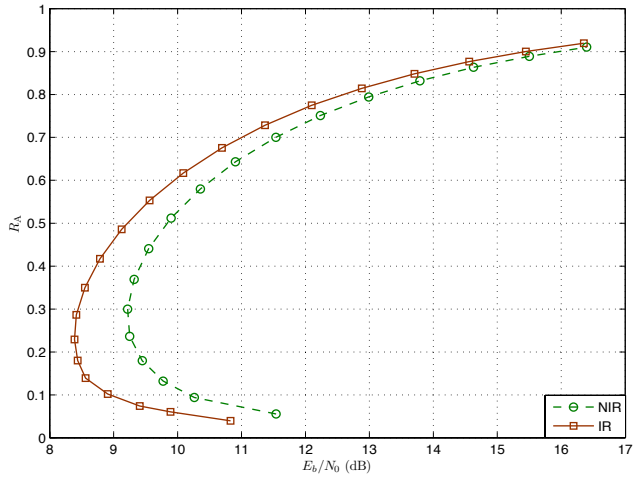

Fig. 23. Achievable rates of the coded M-ary DCSK systems with and without a turbo-like IR over a one-ray Nakagami fading channel. The parameters used are $m = 1$, $f = 20$, and $M = 4$.

it makes sense to evaluate the conditional PDF $f(\mathbf{\Xi}_q|b_q = \mu)$ for facilitating the realization of the turbo-like decoder.

- In each turbo iteration, both $\Pr(b_q = \mu)$ and $\{L_{\rm E,IO}(v_j)\}$ are updated in the inner demapper using the input a-priori LLR sequence $\{L_{\rm A,IO}(v_j)\}$; while $\{L_{\rm E,OI}(v_j)\}$ is updated in the outer decoder using the input a-priori LLR sequence $\{L_{\rm A,OI}(v_j)\}$. Based on such a decoding mechanism, the a-posteriori LLR sequence will converge to an exact value after a sufficient number of iterations, and leads to a performance enhancement.

Example 10: Fig. 22 shows the BER curves of the LDPC-coded M-ary DCSK systems with and without a turbo-like IR over a one-ray Nakagami fading channel with $m = 1$. Here, the rate-$1/2$ accumulate-repeat-by-4-jagged-accumulate (AR4JA) code [140] of length $N_{\rm F} = 500$ is adopted as the channel code. As can be seen from this figure, the IR scheme outperforms the non-IR (NIR) scheme irrespective of the CSI knowledge. As an example, under the scenario with full CSI, the IR scheme achieves a gain of 0.75 dB as compared with the NIR scheme at a BER of 5×10^{-6}. The results indicate the desirable superiority of the turbo-like decoder. Moreover, it is obvious that the error performance when no CSI is available is inferior to that when full CSI is accessible.

Fig. 23 further shows the achievable rate (i.e., $R_{\rm A}$) of the coded M-ary DCSK systems with and without IR over a one-ray Nakagami fading channel, where all parameters used are the same as those listed in Fig. 22[20]. For simplicity, only the case with full CSI is considered here. Similar to Fig. 22, for a given $R_{\rm A}$, the required E_b/N_0 of IR scheme is smaller than that of the NIR scheme. More importantly, there exists a minimum E_b/N_0 (i.e., $(E_b/N_0)_{\min}$), above which reliable transmission can be accomplished when the frame length approaches infinity and the code rate $R \leq R_{\rm A,min}$. Accordingly, the resultant $R_{\rm A,min}$ corresponding to $(E_b/N_0)_{\min}$ is considered as the optimum achievable rate for realizing reliable communications. The above observations are mainly attributed to the nonlinear property of the non-coherent DCSK-related system, which can also be found in other nonlinear communication systems, such as the non-coherent frequency-shift-keying (FSK) systems [144], [145].

Remark: The achievable rate is dependent on the type of receiver, but independent of the particular coding scheme (i.e., the type of code).

F. DCSK-ARQ/CARQ System

As another promising error-control mechanism, ARQ is of great usefulness to enhance the error performance and system throughput, and thus has been widely exploited by a significant amount of wireless communication systems and standards, such as Long Term Evolution (LTE) in 4G wireless communication systems [61], [146]. The basic idea of such a technique is to request the data-link layer of the transmitter to retransmit packets (i.e., data frames) that have not been correctly decoded by the receiver. In recent years, CARQ has emerged as a more attractive error-control method because it enables the advantages of both CC and ARQ [62].

In 2015, the DCSK-ARQ and DCSK-CARQ systems, which are respectively formulated via incorporating novel ARQ and CARQ schemes into the conventional DCSK-NC system, were proposed and analyzed by Fang *et al*. [18]. In this subsection, we will outline the transceiver design of DCSK-CARQ system, while the principle of the DCSK-ARQ system can be referred to [18].

1) Transmission mechanism: Consider a DCSK-CARQ system that contains one user U, $N-1$ relays (i.e, $\mathbf{R} = \{\mathsf{R}_1, \mathsf{R}_2, \ldots, \mathsf{R}_{N-1}\}$), and one destination D[21]. Each transmission period is divided into $\mathcal{Z}+1$ phases, i.e., one transmission phase and $\mathcal{Z}$ retransmission phases, where $\mathcal{Z}$ should be no larger than the maximum number of retransmissions $\mathcal{Z}_{\max}$ (i.e., $0 < \mathcal{Z} \leq \mathcal{Z}_{\max}$). The transmission mechanism of such

[20]For a given E_b/N_0, the achievable rate $R_{\rm A}$ of a system (i.e., the cutoff rate) is defined as the maximum code rate that can achieve reliable transmissions [143]. In other words, $R_{\rm A}$ is the fundamental upper-limit on the code rate of any coding scheme. In [69], the authors have performed the achievable-rate analysis to validate the turbo-like IR design.

[21]In this subsection, N is defined as the total number of users and relays.

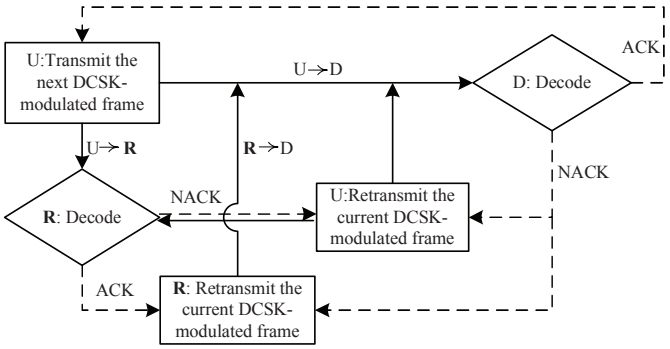

Fig. 24. Transmission mechanism of the DCSK-CARQ system, where the transmission channels and the feedback channels are denoted by solid lines and dashed lines, respectively.

a DCSK-CARQ system is illustrated in Fig. 24. Referring to this figure, the detailed CARQ-based transmission mechanism can be described as below.

(1) Initialize the number of retransmissions to zero, i.e., $z_{\mathrm{RE}} = 0$.
(2) U launches one new transmission by broadcasting a (DCSK-modulated) frame to the other terminals (i.e, $\mathbf{R}$ and D) in the first phase. Afterwards, $\mathbf{R}$ and D try to decode the signal and generate the corresponding feedback messages, i.e., acknowledgement/negative-acknowledgement (ACK/NACK). We further denote the set of relays that make successful decoding (i.e., generate ACKs) and its complementary set (i.e., generate NACKs) by $\mathbf{R}_{\mathrm{A}}$ and $\overline{\mathbf{R}}_{\mathrm{A}} = \mathbf{R} \setminus \mathbf{R}_{\mathrm{A}}$, respectively.
(3) If D correctly decodes the current frame, it sends an ACK to U and go to Step (2); otherwise, go to Step (4).
(4) D sets $z_{\mathrm{RE}} = z_{\mathrm{RE}} + 1$. If the maximum number of retransmissions has been performed, i.e., $z_{\mathrm{RE}} > \mathcal{Z}_{\max}$, terminate the retransmission and go to Step (1).
(5) D stores a copy of the currently received signal and sends a NACK via EF feedback channels[22] to both U and $\mathbf{R}$ for requesting a retransmission.
(6) After receiving the NACK from D, relays in $\mathbf{R}_{\mathrm{A}}$ retransmit the current frame to D in the next phase if $\mathbf{R}_{\mathrm{A}} \neq \varnothing$; otherwise, all the relays in $\overline{\mathbf{R}}_{\mathrm{A}}$ store a copy of the currently received signal and send NACKs to U. We respectively denote the former and latter events by $\mathbf{\Theta} = \mathbf{1}$ and $\mathbf{\Theta} = \mathbf{2}$.
(7) If $\mathbf{\Theta} = \mathbf{1}$, D adopts the maximum-ratio combiner (MRC) [147] to process the currently received signal as well as the previously stored signals, and then employs the GML to estimate the source frame. If $\mathbf{\Theta} = \mathbf{2}$, U rebroadcasts the current frame to $\mathbf{R}$ and D in the next phase; and both $\mathbf{R}$ and D exploit the MRC and GML to combine and decode their corresponding received signals, respectively. Finally, go to Step (3).

2) Modified receiver: According to such a transmission mechanism, a modified receiver architecture, which is utilized by both $\mathbf{R}$ and D, has been proposed in [18]. The block diagram of the proposed receiver is shown in Fig. 25. One can observe that the receiver considers both the characteristics of DCSK signals and CARQ protocol and thus can obtain better performance in contrast to the conventional GML receiver.

[22]It is assumed that all feedback channels used for transmitting the ACK/NACK message are EF in this paper. This assumption is commonly used in the literature [61], [62], because the feedback message can be protected by ECCs to achieve reliable transmission in practical applications.

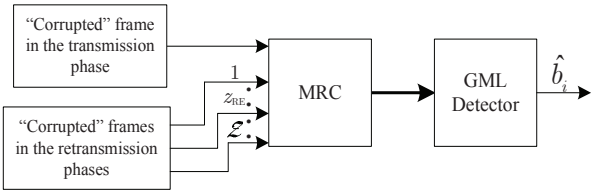

Fig. 25. Block diagram of the modified receiver in the DCSK-CARQ system.

Remarks:

- For the sake of reducing the retransmission delay, $\mathcal{Z}_{\max}$ should be set to a sufficiently small positive integer, e.g., $0 < \mathcal{Z}_{\max} < 5$.
- In [18], it is assumed that the received signals are processed by an MRC prior to being detected. Although the MRC can achieve a high diversity gain, a channel-estimation module should be added in the corresponding system to get the CSI, which is one drawback of such a combining scheme. Alternatively, EGC can be exploited because it not only exhibits desirable performance, but requires no knowledge of CSI as well [148].

Example 11: The frame-error-rate (FER) results of DCSK-NC system, DCSK-ARQ system, DCSK-CC system, and DCSK-CARQ system over a multipath Nakagami fading channel are depicted in Fig. 26. To simplify the comparison, only synchronous systems are considered here. As shown, DCSK-ARQ system and DCSK-CARQ system, which make use of retransmission mechanisms, are respectively superior to their corresponding counterparts (i.e., DCSK-NC system and DCSK-CC system). Especially, the DCSK-CARQ system is the best-performing one among the four systems while the DCSK-NC system is the worst-performing. The normalized-throughput results in Fig. 27 further validate the excellent performance of DCSK-CARQ system. It has also been shown in [18] that the error performance of DCSK-ARQ/CARQ system does not vary much even if the synchronization among different users is not perfectly achieved.

G. Network-Coded DCSK Systems

Reliable and efficient transmission is one of the ultimate objectives of designing modern wireless communication systems. As a powerful solution to improve the transmission efficiency of cooperative networks, network coding was proposed by Li *et al.* in the early 21st century [149]. Typically, a network coding system consists of two users (i.e., U_1 and U_2) and one relay (R), by which a two-way relay channel is constructed. In such a channel, both users exchange information with each other with the assistance from R. There are three classical types of network coding schemes, i.e., straightforward network coding (SNC) [150], physical-layer network coding (PNC) [151], and analog network coding (ANC) [152].

Initially, the SNC that requires three time slots to complete one transmission has been proposed, and it attains a throughput

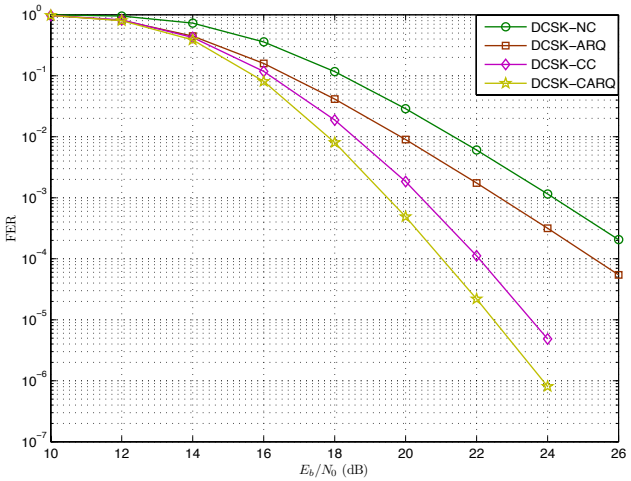

Fig. 26. FER results of DCSK-NC system, DCSK-ARQ system, DCSK-CC system, and DCSK-CARQ system over a multipath Nakagami fading channel. The parameters used are $N = 2, m = 2, L = 2, (\tau_1, \tau_2) = (0, T_s), f = 64, N_{\rm F} = 32,$ and $\mathcal{Z}_{\max} = 1$.

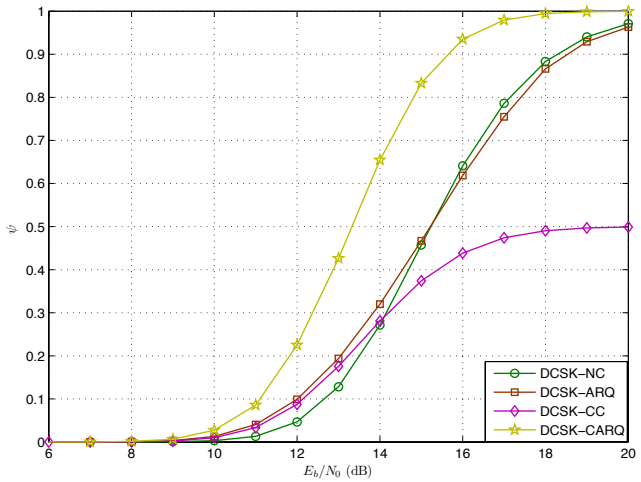

Fig. 27. Normalized throughput of DCSK-NC system, DCSK-ARQ system, DCSK-CC system, and DCSK-CARQ system over a multipath Nakagami fading channel. The parameters used are $N = 2, m = 2, L = 2, (\tau_1, \tau_2) = (0, T_s), f = 64, N_{\rm F} = 32,$ and $\mathcal{Z}_{\max} = 1$.

improvement over the conventional transmission scheme that needs four time slots to do so [150]. In 2006, Zhang *et al*. [151] have found that the concept of network coding can be applied at the physical layer, referred to as PNC, so as to achieve further improvement in throughput. In particular, there are only two time slots in each transmission period for PNC. To be specific, U_1 and U_2 send their corresponding messages to R simultaneously in the first time slot, while R decodes the "corrupted" superimposed signal and broadcasts the retrieved signal to U_1 and U_2 in the second time slot[23]. In PNC, the interfered signal can be perfectly recovered at R by means of appropriate decoding algorithms. Such a superimposed signal is considered as a useful piece of information that helps increasing the reliability of end-to-end transmissions in PNC systems. Inspired by the rate-boosting advantage, more researchers have delved into PNC research. Yet, the encoding algorithm therein is based on the assumption of symbol-level and carrier-phase synchronization, which cannot be easily realized in certain practical applications such as the up-links of wireless communication systems. To overcome this limitation, the concept of ANC, which can be utilized in both synchronous and asynchronous scenarios, has been developed by Katti *et. al*. [152]. Instead of the DF protocol, R always exploits the amplify-and-forward (AF) protocol [153] to deal with the interfered signal in ANC systems.

In [154]–[156], PNC and ANC schemes have been introduced to the conventional SS systems, e.g., CDMA systems, and their error performance and throughput have been thoroughly analyzed over AWGN and multipath fading channels. The results have shown that the network-coded SS system attains a satisfactory enhancement in throughput over the conventional SS systems. In the wake of the success of network-coded CDMA systems, Kaddoum *et al*. [70], [71] have dedicated special attention to applying the PNC and ANC techniques to DCSK-based systems. In these two papers, the authors have also analyzed the theoretical BER performance of PNC-aided DCSK system and ANC-aided DCSK system under the multipath fading condition with delay spread, which has not been considered in [154]–[156].

1) PNC-DCSK system: To the best of our knowledge, the first paper that ventures into the PNC-aided DCSK systems was published in 2015 [70]. However, the authors have found that the PNC-DCSK system cannot produce good error performance in the context of multipath fading because the superimposed signal suffers from a more severe IUI and noise as compared to the case of one-ray fading.

In order to address the interference problem, two improved PNC (IPNC)-DCSK schemes have been developed, which are referred to as *IPNC-DCSK1* and *IPNC-DCSK2*. Aiming to mitigate such interferences, the two users transmit their corresponding messages to R separately by utilizing a time-multiplexing technique (similar to the fundamental SNC system) in the IPNC-DCSK1 system. On the other hand, frequency multiplexing is employed in the IPNC-DCSK2 system to distinguish the two signals that are simultaneously transmitted by the two users. As compared with the conventional PNC-DCSK system, the two IPNC-DCSK systems can effectively mitigate the IUI and thus enhance the error performance via increasing one additional time slot and doubling the bandwidth, respectively.

2) ANC-DCSK system: Apart from the PNC-DCSK system, the ANC-DCSK framework that takes the asynchronous scenario into consideration has been thoroughly discussed in [71]. Unfortunately, the ANC-DCSK system does not show satisfactory performance due to the lack of interference-cancelation algorithms. More importantly, the ANC-DCSK scheme may not be able to support more than two users because of the absence of available MA transmission strategy. As is well known, MA compatibility is one fundamental requirement for the next-generation (5G) wireless communication systems.

To tackle the above-mentioned practical weaknesses, a novel ANC-MC-DCSK architecture that combines ANC scheme with MA-MC-DCSK modulation has been conceived in [71]. In the MA-ANC-MC-DCSK system, N $(N > 2)$ users can be

[23]Such a processing method is also known as the DF protocol.

distinguished in the frequency domain in order to avoid IUI. More precisely, for a given bandwidth, each user is firstly assigned an independent frequency to transmit the reference-chaotic signal, whereas the remaining bandwidth is shared by all users to transmit information-bearing signals. Based on such a frequency-multiplexing method, these users are able to exchange their messages among one another with the help of ANC.

In each transmission period, all the N users send their MC-DCSK signals to R simultaneously in the first time slot. Then, R exploits the ANC operation to process the N received signals. The ANC-coded signal will be directly amplified by R and forwarded to the N users in the second time slot. To improve the decoding performance of MA-ANC-MC-DCSK system over multipath fading channels, a self-interference-mitigation methodology has been proposed in [71]. Using such an algorithm, the ultimate receiver terminal (e.g., U_1) can alleviate its self-interference by subtracting its own "corrupted" signal from the overall received signal[24].

At the end of this subsection, we provide a concise portrayal on the advantages and disadvantages of the aforementioned network-coded DCSK-based systems.

- Among all the two-user network-coded DCSK systems, IPNC-DCSK1/DCSK2 system, PNC-DCSK system, and ANC-DCSK system produce the best, moderate, and the worst error performance, respectively. The main reason is that the first two systems employ DF protocol at R while the last one exploits AF protocol.
- As compared with PNC-based DCSK systems, ANC-MC-DCSK system not only can be applicable to asynchronous scenarios, but also achieve MA capability more easily. However, such advantages are obtained by dramatically increasing the required bandwidth and system complexity.
- PNC-based DCSK systems do not need any CSI at the receiver. However, in ANC-MC-DCSK system, CSI should be estimated in order to execute the self-interference-cancelation algorithm, which is served as an indispensable and intermediate step for achieving good end-to-end performance.

H. Other DCSK-Related Systems

Additionally, some other meritorious DCSK-related systems, such as combined DCSK/CS-DCSK conventional communication systems, MR-based M-ary DCSK system and OFDM-DCSK system, have been proposed, designed and analyzed in recent years [46]–[48], [72], [119]. In [46], [47], the theoretical and simulated error performance of DCSK systems has been intensely studied under the influence of either a coexisting BPSK or DSSS system (i.e., the combined DCSK-BPSK or DCSK-DSSS system) over an AWGN channel. As a further advance, the combined CS-DCSK-BPSK system has been developed in [48], where the corresponding theoretical BER expression has been derived over a multipath Nakagami fading channel. In [72], DCSK modulation has been introduced for multimedia transmissions, in which MR modulation is considered in the M-ary DCSK system and an MR-based M-ary DCSK system is formulated. Moreover, a novel OFDM-DCSK system has been proposed in [119] for the sake of increasing the spectral and energy efficiencies, as well as boosting the MA capability.

In general, all the above-mentioned DCSK-related systems can outperform their corresponding counterparts in certain aspects and have shown sufficient potential in their relevant applications. Due to the space limitation, the design and analysis methodologies of such systems are not elaborated here because they are not the major focus of this paper. Instead, we refer the interested readers to the above-cited articles as well as the references therein for more details. They can serve as a good starting point for further study.

V. Design of FM-DCSK-based UWB Systems

Over the past ten years or so, there has been increasing interest in the research community towards the UWB communication technology [157]–[160]. Robustness against fading together with the potential for low-cost and low-power transceiver design are two main features that make UWB the preferable choice for a range of wireless communication applications, especially for WPAN, WSN, and WBAN. As a TR system, it has been pointed out in [82] that FM-DCSK modulation can capture the entire signal energy without requiring CSI and therefore offers a good candidate for UWB transmission. Motivated by that work, more and more research attention has been moved on to the design and analysis of FM-DCSK UWB systems [79]–[81], [84], [86]–[92], [120]. Furthermore, chaos-based UWB signal has been included in the latest standard for WBAN (i.e., IEEE 802.15.6) recently [96]. In this section, we summarize the research contributions that have been made in FM-DCSK-based UWB systems.

A. Principles of FM-DCSK-UWB System

1) Transceiver structure: Similar to the FM-DCSK systems in Sect. III-A, FM-DCSK UWB systems belong to the category of TR systems. The transmitter configuration of an FM-DCSK UWB system is the same as that shown in Fig. 6, except that the original chaos generator is replaced by a UWB-chaos-pulse generator.

The structure of a generalized (binary) FM-DCSK UWB signal is depicted in Fig. 28. Referring to this figure, each information bit b_i to be transmitted is mapped onto a FM-DCSK UWB signal that includes two ultrashort chaotic pulses (i.e., chips) $g_i(t)$ and $g_i'(t)$. Here, $g_i(t)$ and $g_i'(t) = b_i g_i(t)$ denote the reference FM-chaotic (UWB) pulse and the information-bearing pulse, respectively; T_{c} denotes the duration of each pulse; T represents the duration of the whole signal; T_{g} denotes the guard interval between two component pulses; and T_Δ is the guard gap between two adjacent FM-DCSK UWB signals (i.e., symbols). As a consequence, the overall duration used to transmit a chaotic pulse becomes $T_{\mathrm{D}} = T/M = T_{\mathrm{c}} + T_{\mathrm{g}}$ with $M = 2$ denoting the order of DCSK modulation and $T_{\mathrm{D}} \gg T_{\mathrm{c}}$. Noticeably, T_{D} assures the maximum data

[24]The "corrupted" signal of U_k is defined as components of the overall received signal that include the terms $s_{k,q}(t)$, where $s_{k,q}(t)$ is the transmitted MC-DCSK signal of U_k for the q-th bitstream during the first time slot, as defined in (6).

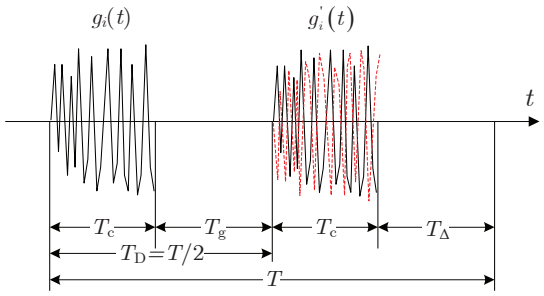

Fig. 28. Structure of a generalized FM-DCSK UWB signal $s(t) = [g_i(t), g_i'(t)]$. The information-bearing chip is denoted by the black-solid line if $b_i = +1$, and is denoted by the red-dotted line otherwise.

rate (i.e., $R_{\rm T} = 1/T$), whereas $T_{\rm g}$ reduces the inter-pulse interference (IPI) caused by multipath transmission as well as the ISI between adjacent signals[25].

At the receiver terminal, the source information bit can be recovered from the received signal by exploiting a DC demodulator because of the special TR signal structure. Normally, the integration interval of the component correlator satisfies $T_{\rm II} = T_{\rm D}$.

2) Critical parameters: In a typical UWB channel model that contains multipath propagation (e.g., multipath fading and delay) [161], the performance of FM-DCSK UWB systems is mainly dependent on the guard interval and integration interval. We now simply analyze the impact of these two key parameters on the system performance.

(1) Guard Interval: As illustrated in [86], the error performance of FM-DCSK UWB systems over a multipath fading channel is dominated by a range of factors such as IPI, ISI, and Gaussian noise. Given a fixed pulse duration $T_{\rm c}$, the data rate $R_{\rm T}$ and integration interval $T_{\rm II}$ are specified by $T_{\rm g}$. As $T_{\rm g}$ increases, IPI and ISI diminish while the noise involved increases. Accordingly, the system performance will undergo an initial-increase-and-then-decrease process. It indicates that there exists an optimal value of $T_{\rm g}$ (denoted as $T_{\rm g,th}$) accomplishing the best error performance.

To be specific, if $T_{\rm g} \in [0, T_{\rm g,th}]$, the error performance improves with $T_{\rm g}$ because the benefit from reducing IPI and ISI can sufficiently offset the increase in noise level. As $T_{\rm g}$ increases beyond $T_{\rm g,th}$ (i.e., $T_{\rm g} \in (T_{\rm g,th}, T_{\rm g,max}]$[26]), the guard interval becomes so large that the extra reduction in IPI and ISI is minimal and negligible. But the noise level is still increasing with $T_{\rm g}$, which results in an overall performance degradation. Besides the error performance, the data rate decreases gradually as $T_{\rm g}$ becomes larger.

(2) Integration Interval: On the other hand, if both $T_{\rm c}$ and $T_{\rm g}$ are kept constant (i.e., $T = 2T_{\rm D} = 2(T_{\rm c} + T_{\rm g})$ is constant), the system performance is solely dependent on the integration interval $T_{\rm II}$ at the receiver. In fact, $T_{\rm II}$ is always set to $T/2$ in the conventional FM-DCSK system over different channel environments [29], [31], whereas it is assumed as $T_{\rm c}$ in the FM-DCSK UWB system over an AWGN channel [82]. When the channel is no longer AWGN, the integration interval can vary within $[T_{\rm c}, T/2]$ under UWB transmission scenarios. So, it needs to explore an optimal balance between the captured signal energy and noise energy.

As an example, the influence of the above two parameters on the performance of FM-DCSK UWB systems has been thoroughly discussed in the context of multipath fading by Min *et al*. [86] so as to verify the feasibility of their potential in IEEE 802.15.4a indoor applications.

[25]In FM-DCSK UWB systems, the guard gap between two adjacent signals is usually set as $T_\Delta = T_{\rm g}$.

[26]For a given FM-DCSK UWB signal duration T, the maximum value of guard interval equals $T_{\rm g,max} = T/2 - T_{\rm c}$.

TABLE VII
LIST OF THE CMS DEFINED IN IEEE 802.15.4A STANDARD.

CM Type	Environment	Bandwidth/GHz
1	Residential LOS	$2 \sim 10$
2	Residential NLOS	$2 \sim 10$
3	Office LOS	$3 \sim 6$
4	Office NLOS	$3 \sim 6$
5	Outdoor LOS	$3 \sim 6$
6	Outdoor NLOS	$3 \sim 6$
7	Industrial LOS	$2 \sim 8$
8	Industrial NLOS	$2 \sim 8$
9	Open-outdoor NLOS	$2 \sim 8$

(3) Channel Model: We restrict ourselves to low-rate and low-power short-range wireless communication applications (e.g., WPANs and WSNs). Having an accurate CM is extremely vital for performance evaluation and design of FM-DCSK UWB systems. Actually, there are two families of CMs that can be used to characterize UWB transmission scenarios, i.e., IEEE 802.15.3a CMs [162] and IEEE 802.15.4a CMs [161], [163].

CMs standardized by IEEE 802.15.4a appear to be a more general and popular family of CMs in UWB research and practice because of the more diverse operating environments and a longer operating range. Therefore, the IEEE 802.15.4a CMs are adopted as the UWB transmission environments in this paper. This family of CMs cover the frequency range from 2 GHz to 10 GHz, and include various testing environments with line-of-sight (LOS) and non-LOS (NLOS) properties. The nine CMs (i.e., CM1 to CM9) defined by IEEE 802.15.4a standard are listed in Table VII. More detailed parameters for each CM in this table can be found in [161]. It has been pointed out in [86], [88] that systems having excellent performance in CM1 can also perform well in other CMs. Therefore, in the following subsections, all simulation results of FM-DCSK-based UWB systems are performed over the CM1 channel for simplicity, where both multipath fading and delay spread are involved.

Example 12: As a simple example, we discuss the impact of guard-interval length on the error performance of the SU-FM-DCSK UWB system over an IEEE 802.15.4a CM1 channel and show the corresponding result in Fig. 29. Suppose that channel parameters are set as follows: the bit duration $T = 1000$ns, the chaotic-pulse duration $T_{\rm c} = 2.5$ns, and the sampling frequency $f_s = 8$GHz. Based on such an assumption, the maximal guard interval becomes $T_{\rm g,max} = 497.5$ns. As a consequence, the guard interval should satisfy $T_{\rm g} \in [0, 497.5{\rm ns}]$. As observed from this figure, the simulated result agrees well with the aforementioned theoretical analysis, and the optimal value of guard interval is $T_{\rm g,th} = 50$ns. *Note also that* there may exist a more accurate value of

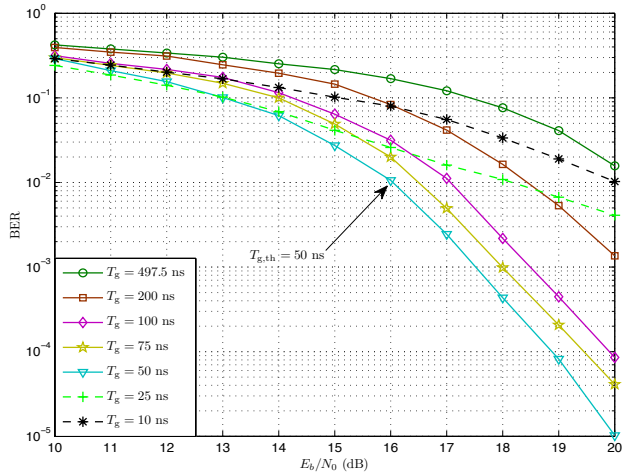

Fig. 29. BER curves of the SU-FM-DCSK UWB system over a CM1 channel with different guard intervals. The parameters used are $T = 1000\text{ns}, T_c = 2.5\text{ns}$, and $f_s = 8\text{GHz}$.

$T_{g,th} \in [25\text{ns}, 75\text{ns}]$ because only three T_g samples within the closed interval are selected in our simulation.

B. Timing-Synchronization Algorithm

Since the information-bearing pulse in TR-UWB systems (e.g., FM-DCSK UWB system) is extremely short, the corresponding error performance is very sensitive to the captured signal energy and noise energy. In this scenario, timing offset may severely deteriorate the performance of TR-UWB systems and thus make them not practically applicable [164], [165]. Thereby, timing synchronization[27] becomes one challenging problem for the UWB receiver design in practical applications.

To date, there have been a variety of articles studying the timing synchronization issue of coherent and non-coherent UWB systems [166]–[169]. In particular, timing-synchronization algorithms for non-coherent TR-UWB systems in [168] and [169] are respectively carried out based on (i) the "peak-picking" operation on a large set of cross-correlation values of the received signals; and (ii) the correlation of two consecutive received signals. Nonetheless, these two approaches may not be suitable for FM-DCSK UWB systems due to the following reasons.

- Different from the conventional TR UWB signal, the transmitted FM-DCSK UWB signal varies even for the same information bits. It is because of the time-varying chaotic waveform being used as the reference UWB pulse.
- The inherent near-random property of chaotic signals yields a very low cross-correlation value.

Accordingly, there is a lack of usable timing-synchronization algorithm for FM-DCSK UWB systems. To complement the previous research work on FM-DCSK UWB systems, a fast data-aided timing-synchronization algorithm, which capitalizes on the good cross-correlation characteristic of chaotic signals, has been proposed by Chen *et al.* [87].

[27]In reality, the exact arrival time of the incoming signal is always not available at the receiver. The timing synchronization, which aims at acquiring the arrival time of the first channel path (i.e., starting point of integration) without any CSI, should be conducted prior to the detecting process [166], [167]. As a consequence, the accuracy of such a technique is of great importance for a TR-UWB system to achieve good error performance.

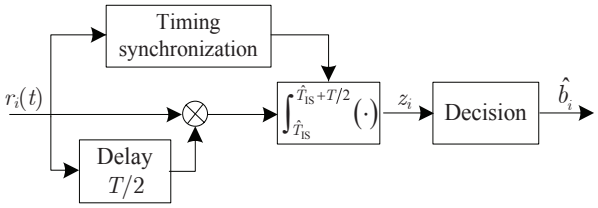

Fig. 30. Block diagram of the receiver in an FM-DCSK UWB system, which includes a timing-synchronization module.

Consider an FM-DCSK UWB system where the arrival time of the incoming signal is not known at the receiver terminal. Fig. 30 depicts the structure of the receiver including a timing-synchronization module, where T denotes the bit duration and $\hat{T}_{IS}$ denotes the estimated starting point of integration. Hence, the objective of the proposed timing-synchronization algorithm is to optimize the value of $\hat{T}_{IS}$ so as to achieve $\hat{T}_{IS} \in [T_{IS} - T_{res}, T_{IS} + T_{res}]$ [87]. Here, T_{IS} is the ideal starting point of integration, $T_{res} = 1/f_s$ is the synchronization resolution defined in [169], and f_s is the sampling frequency of each chaotic pulse.

The data-aided timing-synchronization algorithm for the FM-DCSK UWB system [87] is summarized as follows.

1) Initialize the estimated starting point of integration as $\hat{T}_{IS} = T_{IS,0}$, where $T_{IS,0} \in [0, T)$; and reset the number of optimization steps as $z_{TS} = 0$.
2) Divide the interval $[\hat{T}_{IS}, \hat{T}_{IS} + T]$ into N_{TS} successive uniform subintervals by adding $N_{TS} - 1$ points, i.e., $\hat{T}_{IS} + T/N_{TS}, \hat{T}_{IS} + 2T/N_{TS}, \cdots, \hat{T}_{IS} + (N-1)T/N_{TS}$. For $\mu = 0, 1, 2, \cdots, N_{TS} - 1$, measure the following integration with the starting point $\hat{T}_{IS} + \mu T/N_{TS}$, as

$$\Gamma_{i,\mu}^{(0)} = \left| \int_{\hat{T}_{IS}+\mu T/N_{TS}}^{\hat{T}_{IS}+\mu T/N_{TS}+T'_{II}} r_i(t) r_i^*(t + T/2)\, \mathrm{d}t \right|, \quad (11)$$

where $r_i(t)$ is the received signal corresponding to b_i, $T'_{II} \in (0, T/2]$ is the integral window of the timing synchronization, the subscript "$*$" is the complex-conjugate operator, and $|\cdot|$ is the modulus operator. Based on the vector $\mathbf{\Gamma}_i^{(0)} = \{\Gamma_{i,0}^{(0)}, \Gamma_{i,1}^{(0)}, \cdots, \Gamma_{i,(N_{TS}-1)}^{(0)}\}$, the index Ω_0, for which the maximum signal energy $\Gamma_{i,\Omega_0}^{(0)} = \max_{\mu} \Gamma_{i,\mu}^{(0)}$ is accomplished, is readily found via comparison (i.e., $\Omega_0 = \arg\max_{\mu} \Gamma_{i,\mu}^{(0)}$). Then, $\hat{T}_{IS}$ is updated as

$$\hat{T}_{IS} = \hat{T}_{IS} - (N_{TS} - \Omega_0) T/N_{TS}, \quad (12)$$

and the ideal starting point follows $T_{IS} \in [\hat{T}_{IS} - T/N_{TS}, \hat{T}_{IS} + T/N_{TS}]$. Set $z_{TS} = z_{TS} + 1$.
3) If $z_{TS} > 1$, go to Step 4); otherwise (i.e., $z_{TS} = 1$), the region that T_{IS} lies in is split into two uniform subregions, i.e., $[\hat{T}_{IS} - T/N_{TS}, \hat{T}_{IS}]$ and $[\hat{T}_{IS}, \hat{T}_{IS} + T/N_{TS}]$. Then, utilize the middle points of the above two subregions, i.e., $\hat{T}_{IS} - (-1)^{\iota} T/(2N_{TS})$ $(\iota \in \{0, 1\})$, as two starting points,

respectively, to calculate the following integration

$$\Gamma_{i,\iota}^{(1)} = \left| \int_{\hat{T}_{\rm IS}-(-1)^{\iota}T/(2N_{\rm TS})}^{\hat{T}_{\rm IS}-(-1)^{\iota}T/(2N_{\rm TS})+T'_{\rm II}} r_i(t) r_i^*(t+T/2)\,{\rm d}t \right|. \tag{13}$$

Hence, the ideal starting point is located as $T_{\rm IS} \in [\hat{T}_{\rm IS} - T/N_{\rm TS}, \hat{T}_{\rm IS}]$ if $\Omega_1 = \arg\max_{\iota} \Gamma_{i,\iota}^{(1)} = 0$. Otherwise, $T_{\rm IS} \in [\hat{T}_{\rm IS}, \hat{T}_{\rm IS}+T/N_{\rm TS}]$. The middle point of the resultant region is then considered as the updated value of $\hat{T}_{\rm IS}$, i.e.,

$$\hat{T}_{\rm IS} = \hat{T}_{\rm IS} - (-1)^{\Omega_1} T/(2N_{\rm TS}). \tag{14}$$

Exploiting the updated $\hat{T}_{\rm IS}$, the region that involves $T_{\rm IS}$ can be rewritten as $T_{\rm IS} \in [\hat{T}_{\rm IS} - T/(2N_{\rm TS}), \hat{T}_{\rm IS} + T/(2N_{\rm TS})]$.

4) For $z_{\rm TS} = 2, 3, \cdots$, $\hat{T}_{\rm IS}$ can be promptly obtained through a similar way as Step 3), resulting in

$$\hat{T}_{\rm IS} = \hat{T}_{\rm IS} - \frac{(-1)^{\Omega_{z_{\rm TS}}} T}{(2^{z_{\rm TS}} N_{\rm TS})}, \tag{15}$$

where the original $\hat{T}_{\rm IS}$ on the right-hand side of this equation is give by (12); $\Omega_{z_{\rm TS}} = \arg\max_{\iota} \Gamma_{i,\iota}^{(z_{\rm TS})} \in \{0, 1\}$; and $\Gamma_{i,\iota}^{(z_{\rm TS})}$ is given by [87, eq.(8)]. Accordingly, $T_{\rm IS}$ lies in $[\hat{T}_{\rm IS} - T/(2^{z_{\rm TS}} N_{\rm TS}), \hat{T}_{\rm IS} + T/(2^{z_{\rm TS}} N_{\rm TS})]$.

5) For $z_{\rm TS} = 0, 1, 2, \cdots$, the synchronization error is calculated as $\Delta_{\rm TS} = \left|\hat{T}_{\rm IS} - T_{\rm IS}\right| \leq T/(2^{z_{\rm TS}} N_{\rm TS}) \triangleq \Delta_{\rm TS,max}$. If $\Delta_{\rm TS,max} > T_{\rm res}$, set $z_{\rm TS} = z_{\rm TS} + 1$ and go to Step 3); otherwise, terminate the optimization.

Remarks:

- In the timing-synchronization algorithm, $N_{\rm TS}$ is a small positive number and is usually set as 4. Besides, the integral window $T'_{\rm II}$ is a key parameter to determine the synchronization performance and thus should be appropriately selected [87].
- With respect to the exhaustive-searching algorithm for conventional TR-UWB systems [169], the proposed data-aided algorithm not only can speed up the timing acquisition, but also can remarkably reduce the computational complexity. For example, the time complexity of former one is $\mathcal{O}(1/T_{\rm res})$ while that of the latter one is $\mathcal{O}(\log_2(1/T_{\rm res}))$ $(f_s = 1/T_{\rm res} \gg 1)$.
- Using the proposed timing-synchronization algorithm, the error performance of FM-DCSK UWB system over an IEEE 802.15.4a CM1 channel becomes fairly close to the case of perfect timing acquisition [87].

For the reasons mentioned above, the timing-synchronization algorithm proposed in [87] is particularly suitable for the FM-DCSK UWB architecture, and it further facilitates the application of such type of systems to low-rate and low-power WPANs/WSNs. In the rest of this treatise, we will directly assume that perfect timing synchronization is achieved at the receiver of FM-DCSK-based UWB systems.

C. SIMO FM-DCSK UWB System

Although the critical parameters and timing-synchronization issues of FM-DCSK UWB systems under indoor transmission scenarios have already been extensively studied in the literature, a myriad of interesting issues on the design and analysis, e.g., error performance and throughput enhancement, delay line problem, MA capability, theoretical-analysis tool, etc., are awaiting for further investigation. All of these issues are highly relevant to the application of FM-DCSK UWB to modern wireless communication systems.

To overcome the weaknesses of delay line and user capacity in conventional FM-DCSK UWB systems, a new SIMO CPC-based FM-DCSK UWB system has been conceived by Wang *et al* [89]. In the proposed system, the format of the transmitted FM-DCSK UWB signal has firstly been modified to a so-called *CPC-based FM-DCSK UWB signal* based on an M-order ($M \geq 4$) WC. The goal is to reduce the length of time-delay units. Then a time-division scheme has been introduced to the CPC-based FM-DCSK UWB system to address the limitation on user capacity. To elaborate a little further on the novel FM-DCSK UWB system, we describe the corresponding transceiver design and its application to an MA scenario as follows.

1) Transceiver structure: In the CPC-based SIMO FM-DCSK UWB system, an M-order WC is adopted at the transmitter[28]. Unlike the original SIMO FM-DCSK system [85], where all row vectors of the WC have been utilized to realize multibit transmission, the CPC-based SIMO FM-DCSK UWB system only uses the first two row vectors (i.e., $\mathbf{w}_1$ and $\mathbf{w}_2$) to multiply with the M chaotic pulses and to form the transmitted signal.

For example, assuming that $M = 4$, each information bit $b_i \in \{+1, -1\}$ is represented by an FM-DCSK UWB signal having four ultrashort chaotic pulses, i.e., $s_i(t) = \mathbf{w}_{(3-b_i)/2} * [g_i(t)\ g_i(t)\ g_i(t)\ g_i(t)]$, where $g_i(t)$ denotes the reference FM-chaotic UWB pulse of duration $T_{\rm c}$. However, in this scenario, the distance between the neighboring chaotic pulses in each transmitted signal (i.e., the length of time-delay unit $T_{\rm D}$) is no longer equal to T/M, but is decreased to an acceptable value that satisfies $T_{\rm D} \geq T_{\rm c}$. As a result, the guard gap between two neighboring signals can be promptly calculated as $T_\Delta = T - 3T_{\rm D} - T_{\rm c} \neq T_{\rm g}$, where $T_{\rm g} = T_{\rm D} - T_{\rm c}$. Based on the aforementioned discussion, the structures of the transmitted signals in the CPC-based SIMO FM-DCSK UWB system and conventional SIMO FM-DCSK system are illustrated in Fig. 31.

At the receiver terminal, the received signals corresponding to different transmit-receive antenna pairs are firstly detected by independent DC/GML demodulators, in which the integration interval satisfies $T_{\rm II} = T_{\rm D}$. The obtained energies are combined by either EGC or MRC and then the estimated bit is decoded by an appropriate decision-making rule.

Remarks:

- For a given demodulator (DC or GML), the CPC-based scheme outperforms the conventional scheme over multi-path fading channels, especially in the high-SNR region, provided that $T_{\rm D} \geq T_{\rm c}$. It is because a shorter integration interval and a larger guard gap ensure less captured noise energy and smaller ISI. Although a more severe IPI is

[28] M is also defined as the order of the CPC-based SIMO FM-DCSK UWB system in this subsection.

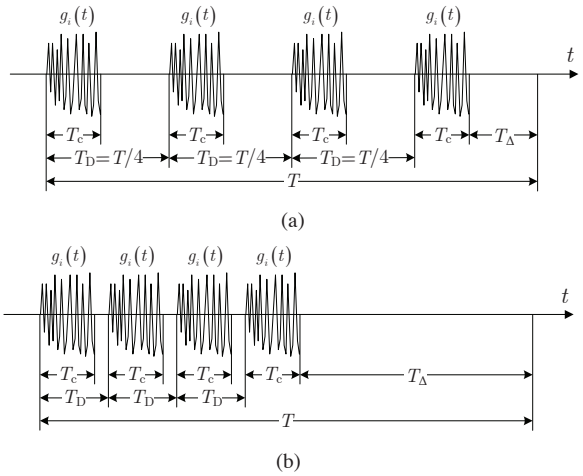

Fig. 31. Structure of the transmitted signal in the (a) conventional SIMO FM-DCSK UWB system and (b) CPC-based SIMO FM-DCSK UWB system. The parameters used are $b_i = 1$ and $M = 4$.

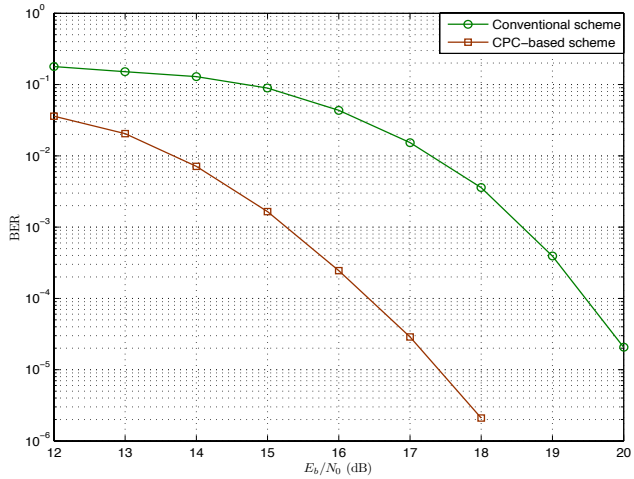

Fig. 32. BER curves of the CPC-based SIMO FM-DCSK system and conventional SIMO FM-DCSK UWB system over a CM1 channel. The parameters used are $N_R = 2, M = 4, T = 1000\text{ns}, T_c = 2.5\text{ns}$, and $f_s = 8\text{GHz}$. The lengths of time-delay unit for the CPC-based and conventional schemes are equal to $T_{D,th} = 15.625\text{ns}$ and $T_{D,conv} = 250\text{ns}$, respectively.

observed simultaneously, this effect is inferior to that of the attainable advantages. Consequently, the CPC-based scheme can exhibit a better error performance, and the performance gain will increase gradually as T_D becomes smaller until an optimal value is achieved (see the forthcoming *Example 13*).

- As long delay lines are very difficult to be implemented by the existing technologies [170], M should be set to a sufficiently large integer for the sake of reducing the length of time-delay units to a desirable value. Along with a larger value of M, the required number of delay lines in both transmitter and receiver increase. Meanwhile, the energy per pulse may become too weak to resist the noise, which leads to a performance degradation. In accordance to the aforementioned reasons, one should carefully select the value of M to obtain a good balance between implementation complexity and error performance. As reported in [89], $M = 4$ has been proved to be an optimal value when the above two issues are taken into account.
- Between the two types of demodulators (i.e., DC and GML), the GML scheme can perform better but requires more delay lines.

2) MA scheme: In the CPC-based SIMO FM-DCSK UWB system, all the component pulses are located at the front part of one bit duration, as shown in Fig. 31(b). In fact, the effective signal that includes all the pulses has a duration of $T_{ES} = MT_D \ll T$. There is still an idle time (i.e., duration of an idle period) $T_{ID} = T - T_{ES}$ in each bit duration, which can be substantially utilized to accommodate more users.

Without loss of generality, we consider an M-order CPC-based SIMO FM-DCSK UWB system. Exploiting the time-division technique, the maximum number of users that can be accommodated in each transmission period is expressed as $\mathcal{C}_{TD} = \lfloor T/T_{ES} \rfloor$, where $\lfloor x \rfloor$ denotes the floor of x. Also, the M-order WC can be assigned to $M/2$ user groups[29]. In this way, the user capacity, i.e., the total number of users that can be accommodated, is finally given as $\mathcal{C}_u = \mathcal{C}_{TD} \cdot (M/2) = \lfloor T/(2T_D) \rfloor$.

Remark: The user capacity of the CPC-based SIMO FM-DCSK UWB system is no longer limited by the order of WC (i.e., M), but is only dependent on the integration interval T_D.

Example 13: We consider an SU-CPC-based SIMO FM-DCSK UWB system in an IEEE 802.15.4a CM1 channel. Suppose that the channel-parameter setting here is the same as that in *Example 12*, while the system parameters are set as follows: the order of WC $M = 4$ and the number of receive antennas $N_R = 2$. As a validation of the design in [89], we compare the BER performance of the CPC-based and conventional SIMO FM-DCSK UWB systems in Fig. 32. It is clear that the CPC-based scheme is remarkably superior to the conventional scheme. For instance, at a BER of 2×10^{-5}, the former one possesses a gain of about 3 dB over the latter one.

D. Cooperative FM-DCSK UWB system

As an application of DCSK-CC systems to UWB scenarios, a two-user cooperative FM-DCSK UWB system has been developed by Fang *et. al* [88]. In that work, the authors have evaluated the theoretical BER performance of cooperative FM-DCSK UWB system in the IEEE 802.15.4a CMs with small-scale fading statistics. Also, the integration interval has been optimized by employing a *binary-search algorithm*. Aiming at obtaining further improvement, the SIMO architecture has been introduced to the cooperative FM-DCSK UWB system to form a cooperative SIMO FM-DCSK UWB system. Straightforwardly, the cooperative FM-DCSK UWB system can outperform the traditional FM-DCSK-NC UWB system owing to the same reasons mentioned in Sect. IV-D. Thus, we only perform simulations on the cooperative SIMO FM-DCSK UWB system to further demonstrate the merit of optimizing the integration interval over a CM1 multipath fading channel.

Example 14: Fig. 32 plots the BER results of the cooperative SIMO FM-DCSK UWB system over a CM1 channel

[29]Here, the user group is defined as a set of $\mathcal{C}_{TD}$ users accommodated in each transmission period via time-division technique.

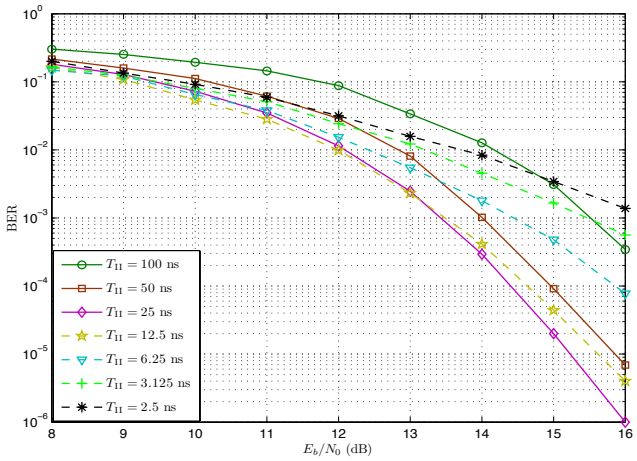

Fig. 33. BER curves of cooperative SIMO FM-DCSK UWB system over a CM1 channel with different integration intervals. The parameters used are $N_{\rm R} = 2, M = 4, T = 400{\rm ns}, T_{\rm c} = 2.5{\rm ns},$ and $f_s = 8{\rm GHz}$.

with different integration intervals. Here, the parameters used are the same as those listed in *Example 13*, except that T is changed to $400{\rm ns}$. Referring to this figure, systems with integration intervals $T_{\rm II} \in (T_{\rm c}, T/M)$ achieve better performance than the original cooperative system with $T_{\rm II} = T/M = 100{\rm ns}$. However, the system suffers from severe performance deterioration when $T_{\rm II} = T_{\rm c} = 2.5{\rm ns}$, and thus it is outperformed by the original system. In this case, the energy captured from the desired signal is so small that it can no longer overcome the noise energy. In summary, the best error performance can be achieved when $T_{\rm II} = T/M = 25{\rm ns}$, and this value can be served as the optimal integration interval for the given parameter setting.

Remark: The authors in [88] have limited their attention to the two-user scenario and have not generalized the cooperative FM-DCSK UWB system to the scenario of more users.

E. Other FM-DCSK-based UWB Systems

Similar to the SIMO and cooperative FM-DCSK UWB systems elaborated in Sects. V-C and V-D, most of the other DCSK-related frameworks can be applied to the UWB scenarios. For example, STBC-FM-DCSK UWB system, MIMO-relay FM-DCSK UWB system and ARQ-based FM-DCSK UWB system, have been carefully studied in [52], [90], and [91], respectively, so as to meet the low-rate and low-power requirement of WPAN and WSN applications. Furthermore, the CS-DCSK modulation has been extended to UWB transmission environments in [79]. In that work, the authors have roughly analyzed the BER performance of FM-CS-DCSK UWB system in the presence of narrowband interference over IEEE 802.15.4a indoor channels.

Recently, the performance of FM-DCSK UWB system has been briefly investigated for wireless medical applications [92]. In particular, the key parameter, e.g., integration interval, has been discussed in order to fit well with the QoS requirements of different medical environments.

Nonetheless, there may exist some other FM-DCSK UWB systems in the vast volume of literature which have not been enumerated explicitly in this article.

VI. Concluding Remarks and Future Research Directions

A. Concluding Remarks

In this treatise, we have provided a comprehensive survey of the open literature related to DCSK-based communication systems and their underlying application to UWB scenarios. We have considered DCSK modulation and its valuable variants, DCSK-related communication systems, as well as FM-DCSK-based UWB systems under various transmission scenarios from the design and analysis perspectives. Specifically, we have restricted our elaborations to the design principles of such modulations and systems in the theory aspect but have slightly touched upon the corresponding hardware implementations.

We have commenced the discourse by summarizing the fundamental knowledge of CSK and DCSK modulations, including the related terminology and definitions, in Sect II. Therein, the classical MA strategies and CMs of DCSK-based systems have also been reviewed, followed by a compact historical overview of the contributions related to such communication systems.

Based on these preliminary foundations, in Sect. III we have proceeded to present a range of meritorious variants of DCSK modulation scheme. In Sect. III-A, we have given a concise portrayal of the FM-DCSK and its corresponding improved version (i.e., IFM-DCSK), both of which can overcome the drawback of unstable bit-energy in DCSK and keep the error performance unchanged. In Sects. III-B and III-C, we have outlined the research achievements in designing multilevel DCSK schemes, i.e., QCSK scheme and three types of M-ary DCSK schemes. All these multilevel methods can achieve much higher data rate via either increasing the implementation complexity or reducing the spectral efficiency. Afterwards, the CS-DCSK and DDCSK have been briefly introduced in Sects. III-D and III-E, respectively. The last subsection (i.e., Sect. III-F) has portrayed the newly developed MC-DCSK and its corresponding advantages.

In Sect. IV, we have turned our attention to the current research topics related to designing DCSK-related wireless communication systems over multipath fading channels. We have started this section by explaining the configuration of a WC-based SIMO FM-DCSK system that accomplishes improvement in both error performance and data rate in Sect. IV-A. Subsequently, we have summarized the design methodologies of two different types of STBC-DCSK systems in Sect. IV-B. However, some practical wireless communication systems may not install multiple transmit antennas, which limits the further applications of STBC-based architecture. Then we have surveyed some preferable DCSK-related systems that only equip one antenna at the transmitter, such as the MIMO relay DCSK-CD system in Sect. IV-C and DCSK-CC system in Sect. IV-D. The joint design of DCSK and error-control techniques (i.e., ECC and ARQ/CARQ) has been presented in Sects. IV-E and IV-F. In addition, we have discussed the PNC-DCSK and ANC-DCSK systems in Sect. IV-G and have taken a quick glance at other DCSK-related communication systems developed in recent years in Sect. IV-H.

Apart from the relevant contributions achieved under the DCSK-based frameworks, the application of such techniques to UWB scenarios has been introduced in Sect. V. In this section, we have dedicated special attention to the employment of FM-DCSK-based modulation schemes, which are particularly feasible for low-power short-range UWB transmissions. In Sect. V-A, we continued to survey the basic principles of FM-DCSK UWB system including transceiver structure, critical parameters, and channel models. It has been emphasized that the guard interval and integration interval are the two most important parameters of such a system. We have also outlined the emerging issue of timing synchronization and the corresponding solution in Sect. V-B. Moreover, in Sects. V-C and V-D, the design and optimization of SIMO and cooperative FM-DCSK UWB systems have been discussed, respectively, in which the inherent feature of FM-DCSK UWB signal is taken into consideration. Besides, other state-of-the-art FM-DCSK-based UWB systems have been briefly reviewed in Sect. V-E.

To summarize, as a new type of SS techniques, the DCSK-based modulations have demonstrated their potential and superiorities for use in a great deal of wireless communication applications, especially for low-power and low-complexity short-range WPANs, WSNs, and WBANs. Certainly, such novel type of modulations creates new opportunities as well as challenges for modern SS communications.

B. Future Research Directions

DCSK-based modulations have received significant attention since its first appearance. Some chaotic modulation schemes, such as TR-like FM-DCSK-based scheme and chaos-based UWB scheme, have already been proposed for the WPAN applications within the IEEE 802.15.4a standard and the WBAN applications within the IEEE 802.15.6 standard. There is no doubt that DCSK may find more deployment in other potential applications and be considered by some new standards in the near future. However, much more effort should be spent for practical applications of DCSK. Based on our discussions in the preceding sections, some of the open research issues and practical challenges are listed as follows.

1) Although the capacity of DCSK-modulated system over an AWGN channel has been analyzed by means of Monte-Carlo simulations [25], it is more interesting to propose some sophisticated approaches in order to derive the corresponding capacity bound over a multipath Nakagami fading channel, which can accurately characterize the fading statistics of realistic wireless transmission environments.
2) As argued in Sect. IV-E, the performance of DCSK system is still far away from the channel capacity and hence it can be significantly boosted by using LDPC codes. Nevertheless, the current research endeavor has been to directly use the existing LDPC codes in DCSK systems without any modification [63], [64]. Recent works like [69] have only focused on the decoding aspect in such coded-modulation systems. So, it makes sense to develop an appropriate approach for designing a code structure that fits better with the LDPC-coded DCSK systems. It is believed that the performance gap to the channel capacity can be further reduced with the use of an optimized LDPC code.
3) FM-DCSK UWB systems have been widely studied in the past decade and appear to be a major direction for the DCSK research community. As the UWB CMs in IEEE 802.15.4a standard are more complicated compared with the multipath Nakagami fading CM, the theoretical performance analysis of FM-DCSK UWB system in such transmission scenarios becomes an intractable problem. Till now, this research topic has only been preliminarily discussed by a few articles [79], [88], and it is definitely worth further investigation.
4) According to Sect. V-E, FM-DCSK UWB systems can also be utilized in wireless medical applications, such as WBANs, by adjusting some critical parameters. Nowadays, the interest in WBAN has grown significantly towards real applications such as wearable and portable e-Health systems [96], [171], [172]. Due to the low-power and low-complexity requirement of WBAN applications, the combination of simple ECCs and modulations may offer a good choice for the corresponding physical-layer design. Therefore, the design of low-complexity ECCs (e.g., cyclic LDPC codes and protograph LDPC codes) concatenated with FM-DCSK-based UWB modulations deserves for a future line.
5) We also anticipate that another potential research direction is to further study other excellent variants of DCSK. As can be observed from Sect. III, a significant amount of DCSK variants have been constructed respectively for the SU and MA scenarios. Unfortunately, the inherent drawbacks of DCSK, e.g., relatively low energy and spectral efficiencies, have not been addressed adequately. As power consumption and bandwidth consumption are always seriously concerned in the implementation of wireless communication devices, more research attempt is expected for designing more efficient non-coherent chaos-based modulations without sacrificing error performance.
6) As far as we know, most research in the open literature has been endeavored to the theoretical advancement of the DCSK-based communication systems rather than hardware implementation. Recently, the authors in [120], [173] have attempted to implement DCSK and FM-DCSK modulations and have measured their corresponding performance in software-radio-based platforms. Yet, there is still a lack of hardware-based platform for real measurement of such modulations, and hence a good solution to this problem will be truly encouraging.

REFERENCES

[1] R. L. Devaney, *A First Course in Chaotic Dynamical Systems: Theory and Experiment*. New York, NY, USA: Addison-Wesley, 1992.
[2] M. K. Simon, J. K. Omura, R. A. Scholtz, and B. K. Levitt, *Spread Spectrum Communications*. New York, NY, USA: Computer Science Press, 1985.
[3] U. Madhow and M. Pursley, "Acquisition in direct-sequence spread-spectrum communication networks: an asymptotic analysis," *IEEE Trans. Inf. Theory*, vol. 39, no. 3, pp. 903–912, May 1993.
[4] C. Kchao and G. Stubeer, "Analysis of a direct-sequence spread-spectrum cellular radio system," *IEEE Trans. Commun.*, vol. 41, no. 10, pp. 1507–1517, Oct. 1993.
[5] M. Pursley and D. Sarwate, "James L. Massey's contributions in the early years of spread-spectrum communication theory research," *IEEE*

Commun. Surveys & Tutorials, vol. 17, pp. 1500–1510, Third Quarter 2015.

[6] G. Heidari-Bateni and C. McGillem, "Chaotic sequences for spread spectrum: an alternative to PN-sequences," in *Proc. IEEE Int. Conf. Selected Topics in Wireless Commun.*, Jun. 1992, pp. 437–440.

[7] ——, "A chaotic direct-sequence spread-spectrum communication system," *IEEE Trans. Commun.*, vol. 42, no. 234, pp. 1524–1527, Feb. 1994.

[8] U. Parlitz, L. O. Chua, L. Kocarev, K. S. Halle, and A. Shang, "Transmission of digital signals by chaotic synchronization," *Int. J. Bifurcation and Chaos*, vol. 2, no. 4, pp. 973–977, Apr. 1992.

[9] H. Dedieu, M. Kennedy, and M. Hasler, "Chaos shift keying: modulation and demodulation of a chaotic carrier using self-synchronizing Chua's circuits," *IEEE Trans. Circuits Syst. II: Exp. Briefs*, vol. 40, no. 10, pp. 634–642, Oct. 1993.

[10] M. Itoh and H. Murakami, "New communication systems via chaotic synchronizations and modulation," *IEICE Trans. Fund.*, vol. E78-A, no. 3, pp. 285–290, Mar. 1995.

[11] U. Feldmann, M. Hasler, and W. Schwarz, "Communication by chaotic signals: the inverse system approach," *Int. J. Circuit Theory Appl.*, vol. 24, no. 5, pp. 551–579, Sept. 1996.

[12] G. Kolumban, B. Vizvari, W. Schwarz, and A. Abel, "Differential chaos shift keying: A robust coding for chaotic communication," in *Proc. Int. Workshop Nonlinear Dynam. Electron. Syst. (NDES)*, Jun. 1996, pp. 87–92.

[13] L. M. Pecora and T. L. Carroll, "Synchronization in chaotic systems," *Phys. Rev. A*, vol. 64, no. 8, pp. 821–824, Feb. 1990.

[14] G. Kolumban, M. Kennedy, and L. Chua, "The role of synchronization in digital communications using chaos-Part I: Fundamentals of digital communications," *IEEE Trans. Circuits Syst. I: Reg. Papers*, vol. 44, no. 10, pp. 927–936, Oct. 1997.

[15] ——, "The role of synchronization in digital communications using chaos-Part II: Chaotic modulation and chaotic synchronization," *IEEE Trans. Circuits Syst. I: Reg. Papers*, vol. 45, no. 11, pp. 1129–1140, Nov. 1998.

[16] G. Kolumban and M. Kennedy, "The role of synchronization in digital communications using chaos-Part III: Performance bounds for correlation receivers," *IEEE Trans. Circuits Syst. I: Reg. Papers*, vol. 47, no. 12, pp. 1673–1683, Dec. 2000.

[17] W. Xu, L. Wang, and G. Chen, "Performance of DCSK cooperative communication systems over multipath fading channels," *IEEE Trans. Circuits Syst. I: Reg. Papers*, vol. 58, no. 1, pp. 196 –204, Jan. 2011.

[18] Y. Fang, L. Wang, P. Chen, J. Xu, G. Chen, and W. Xu, "Design and analysis of a DCSK-ARQ/CARQ system over multipath fading channels," *IEEE Trans. Circuits Syst. I: Reg. Papers*, vol. 62, no. 6, pp. 1637–1647, Jun. 2015.

[19] G. Kaddoum, F. Gagnon, P. Charge, and D. Roviras, "A Generalized BER prediction method for differential chaos shift keying system through different communication channels," *Wireless Pers. Commun.*, vol. 60, pp. 1–13, Dec. 2010.

[20] G. Kolumban, M. P. Kennedy, Z. Jako, and G. Kis, "Chaotic communications with correlator receivers: Theory and performance limits," *Proc. IEEE*, vol. 90, no. 5, pp. 711–732, May 2002.

[21] A. Abel, W. Schwarz, and M. Gotz, "Noise performance of chaotic communication systems," *IEEE Trans. Circuits Syst. I: Reg. Papers*, vol. 47, no. 12, pp. 1726–1732, Dec. 2000.

[22] G. Kolumban, "Theoretical noise performance of correlator-based chaotic communications schemes," *IEEE Trans. Circuits Syst. I: Reg. Papers*, vol. 47, no. 12, pp. 1692–1701, Dec. 2000.

[23] F. C. M. Lau and C. K. Tse, *Chaos-Based Digital Communication Systems*. Heidelberg, Germany: Springer-Verlag, 2003.

[24] G. Kolumban, B. Vizvari, W. Schwarz, and A. Abel, "Basis function description of chaotic modulation scheme," in *Proc. Int. Workshop Nonlinear Dynam. Electron. Syst. (NDES)*, May 2000, pp. 165–169.

[25] G. Cai, L. Wang, and T. Huang, "Channel capacity of M-ary Differential Chaos Shift Keying modulation over AWGN channel," in *Proc. Int. Symp. Commun. Inf. Technol. (ISCIT)*, Sept. 2013, pp. 91–95.

[26] G. Kaddoum, P. Charge, and D. Roviras, "A generalized methodology for bit-error-rate prediction in correlation-based communication schemes using chaos," *IEEE Commun. Lett.*, vol. 13, no. 8, pp. 567–569, Aug. 2009.

[27] S. Mandal and S. Banerjee, "Performance of differential chaos shift keying over multipath fading channels," in *Proc. Indian Nat. Conf. Nonlinear Systems and Dynamics*, Dec. 2003, pp. 1–4.

[28] Y. Xia, C. K. Tse, and F. C. M. Lau, "Performance of differential chaos-shift-keying digital communication systems over a multipath fading channel with delay spread," *IEEE Trans. Circuits Syst. II: Exp. Briefs*, vol. 51, no. 12, pp. 680–684, Dec. 2004.

[29] G. Kolumban, G. Kis, F. C. M. Lau, and C. K. Tse, "Optimum noncoherent FM-DCSK detector: Application of chaotic GML decision rule," in *Proc. IEEE Int. Symp. Circuits Syst. (ISCAS)*, vol. 4, May 2004, pp. 597–600.

[30] G. Kis, "Performance analysis of chaotic communication systems," Ph.D. dissertation, Budapest University of Technology and Economics, Budapest, Hungary, Sept. 2005.

[31] G. Kolumban, M. Kennedy, G. Kis, and Z. Jako, "FM-DCSK: A novel method for chaotic communications," in *Proc. IEEE Int. Symp. Circuits Syst. (ISCAS)*, vol. 4, May 1998, pp. 477–480.

[32] G. Kolumban, Z. Jako, and M. Kennedy, "Enhanced versions of DCSK and FM-DCSK data transmission systems," in *Proc. IEEE Int. Symp. Circuits Syst. (ISCAS)*, vol. 4, Jul. 1999, pp. 475–478.

[33] G. Kaddoum, E. Soujeri, C. Arcila, and K. Eshteiwi, "I-DCSK: An improved non-coherent communication system architecture," *IEEE Trans. Circuits Syst. II: Exps Briefs,* accepted for publication, Aug. 2015. [Online]. Available: http://ieeexplore.ieee.org/

[34] Z. Galias and G. M. Maggio, "Quadrature chaos-shift keying: Theory and performance analysis," *IEEE Trans. Circuits Syst. I: Reg. Papers*, vol. 48, no. 12, pp. 1510–1519, Dec. 2001.

[35] W. Xu, L. Wang, and G. Kolumban, "A novel differential chaos shift keying modulation scheme," *Int. J. Bifurcation and Chaos*, vol. 21, no. 3, pp. 799–814, Jun. 2011.

[36] H. Yang and G.-P. Jiang, "High-efficiency differential-chaos-shift-keying scheme for chaos-based noncoherent communication," *IEEE Trans. Circuits Syst. II: Exp. Briefs*, vol. 59, no. 5, pp. 312–316, May 2012.

[37] G. Kaddoum, F. Richardson, and F. Gagnon, "Design and analysis of a multi-carrier differential chaos shift keying communication system," *IEEE Trans. Commun.*, vol. 61, no. 8, pp. 3281–3291, Aug. 2013.

[38] G. Kaddoum and F. Gagnon, "Design of a high-data-rate differential chaos-shift keying system," *IEEE Trans. Circuits Syst. II: Exp. Briefs*, vol. 59, no. 7, pp. 448–452, Jul. 2012.

[39] G. Kolumban, M. P. Kennedy, and G. Kis, "Multilevel differential chaos shift keying," in *Proc. Int. Workshop Nonlinear Dynam. Electron. Syst. (NDES)*, Jun. 1997, pp. 191–196.

[40] F. C. M. Lau, M. Yip, C. Tse, and S. Hau, "A multiple-access technique for differential chaos-shift keying," *IEEE Trans. Circuits Syst. I: Reg. Papers*, vol. 49, no. 1, pp. 96–104, Jan. 2002.

[41] F. C. M. Lau, K. Y. Cheong, and C. K. Tse, "Permutation-based DCSK and multiple-access DCSK systems," *IEEE Trans. Circuits Syst. I: Reg. Papers*, vol. 50, no. 6, pp. 733–742, Jun. 2003.

[42] Z. Zhou, T. Zhou, and J. Wang, "Performance of multiple-access DCSK communication over a multipath fading channel with delay spread," *Circuits Syst. Signal Process.*, vol. 27, no. 4, pp. 733–742, Aug. 2008.

[43] G. Kaddoum, F.-D. Richardson, S. Adouni, F. Gagnon, and C. Thibeault, "Multi-user multi-carrier differential chaos shift keying communication system," in *Proc. IEEE Int. Wireless Commun. Mobile Comput. Conf. (IWCMC)*, Jul. 2013, pp. 1798–1802.

[44] P. Chen, L. Wang, and G. Chen, "DDCSK-Walsh coding: A reliable chaotic modulation-based transmission technique," *IEEE Trans. Circuits Syst. II: Exp. Briefs*, vol. 59, no. 2, pp. 128–132, Feb. 2012.

[45] P. Chen, K. Su, L. Wang, and Y. Fang, "An improved DDCSK-Walsh coding technique with BCJR decoding," in *Proc. Int. Symp. Commun. Inf. Technol. (ISCIT)*, Oct. 2015, pp. 1–4.

[46] F. C. M. Lau, C. K. Tse, M. Ye, and S. Hau, "Coexistence of chaos-based and conventional digital communication systems of equal bit rate," *IEEE Trans. Circuits Syst. I: Reg. Papers*, vol. 51, no. 2, pp. 391–408, Feb. 2004.

[47] F. C. M. Lau and C. K. Tse, "Performance of chaos-based communication systems under the influence of coexisting conventional spread-spectrum systems," *IEEE Trans. Circuits Syst. I: Reg. Papers*, vol. 50, no. 11, pp. 1475–1481, Nov. 2003.

[48] W. Xu, L. Wang, and G. Chen, "Performance analysis of the CS-DCSK/BPSK communication system," *IEEE Trans. Circuits Syst. I: Reg. Papers*, vol. 61, no. 9, pp. 2624–2633, Sept. 2014.

[49] S. Wang and X. Wang, "M-DCSK-based chaotic communications in MIMO multipath channels with no channel state information," *IEEE Trans. Circuits Syst. II: Exp. Briefs*, vol. 57, no. 12, pp. 1001–1005, Dec. 2010.

[50] H. Ma and H. Kan, "Space-time coding and processing with differential chaos shift keying scheme," in *Proc. IEEE Int. Conf. Commun. (ICC)*, Jun. 2009, pp. 1–5.

[51] G. Kaddoum, M. Vu, and F. Gagnon, "Performance analysis of differential chaotic shift keying communications in MIMO systems," in *Proc. IEEE Int. Symp. Circuits Syst. (ISCAS)*, May 2011, pp. 1580–1583.

[52] P. Chen, L. Wang, and F. C. M. Lau, "One analog STBC-DCSK transmission scheme not requiring channel state information," *IEEE Trans. Circuits Syst. I: Reg. Papers*, vol. 60, no. 4, pp. 1027–1037, Apr. 2013.

[53] Y. Fang, J. Xu, L. Wang, and G. Chen, "Performance of MIMO relay DCSK-CD systems over Nakagami fading channels," *IEEE Trans. Circuits Syst. I: Reg. Papers*, vol. 60, no. 3, pp. 757–767, Mar. 2013.

[54] A. Sendonaris, E. Erkip, and B. Aazhang, "User cooperation diversity–Part I: System description," *IEEE Trans. Commun.*, vol. 51, no. 11, pp. 1927–1938, Nov. 2003.

[55] ——, "User cooperation diversity-Part II: Implementation aspects and performance analysis," *IEEE Trans. Commun.*, vol. 51, no. 11, pp. 1939–1948, Nov. 2003.

[56] J. Xu, W. Xu, L. Wang, and G. Chen, "Design and simulation of a cooperative communication system based on DCSK/FM-DCSK," in *Proc. IEEE Int. Symp. Circuits Syst. (ISCAS)*, Jun. 2010, pp. 2454–2457.

[57] Y. Fang, L. Wang, and G. Chen, "Performance of a multiple-access DCSK-CC system over Nakagami-m fading channels," in *Proc. IEEE Int. Symp. Circuits Syst. (ISCAS)*, May 2013, pp. 277–280.

[58] A. Magableh, M. Al-Mistarihi, and M. Al-Khasawneh, "Performance evaluation of bit error probability in DCSK cooperative communication systems over Nakagami-m fading channels," in *Proc. Int. Multi-Conf. Syst., Signals Devices (SSD)*, Feb. 2014, pp. 1–4.

[59] N. Bonello, S. Chen, and L. Hanzo, "Low-density parity-check codes and their rateless relatives," *IEEE Commun. Surveys & Tutorials*, vol. 13, no. 1, pp. 3–26, First Quarter 2011.

[60] Y. Fang, G. Bi, Y. Guan, and F. C. M. Lau, "A survey on protograph LDPC codes and their applications," *IEEE Commun. Surveys & Tutorials*, vol. 17, no. 4, pp. 1–28, Fourth Quarter 2015.

[61] H. Chen, R. Maunder, and L. Hanzo, "A survey and tutorial on low-complexity turbo coding techniques and a holistic hybrid ARQ design example," *IEEE Commun. Surveys & Tutorials*, vol. 15, no. 4, pp. 1546–1566, Fourth Quarter 2013.

[62] S. Lee, W. Su, S. Batalama, and J. Matyjas, "Cooperative decode-and-forward ARQ relaying: Performance analysis and power optimization," *IEEE Trans. Wireless Commun.*, vol. 9, no. 8, pp. 2632–2642, Aug. 2010.

[63] L. Wang and G. Chen, "Using LDPC codes to enhance the performance of FM-DCSK," in *Proc. Midwest Symp. Circuits Syst. (MWSCAS)*, vol. 1, Jul. 2004, pp. 401–404.

[64] C. Zhang, L. Wang, and G. R. Chen, "Promising performance of PA coded SIMO FM-DCSK communication systems," *Circuits Syst. Signal Process.*, vol. 27, no. 6, pp. 915–926, Aug. 2008.

[65] G. Kaddoum and F. Gagnon, "Error correction codes for secure chaos-based communication system," in *Proc. Biennial Symp. Communications (QBSC)*, May 2010, pp. 193–196.

[66] A. Wagemakers, F. J. Escribano, L. Lopez, and M. A. F. Sanjuan, "Competitive decoders for turbo-like chaos-based systems," *IET Commun.*, vol. 6, no. 10, pp. 1278–1283, Jul. 2012.

[67] F. Escribano, S. Kozic, L. Lopez, M. Sanjuan, and M. Hasler, "Turbo-like structures for chaos encoding and decoding," *IEEE Trans. Commun.*, vol. 57, no. 3, pp. 597–601, Mar. 2009.

[68] Y. Lyu, G. Cai, and L. Wang, "Iterative demodulation and decoding of LDPC-coded M-ary DCSK modulation over AWGN channel," in *Proc. Int. Symp. Medical Inf. Commun. Technol. (ISMICT)*, Apr. 2014, pp. 1–5.

[69] Y. Lyu, L. Wang, G. Cai, and G. Chen, "Iterative receiver for M-ary DCSK systems," *IEEE Trans. Commun.,* accepted for publication, 2015. [Online]. Available: http://ieeexplore.ieee.org/

[70] G. Kaddoum and M. El-Hajjar, "Analysis of network coding schemes for differential chaos shift keying communication system," *CoRR*, vol. abs/1505.02851, May 2015. [Online]. Available: http://arxiv.org/abs/1505.02851

[71] G. Kaddoum and F. Shokraneh, "Analog network coding for multi-user multi-carrier differential chaos shift keying communication system," *IEEE Trans. Wireless Commun.*, vol. 14, no. 3, pp. 1492–1505, Mar. 2015.

[72] L. Wang, G. Cai, and G. Chen, "Design and performance analysis of a new multiresolution M-ary differential chaos shift keying communication system," *IEEE Trans. Wireless Commun.*, vol. 14, no. 9, pp. 5197–5208, Sept. 2015.

[73] R. Ahlswede, N. Cai, S.-Y. Li, and R. W. Yeung, "Network information flow," *IEEE Trans. Inf. Theory*, vol. 46, no. 4, pp. 1204–1216, Jul. 2000.

[74] B. Zhang, J. Hu, Y. Huang, M. El-Hajjar, and L. Hanzo, "Outage analysis of superposition-modulation-aided network-coded cooperation in the presence of network coding noise," *IEEE Trans. Veh. Technol.*, vol. 64, no. 2, pp. 493–501, Feb. 2015.

[75] B. Nazer and M. Gastpar, "Reliable physical layer network coding," *Proc. IEEE*, vol. 99, no. 3, pp. 438–460, Mar. 2011.

[76] K. Ramchandran, A. Ortega, K. Uz, and M. Vetterli, "Multiresolution broadcast for digital HDTV using joint source/channel coding," *IEEE J. Sel. Areas Commun.*, vol. 11, no. 1, pp. 6–23, Jan. 1993.

[77] L.-F. Wei, "Coded modulation with unequal error protection," *IEEE Trans. Commun.*, vol. 41, no. 10, pp. 1439–1449, Oct. 1993.

[78] M. P. Kennedy, G. Kolumban, and G. Kis, "Simulation of the multipath performance of FM-DCSK digital communications using chaos," in *Proc. IEEE Int. Symp. Circuits Syst. (ISCAS)*, vol. 4, Jul. 1999, pp. 568–571.

[79] Z. Chen, W. Xu, J. Huang, and L. Wang, "Performances of CS-DCSK UWB communication system in the presence of narrow band interferers," in *Proc. IEEE Int. Conf. Trust, Secur. Priv. Comput. Commun. (TrustCom)*, Jun. 2012, pp. 1475–1480.

[80] S. Erkucuk and D. I. Kim, "Combined M-ary code shift/differential chaos keying for low-rate UWB communications," in *Proc IEEE Int. Conf. Ultra-Wideband (ICUWB)*, Sept. 2005, pp. 33–37.

[81] C.-C. Chong and S. K. Yong, "UWB direct chaotic communication technology for low-rate WPAN applications," *IEEE Trans. Veh. Technol.*, vol. 57, no. 3, pp. 1527–1536, May 2008.

[82] G. Kolumban, "UWB technology: Chaotic communications versus noncoherent impulse radio," in *Proc. European Conf. Circuit Theory Des.*, vol. 2, Aug. 2005, pp. 79–82.

[83] M. P. Kennedy, G. Kolumban, G. Kis, and Z. Jako, "Performance evaluation of FM-DCSK modulation in multipath environments," *IEEE Trans. Circuits Syst. I: Reg. Papers*, vol. 47, no. 12, pp. 1702–1711, Dec. 2000.

[84] S. Mukherjee and D. Ghosh, "Design and performance analysis of a novel FM-chaos based modulation technique," in *Proc. IEEE Wireless Commun. Netw. Conf. (WCNC)*, Apr. 2014, pp. 594–599.

[85] L. Wang, C. Zhang, and G. Chen, "Performance of an SIMO FM-DCSK communication system," *IEEE Trans. Circuits Syst. II: Exp. Briefs*, vol. 55, no. 5, pp. 457–461, May 2008.

[86] X. Min, W. Xu, L. Wang, and G. Chen, "Promising performance of a frequency-modulated differential chaos shift keying ultra-wideband system under indoor environments," *IET Commun.*, vol. 4, no. 2, pp. 125–134, Jan. 2010.

[87] S. Chen, L. Wang, and G. Chen, "Data-aided timing synchronization for FM-DCSK UWB communication systems," *IEEE Trans. Ind. Electron.*, vol. 57, no. 5, pp. 1538–1545, May 2010.

[88] Y. Fang, P. Chen, and L. Wang, "Performance analysis and optimisation of a cooperative frequency-modulated differential chaos shift keying ultra-wideband system under indoor environments," *IET Networks*, vol. 1, no. 2, pp. 58–65, Jun. 2012.

[89] L. Wang, X. Min, and G. Chen, "Performance of SIMO FM-DCSK UWB system based on chaotic pulse cluster signals," *IEEE Trans. Circuits and Syst. I, Reg. Papers*, vol. 58, no. 9, pp. 2259–2268, Sept. 2011.

[90] Y. Fang, S. Hong, and L. Wang, "A novel MIMO relay FM-DCSK UWB system for low-rate and low-power WPAN applications," in *Proc. Int. Symp. Commun. Inf. Technol. (ISCIT)*, Oct. 2011, pp. 159–162.

[91] T. Huang, L. Wang, W. Xu, and G. Cai, "An adaptive retransmission scheme of SIMO FM-DCSK UWB system," in *Proc. Int. Symp. Communications and Inf. Technol. (ISCIT)*, Sept. 2013, pp. 128–132.

[92] T. Huang, L. Wang, and W. Xu, "System parameter adjustment of FM-DCSK UWB for different medical environments," in *Proc. Int. Symp. Medical Inf. Commun. Technol. (ISMICT)*, Mar. 2015, pp. 162–165.

[93] C.-C. Chong *et al.*, *Samsung Electronics (SAIT) CFP Presentation for IEEE 802.15.4a Alternative PHY*. Monterey, CA, IEEE 802.15-05-0030-02-004a, Jan. 2005.

[94] N. Kim and I. Kim, *Samsung DM R&D Center Proposal*. Monterey, CA, IEEE 802.15-05-0042-00-004a, Jan. 2005.

[95] H. S. Lee *et al.*, *Chaotic Pulse Based Communication System Proposal*. Monterey, CA, IEEE 802.15-05-0010-04-004a, Jan. 2005.

[96] *IEEE Standard for Local and metropolitan area networks - Part 15.6: Wireless Body Area Networks*. IEEE Std 802.15.6-2012, New York, NY, USA: IEEE Press, Feb. 2012.

[97] Y. Xia, C. K. Tse, and F. C. M. Lau, "Some benchmark multipath performance data of coherent CSK digital communication systems," in *Proc. Int. Workshop on Nonlinear Circuits & Signal Process. (NCSP)*, Mar. 2004, pp. 261–264.

[98] S. Tzafestas, *Walsh Functions in Signal and Systems Analysis and design*. Heidelberg, Germany: Springer-Verlag, 1985.

[99] D. M. Novakovic and M. Dukic, "Evolution of the power control techniques for DS-CDMA toward 3G wireless communication systems," *IEEE Commun. Surveys & Tutorials*, vol. 3, no. 4, pp. 2–15, Fourth Quarter 2000.

[100] S. Berber, "Probability of error derivatives for binary and chaos-based CDMA systems in wide-band channels," *IEEE Trans. Wireless Commun.*, vol. 13, no. 10, pp. 5596–5606, Oct. 2014.

[101] Z. Zhou, J. Wang, and Y. Ye, "Exact BER analysis of differential chaos shift keying communication system in fading channels," *Wireless Pers. Commun.*, vol. 53, no. 2, pp. 299–310, Jan. 2010.

[102] H. Li, X. Dai, and P. Xu, "A CDMA based multiple-access scheme for DCSK," in *Proc. , 2004. Proc. IEEE Circuits Syst. Symp. Emerging Technol: Frontiers of Mobile & Wireless Commun.*, vol. 1, May 2004, pp. 313–316.

[103] X. Yang and B. Vucetic, "A frequency domain multi-user detector for TD-CDMA systems," *IEEE Trans. Commun.*, vol. 59, no. 9, pp. 2424–2433, Sept. 2011.

[104] T. Eng and L. B. Milstein, "Coherent DS-CDMA performance in Nakagami multipath fading," *IEEE Trans. Commun.*, vol. 43, no. 234, pp. 1134–1143, Feb. 1995.

[105] Y. Lee and M. H. Tsai, "Performance of decode-and-forward cooperative communications over Nakagami-m fading channels," *IEEE Trans. Veh. Technol.*, vol. 58, no. 3, pp. 1218–1228, Mar. 2009.

[106] J. Moualeu, W. Hamouda, H. Xu, and F. Takawira, "Multi-relay turbo-coded cooperative diversity networks over Nakagami-m fading channels," *IEEE Trans. Veh. Technol*, vol. 62, no. 9, pp. 4458–4470, Nov. 2013.

[107] L.-L. Yang and L. Hanzo, "Acquisition of m-sequences using recursive soft sequential estimation," *IEEE Trans. Commun.*, vol. 52, no. 2, pp. 199–204, Feb. 2004.

[108] G. Ye, J. Li, A. Huang, and H.-H. Chen, "A Novel ZCZ code based on m-sequences and its applications in CDMA systems," *IEEE Commun. Lett.*, vol. 11, no. 6, pp. 465–467, Jun. 2007.

[109] W. M. Tam, F. C. M. Lau, and C. K. Tse, *Digital Communications with Chaos: Multiple Access Techniques and Performance Evaluation*. Oxford, Great Britain: Elsevier, 2007.

[110] Z. Zhou, T. Zhou, and J. Wang, "Performance of multi-user DCSK communication system over multipath fading channels," in *Proc. IEEE Int. Symp. Circuits Syst. (ISCAS)*, May 2007, pp. 2478–2481.

[111] L. Chen, W. Xu, and L. Wang, "Performance of improved FM-DCSK system based on differential-coding method," in *Proc. Int. Conf. Commun., Circuits Syst. (ICCAS)*, May 2008, pp. 1224–1227.

[112] W. Xu, L. Wang, and G. Kolumban, "A new data rate adaption communications scheme for code-shifted differential chaos shift keying modulation," *Int. J. Bifurcation Chaos*, vol. 22, no. 8, pp. 1–8, Aug. 2012.

[113] W. M. Tam, F. C. M. Lau, C. Tse, and A. J. Lawrance, "Exact analytical bit error rates for multiple access chaos-based communication systems," *IEEE Trans. Circuits Syst. II: Exp. Briefs*, vol. 51, no. 9, pp. 473–481, Sept. 2004.

[114] K. Krol, L. Azzinnari, E. Korpela, A. Mozsary, M. Talonen, and V. Porra, "An experimental FM-DCSK chaos radio system," in *Proc. European Conf. Circuit Theory & Design*, Aug. 2001, pp. 17–20.

[115] G. Kolumban and G. Kis, "Reception of M-ary FM-DCSK signals by energy detector," in *Proc. Int. Workshop Nonlinear Dynam. Electron. Syst. (NDES)*, May 2003, pp. 133–136.

[116] L. Ye, G. Chen, and L. Wang, "Essence and advantages of FM-DCSK technique versus conventional spreading spectrum communication method," *Circ., Syst. Signal Process.*, vol. 24, no. 5, pp. 657–673, Oct. 2005.

[117] A.-B. Salberg and A. Hanssen, "A subspace theory for differential chaos-shift keying," *IEEE Trans. Circuits Syst. II: Exp. Briefs*, vol. 53, no. 1, pp. 51–55, Jan. 2006.

[118] G. Mazzini, R. Rovatti, and G. Setti, "Chaos-based spreading in DS-UWB sensor networks increases available bit rate," *IEEE Trans. Circuits Syst. I: Reg. Papers*, vol. 54, no. 6, pp. 1327–1339, Jun. 2007.

[119] G. Kaddoum, "Analysis of a multi-user OFDM based differential chaos shift keying communication system," *Submitted to IEEE Trans. Commun.*, May 2015.

[120] T. Krebesz, G. Kolumban, C. Tse, and F. C. Lau, "Implementation of FM-DCSK modulation scheme on USRP platform based on complex envelope," in *Proc. Int. Symp. Nonlinear Theory & Its Appl. (ISNTA)*, Oct. 2012, pp. 797–800.

[121] H. Leib, "Data-aided noncoherent demodulation of DPSK," *IEEE Trans. Commun.*, vol. 43, no. 2/3/4, pp. 722–725, Feb. 1995.

[122] L. Bahl, J. Cocke, F. Jelinek, and J. Raviv, "Optimal decoding of linear codes for minimizing symbol error rate," *IEEE Trans. Inf. Theory*, vol. 20, no. 2, pp. 284–287, Mar. 1974.

[123] L. Hanzo, T. Keller, M. Muenster, , and B.-J. Choi, *OFDM and MC-CDMA for Broadband Multi-User Communications*. New York, NY, USA: Wiley-IEEE Press, 2003.

[124] D. Guo, "Performance of multicarrier CDMA in frequency-selective fading via statistical physics," *IEEE Trans. Inf. Theory*, vol. 52, no. 4, pp. 1765–1774, Apr. 2006.

[125] S. Kondo and L. Milstein, "Performance of multicarrier DS CDMA systems," *IEEE Trans. Commun.*, vol. 44, no. 2, pp. 238–246, Feb. 1996.

[126] T. Tsiftsis, H. Sandalidis, G. Karagiannidis, and M. Uysal, "Optical wireless links with spatial diversity over strong atmospheric turbulence channels," *IEEE Trans. Wireless Commun.*, vol. 8, no. 2, pp. 951–957, Feb. 2009.

[127] Y. Fang, P. Chen, L. Wang, F. C. M. Lau, and K.-K. Wong, "Performance analysis of protograph-based low-density parity-check codes with spatial diversity," *IET Commun.*, vol. 6, no. 17, pp. 2941–2948, Nov. 2012.

[128] D. So and R. Cheng, "Detection techniques for V-BLAST in frequency selective fading channels," in *Proc. IEEE Wireless Commun. & Netw. Conf. (WCNC)*, vol. 1, Mar. 2002, pp. 487–491.

[129] Y. Fan and J. Thompson, "MIMO configurations for relay channels: Theory and practice," *IEEE Trans. Wireless Commun.*, vol. 6, no. 5, pp. 1774–1786, May 2007.

[130] S. Sugiura, S. Chen, and L. Hanzo, "MIMO-aided near-capacity turbo transceivers: taxonomy and performance versus complexity," *IEEE Commun. Surveys & Tutorials*, vol. 14, no. 2, pp. 421–442, Second Quarter 2012.

[131] S. M. Alamouti, "A simple transmit diversity technique for wireless communications," *IEEE J. Sel. Areas Commun.*, vol. 16, no. 8, pp. 1451–1458, Oct. 1998.

[132] H. Jafarkhani, *Space-time Coding: Theory and Practice*. New York, NY, USA: Cambridge University Press, 2005.

[133] R. Nabar, H. Bolcskei, and F. Kneubuhler, "Fading relay channels: performance limits and space-time signal design," *IEEE J. Sel. Areas Commun.*, vol. 22, no. 6, pp. 1099–1109, Aug. 2004.

[134] H. Bolcskei, R. Nabar, O. Oyman, and A. Paulraj, "Capacity scaling laws in MIMO relay networks," *IEEE Trans. Wireless Commun.*, vol. 5, no. 6, pp. 1433–1444, Jun. 2006.

[135] B. Wang, J. Zhang, and A. Host-Madsen, "On the capacity of MIMO relay channels," *IEEE Trans. Inf. Theory*, vol. 51, no. 1, pp. 29–43, Jan. 2005.

[136] K. Azarian, H. El Gamal, and P. Schniter, "On the achievable diversity-multiplexing tradeoff in half-duplex cooperative channels," *IEEE Trans. Inf. Theory*, vol. 51, no. 12, pp. 4152–4172, Dec. 2005.

[137] T. Richardson and R. Urbanke, "The capacity of low-density parity-check codes under message-passing decoding," *IEEE Trans. Inf. Theory*, vol. 47, no. 2, pp. 599–618, Feb. 2001.

[138] J. Li, K. Narayanan, and C. Georghiades, "Product accumulate codes: a class of codes with near-capacity performance and low decoding complexity," *IEEE Trans. Inf. Theory*, vol. 50, no. 1, pp. 31–46, Jan. 2004.

[139] C. Douillard, M. Jezequel, C. Berrou, A. Picart, P. Didier, and A. Glavieux, "Iterative correction of intersymbol interference: Turbo-equalization," *European Trans. on Telecommun.*, vol. 6, no. 5, pp. 507–511, Sept. 1995.

[140] Y. Fang, P. Chen, L. Wang, and F. C. M. Lau, "Design of protograph LDPC codes for partial response channels," *IEEE Trans. Commun.*, vol. 60, no. 10, pp. 2809–2819, Oct. 2012.

[141] T. Chaitanya and E. Larsson, "Bits-to-symbol mappings for superposition coding based HARQ systems," in *Proc. IEEE Wireless Commun. & Netw. Conf.*, Apr. 2013, pp. 2468–2472.

[142] S. ten Brink, "Convergence behavior of iteratively decoded parallel concatenated codes," *IEEE Trans. Commun.*, vol. 49, no. 10, pp. 1727–1737, Oct. 2001.

[143] G. Caire, G. Taricco, and E. Biglieri, "Bit-interleaved coded modulation," *IEEE Trans. Inf. Theory*, vol. 44, no. 3, pp. 927–946, May 1998.

[144] W. Stark, "Capacity and cutoff rate of noncoherent FSK with nonselective Rician fading," *IEEE Trans. Commun.*, vol. 33, no. 11, pp. 1153–1159, Nov. 1985.

[145] A. G. Fabregas and A. J. Grant, "Capacity approaching codes for non-coherent orthogonal modulation," *IEEE Trans. Wireless Commun.*, vol. 6, no. 11, pp. 4004–4013, Nov. 2007.

[146] H. El Gamal, G. Caire, and M. Damen, "The MIMO ARQ channel: Diversity-multiplexing-delay tradeoff," *IEEE Trans. Inf. Theory*, vol. 52, no. 8, pp. 3601–3621, Aug. 2006.

[147] A. Shah and A. Haimovich, "Performance analysis of maximal ratio combining and comparison with optimum combining for mobile radio communications with cochannel interference," *IEEE Trans. Veh. Technol.*, vol. 49, no. 4, pp. 1454–1463, Jul. 2000.

[148] Q. Zhang, "Probability of error for equal-gain combiners over Rayleigh channels: Some closed-form solutions," *IEEE Trans. Commun.*, vol. 45, no. 3, pp. 270–273, Mar. 1997.

[149] S.-Y. Li, R. Yeung, and N. Cai, "Linear network coding," *IEEE Trans. Inf. Theory*, vol. 49, no. 2, pp. 371–381, Feb. 2003.

[150] C. Fragoul, J. Y. Boudec, and J. Widmer, "Network Coding: An Instant Primer," *ACM SIGCOMM Comput. Commun. Rev.*, vol. 36, no. 1, pp. 63–68, Jan. 2006.

[151] S. Zhang, S.-C. Liew, , and P. Lam, "Hot topic: Physical layer network coding," in *Proc. MobiCom'06*, Sept. 2006, pp. 358–365.

[152] S. Katti, S. Gollakota, and D. Katabi, "Embracing wireless interference: analog network coding," *ACM SIGCOMM Comput. Commun. Rev.*, vol. 37, no. 4, pp. 397–408, Apr. 2007.

[153] Y. Bi and Y. Ding, "Ergodic channel capacity of an amplify-and-forward relay system at low SNR in a generic noise environment," *IEEE Trans. Signal Process.*, vol. 60, no. 5, pp. 2694–2700, May 2012.

[154] M. Chen and A. Yener, "Multiuser two-way relaying: detection and interference management strategies," *IEEE Trans. Wireless Commun.*, vol. 8, no. 8, pp. 4296–4305, Aug. 2009.

[155] M. Riemensberger, Y. Sagduyu, M. Honig, and W. Utschick, "Comparison of analog and digital relay methods with network coding for wireless multicast," in *Proc. IEEE Int. Conf. Commun. (ICC)*, Jun. 2009, pp. 1–5.

[156] S. Mao, J. Kim, and J. Lee, "Multi-User analog network coding with spread spectrum," in *Proc. IEEE Veh. Technol. Conf. (VTC)*, May 2012, pp. 1–5.

[157] L. Yang and G. Giannakis, "Ultra-wideband communications: an idea whose time has come," *IEEE Signal Process. Mag.*, vol. 21, no. 6, pp. 26–54, Nov. 2004.

[158] M. Pausini and G. Janssen, "Performance analysis of UWB autocorrelation receivers over Nakagami-fading channels," *IEEE J. Sel. Top. Signal Process.*, vol. 1, no. 3, pp. 443–455, Oct. 2007.

[159] A. Dezfooliyan and A. Weiner, "Spatio-temporal focusing of phase compensation and time reversal in ultra-wideband systems with limited rate feedback," *IEEE Trans. Veh. Technol.* accepted for publication, 2015. [Online]. Available: http://ieeexplore.ieee.org/

[160] S. Won and L. Hanzo, "Initial synchronisation of wideband and UWB direct sequence systems: Single- and multiple-antenna aided solutions," *IEEE Commun. Surveys & Tutorials*, vol. 14, no. 1, pp. 87–108, First Quarter 2012.

[161] A. F. Molisch and *et al.*, *IEEE 802.15.4a Channel Model - Final Report*. Sam Amtpmop, TX, IEEE 802.15-04-0662-02-004a, Nov. 2004. [Online]. Available: http://www.ieee802.org/15/pub/2004/

[162] J. Foerster, *Channel Modeling Sub-Committee Final Report*. IEEE P802.15-02/490r1-SG3a, Feb. 2003.

[163] A. Molisch, D. Cassioli, C.-C. Chong, S. Emami, A. Fort, B. Kannan, J. Karedal, J. Kunisch, H. Schantz, K. Siwiak, and M. Win, "A comprehensive standardized model for ultra-wideband propagation channels," *IEEE Trans. Antennas Propag.*, vol. 54, no. 11, pp. 3151–3166, Nov. 2006.

[164] N. He and C. Tepedelenlioglu, "Performance analysis of non-coherent UWB receivers at different synchronization levels," *IEEE Trans. Wireless Commun.*, vol. 5, no. 6, pp. 1266–1273, Jun. 2006.

[165] A. D'Amico and U. Mengali, "Code-multiplexed transmitted-reference UWB systems in a multi-user environment," *IEEE Trans. Commun.*, vol. 58, no. 3, pp. 966–974, Mar. 2010.

[166] Z. Tian and G. Giannakis, "A GLRT approach to data-aided timing acquisition in UWB radios-Part II: Training sequence design," *IEEE Trans. Wireless Commun.*, vol. 4, no. 6, pp. 2994–3004, Nov. 2005.

[167] L. Wu, V. Lottici, and Z. Tian, "Maximum likelihood multiple access timing synchronization for UWB communications," *IEEE Trans. Wireless Commun.*, vol. 7, no. 11, pp. 4497–4501, Nov. 2008.

[168] L. Yang and G. Giannakis, "Timing ultra-wideband signals with dirty templates," *IEEE Trans. Commun.*, vol. 53, no. 11, pp. 1952–1963, Nov. 2005.

[169] R. Zhang and X. Dong, "Synchronization and integration region optimization for UWB signals with non-coherent detection and autocorrelation detection," *IEEE Trans. Commun.*, vol. 56, no. 5, pp. 790–798, May 2008.

[170] M. Casu and G. Durisi, "Implementation aspects of a transmitted reference UWB receiver," *Wireless Commun. Mobile Comput.*, vol. 5, no. 5, pp. 537–549, Aug. 2005.

[171] M. Koohestani, J.-F. Zurcher, A. Moreira, and A. Skrivervik, "A novel, low-profile, vertically-polarized UWB antenna for WBAN," *IEEE Trans. Antennas Propag.*, vol. 62, no. 4, pp. 1888–1894, Apr. 2014.

[172] A. Pantelopoulos and N. Bourbakis, "A survey on wearable sensor-based systems for health monitoring and prognosis," *IEEE Trans. Syst., Man Cybern.-Part C: Appl. Rev.*, vol. 40, no. 1, pp. 1–12, Jan. 2010.

[173] G. Kaddoum, J. Olivain, G. Beaufort Samson, P. Giard, and F. Gagnon, "Implementation of a differential chaos shift keying communication system in GNU radio," in *Proc. Int. Symp. Wireless Commun. Syst. (ISWCS)*, Aug. 2012, pp. 934–938.

[174] L. O. Chua, T. Yang, G. Q. Zhong, and C. W. Wu, "Synchronization of Chua's circuits with time-varying channels and parameters," *IEEE Trans. Circuits Syst. I*, vol. 43, no. 10, pp. 862–868, Oct. 1996.

[175] J. Feng, C. K. Tse, and F. C. M. Lau, "A neural-network-based channel equalization strategy for chaos-based communication systems," *IEEE Trans. Circuits Syst. I*, vol. 50, no. 7, pp. 954–957, Jul. 2003.